DESIGN AND MICROFABRICATION OF A DROPLET-BASED MICROFLUIDIC PROBE FOR SAMPLING AND DELIVERY

By

SHILUN FENG

A thesis submitted to Macquarie University

for the degree of

Doctor of Philosophy

School of Engineering

September 2018

MACQUARIE University
SYDNEY·AUSTRALIA

Abstract

Conventional needles (or similar probes) cannot deliver sequences of different drugs in one insertion. Neither can they transport a rapidly changing chemical signal from the insertion point to an analytical instrument. Both of these limitations are caused by the phenomenon known as Taylor dispersion. Delivery of sequences of drugs (multi-drug delivery) requires multiple injection lines/tubes, each carrying different drugs. Measurement of rapidly changing chemical signals requires that we bring the instrument directly to the sampling point (expensive and impractical).

In a droplet-based microfluidic system, water-based liquids are carried by an immiscible oil (continuous phase) in a hydrophobic channel. If we discretise the fluid into droplets (delivery or sampling), each droplet is isolated and does not mix with neighbouring droplets. This overcomes the signal distortion caused by Taylor dispersion in continuous flow for both sampling and delivery of chemical signals.

If the droplet-based microfluidic device is to be used as a needle, the oil phase cannot be injected into the tissue. However, the oil must be provided at the injection site to partition the sampled liquid. This thesis is focused on developing new droplet-based microfluidic probes with the flow barrier at the tip.

We have successfully developed two kinds of droplet-based microfluidic probes, one for silicon-based microfluidic probes, another for membrane-based microfluidic probes. Each system incorporates a Laplace pressure flow barrier that prevents oil from exiting into the tissue but allows easy passage of water.

This new version of an ancient medical device may allow research into rapidly changing chemical signals such as neurotransmitters. With further development, it may also find applications in disease and trauma diagnostics and treatments.

Keyword: Sampling, delivery, droplet, microfabrication, probe, biomedical microfluidics.

List of Publications

This thesis is based on the following papers, which will be included and presented in the text.

Publications:

1. **S.L. Feng**, G.Z. Liu, L.M. Jiang, Y.G. Zhu, E. M. Goldys, D. W. Inglis, "A Microfluidic Needle for Sampling and Delivery of Chemical Signals by Segmented Flows," **Applied Physics Letters**,111 (18), 183702, 2017. **[Publication I]**

2. **S.L. Feng**, S. Clement, Y.G. Zhu, E. M. Goldys, D. W. Inglis, "Microfabricated probe for hydrogen peroxide detection," **Sensors and Actuators B: Chemical**, submitted on 3rd of September 2018. **[Publication II]**

Manuscripts in preparation:

3. **S.L. Feng**, D. W. Inglis, "Sampling and transport of chemical signals using droplets: a review," manuscript in preparation.

4. **S.L. Feng**, D. W. Inglis, "Laplace pressure as a flow barrier in microchannel: a review," manuscript in preparation.

5. **S.L. Feng**, J. Chan, D. Arrua, E. Hilder, E. M. Goldys and D. W. Inglis, "A cheap Membrane-in-pipette tip droplet logger system capable of sampling and delivery chemicals with chemical resolution," manuscript in preparation.

Related Publications and Conferences

The following publications by the author do not constitute an integral part of this thesis and are therefore not included.

Journals:

6. **S.L. Feng**, A. Skelley, A. Anwer, G.Z. Liu, D.W. Inglis, "Maximizing Particle Concentration in Deterministic Lateral Displacement Arrays," **Biomicrofluidics**, 11 (2), 024121, 2017; doi.org/10.1063/1.4981014.

7. **S.L. Feng**, M. M. Nguyen, D.W. Inglis, "Microfluidic droplet extraction by hydrophilic membrane," **Micromachines**, 8(11), 331, 2017; doi.org/10.3390/mi8110331.

8. A. Naga, **S.L. Feng (co-first author),** S. C. Mukhopadhyay and D. Inglis, "Development of 3-D printed mould based highly flexible graphite sensors for tactile sensing applications," **Sensors & Actuators: A. Physical**, 280, 525-534, 2018; doi.org/10.1016/j.sna.2018.08.028.

9. M. Qi, E. M. Goldys, J.W. Huang, H. Wei, C.M. Cao, **S.L. Feng**, Q. Guo, R. Li, G.Z. Liu, "Graphene Oxide Thin Film with Dual Function Integrated Into a Nano-Sandwich Device for In Vivo Monitoring of Interleukin-6," **ACS Applied Materials & Interfaces**, 9 (48), pp 41659–41668, 2017.

10. A. Naga, N. Afsarimanesh, **S.L. Feng**, S. C. Mukhopadhyay, "Strain−Induced Graphite/PDMS sensors for Biomedical Applications," **Sensors & Actuators: A. Physical**, 271, 257-269, 2018.

Conferences:

11. **S.L. Feng**, G.Z Liu, L.M. Jiang, Y.G. Zhu, E. M. Goldys, D. W. Inglis, "Microfluidic Needle for Segmented Flow," **ANZMNT 2017**, Hobart, Tasmania, June 27-29, 2017.

12. **S.L. Feng**, G.Z Liu, L.M. Jiang, Y.G. Zhu, E. M. Goldys, D. W. Inglis, "Microfluidic Needle for Segmented Flow," **MicroTAS 2017**, Savannah, USA, October 22-26, 2017.

13. **S.L. Feng**, A. Skelley, A. Anwer, G.Z. Liu, D. W. Inglis, "Maximizing Particle Concentration in Deterministic Lateral Displacement Arrays," **MicroTAS 2017**, Savannah, USA, October 22-26, 2017.

14. **S.L. Feng,** Y.G. Zhu, E. M. Goldys, D. W. Inglis, "Real-time detection of H_2O_2 concentration around the cell with a temporal resolution by microfluidic needle," **ANZMNT 2018**, Auckland, New Zealand, June 26-29, 2018.

15. **S.L. Feng**, A. Skelley, D. W. Inglis, "Solving the DLD Boundary problem using AI iterative CFD," accepted, **MicroTAS 2018,** Kaohsiung, Taiwan, November 11-15, 2018.

Preface and Acknowledgement

I wish to thank my supervisor, David Inglis with whom I share an incredible PhD journey. It has been said that a swift horse is usually found but not the same as ‘Pak Lok" (i.e. the person who knew how to spot a ‘Long Distance Running Horse’). He is the kind of person who can cultivate my skills to be a qualified PhD research student. It was David who helped me to become familiar with microfabrication facilities, fundamental microfluidic setup, and everything he knows in the laboratory. He tolerated my mistakes and having to develop my skills slowly.

Furthermore, David encouraged and helped me to do things that will benefit my career development. Moreover, David provided me with so many valuable directions for developing my own philosophy and worldview and conception of research. As David said, “As an engineer, I love problems and think about ways to solve them!”

Also, I thank my family, including my girlfriend for their support, selfless sacrifice and endless patience throughout my three-years PhD journey.

I am also grateful to several other people and organizations for their help and support.

To my co-supervisor, Professor Ewa Goldys, for sharing her scientific knowledge, for guiding my decisions, for being a friend as well as a supervisor and for being an infinite source of motivation and energy.

To Prof. Yonggang Zhu, for the useful discussions and timely advice in my research projects and career development.

To my BMMD (Biomedical Microdevices) group, Dr Lianmei Jiang, Dr Mohsen Asadnia, Dr Ming Li, Mr Bhuwan Ghimire, Mr Mohammadamin Raoufi, James White, Michael Nguyen and Mr Hangrui Liu for keeping me company. Often, I was alone when conducting experiments,

and it was good to share the experimental resources. Most importantly, they helped me to proof-read my thesis. Thanks for being a group.

To my CNBP (Centre for Nanoscale BioPhotonics) group, Dr Sandya Clement, Dr Wei Deng, Zarha, Dr Anna Gular, Dr Kai Zhang, Dr Guozhen Liu, and Dr Ayad. You all helped me to develop my biomedical skills and run all of the biomedical applications. Thanks for being a group.

To the researchers in Mq (Macquarie University), thanks to Walther Adendorff and other staffs from the METS for the workshop fabrication; thanks to Sue Lindsay and Chao Shen from the SEM microscope unit and helping with the SEM and thermal evaporation; thanks to the MQ OptoFab staff, Benjamin Johnston, Alex, Peter and others. These three groups above provided me with endless help over the 3 years of my research. I can show these three groups' facilities to all my visitors. Moreover, these people always made time for our visits and discussed the troubleshooting of certain problems that arose.

Thanks to HDRO officer Megan Brewer for proofreading my thesis; thanks for HDRO officer Jane Yang for all of the help during my 3 years PhD study.

Finally, to my wonderful friends who contributed directly or indirectly with their encouragement. They are: Zizhen Ming, Jin Li (Jim), Zhengnan Shan, Yan Wang, Xin Xu, Ping Tang, Yulong Sun, Yibin Wei, Mingzi Zhang, Mike Pai, Shiyang Tang, Dan Yuan, Shen Yan, Anindya Nag, Nasrin, Alahi, Roy, Edy, Saadi, baba, Sicong Tian, Carlos, Saleha, Luca Marchetti, Xiaoxia Yang, Shengshen Gu, Yuxiang Zhu, Haimei Xu, Yongtao Liu, Chaohao Chen, Jingjing Li, Osmond Lao,Yuan Li, Kajal, Forest Zhu, Wendy Tao, Yang Yang, Xiaoteng Jia, Guoying, Libing Fu, Jimmy, Sheran Li, Baoming Wang, Shusen Liu, Yifan Zuo, Fuyuan Zhang, Kai Zhang, Guanglou Zheng, Min Li, Chunshan Liu, Wei Xu, Wendy Tao, Shuaizhong Zhang and others.

Contents

Abstract I

List of Publications III

Related Publications and Conferences IV

Preface and Acknowledgement VI

Contents VIII

List of Figures XI

Chapter 1: Introduction 1

1.1 Research background 1

1.2 Aims and Objectives 4

1.3 Thesis Organization 5

Chapter 2：Literature reviews 9

2.1 Droplet-based microfluidic probe systems 9

2.1.1 Background 9

2.1.2 Theory of Taylor dispersion and measurement Theory 10

2.1.3 Methods 14

2.1.4 Potential applications 24

2.1.5 Conclusion of droplet-based microfluidic probe systems 25

2.2 Laplace pressure as a flow barrier 26

2.2.1 Background 26

2.2.2 Theory of Laplace pressure 28

2.2.3 Conclusion of Laplace pressure as a flow barrier 35

2.3 Droplet generation, droplets merging, and mixing in a droplet 35

2.3.1 Droplet generation 36

2.3.2 Diffusion 37

2.3.3 Droplets merging 39

2.3.4 Mixing in a droplet 43

2.4 Conclusion 44

Chapter 3: Design and microfabrication of a silicon-based microfluidic probe system 47

3.1 Background 47

3.2 Introduction to publication I 50

3.3 Author's contribution 51

3.4 Publication I 52

Chapter 4: Biomedical application of a silicon-based microfluidic probe system 58

4.1 Background 58

4.2 Introduction to publication II 59

4.3 Author's contribution 59

4.4 Publication II 59

Chapter 5: Design and fabrication of a membrane-in-pipette-tip system 73

5.1 Background 73

5.2 Theory of membrane-based microfluidic probe systems 74

5.3 Design and fabrication 74

5.3.1 Membrane-at-needle-tip design and fabrication 75

5.3.2 Membrane-on-chip design and fabrication 75

5.3.3 Membrane-in-pipette-tip system design and fabrication 77

5.4 Results 79

5.4.1 Measurement of the wet membrane Laplace pressure 79

5.4.2 Demonstration of sampling and delivery 80

5.4.3 Use of the automatic platform 81

5.4.4 Chemical resolution analysis 82

5.5 Discussion and perspective 82

5.6 Conclusion 84

Chapter 6 Conclusion and outlook 86

6.1 Conclusions 86

6.2 Future directions 88

Appendix 90

Protocol 1: Chuck design and fabrication for lab use 90

Protocol 2: Dicing of the silicon chip 91

List of Figures

Figure 1. Thesis layout. 5

Figure 2. The picture to show how to use segmented flow to avoid the Taylor dispersion. Top part shows the continous flow, where a and b are two different single phase, after transporting a distance, the signal dispersion happended at their connecting part, as part c. After a long distance, they all turned to be part c. Bottom is the picture to show how to use segmented flow to avoid the taylor dispersion. A different phase 2 was used to separate the component a and component b as phase 1. After transporting for a long distance, the signal still keep instant [21]. 10

Figure 3. Microdialysis probe for serial, loop, side-by-side and concentric design. 15

Figure 4. Aqueous phase sampling with downstream droplet formation methods. a) Robert Kennedy's group used the microdialysis probe for sampling, coupled with a droplet generation chip to transport chemicals to a CE system [51]; b) this group's research on low-flow push-pull probe system worked with a droplet system [42]; c) capillary was also used as the sampling probe, and attached is one with a 0.5mm probe and combined with droplet generator during the post-processing process [52]; d) a side hole closing channel provides droplet and merged with droplets for post-processing. 16

Figure 5. Pre-formed droplets and extracted sample from tissue methods. a) A conceptual schematic drawing of stimulation, recording, and analysis; b) schematic showing how the chemistrode works; c) time-lapse bright-field images (side view) of the droplet extracting contents at 0 ms, 30 ms, 60ms and 90 ms [43]. 19

Figure 6. Droplets formed nearby the source methods. a). One device from professor Qun Fang's group [71] that has three channels; the middle channel can impart significant pressure that sucks the liquid in; b) droplets

generated at the tip as flow. A simple demonstration of sampling at the tip for 3-bromopropan-1-ol detection{Gielen, 2014 #269}; c) sampling probe from our group with controlled barrier [41]. 21

Figure 7. Off-chip water-based droplets enrichment methods. a) Schematic of droplet creation and spotting on a MALDI plate, where the hydrophobic carrier (oil) will evaporate quickly; b). schematic of the device from DeMello group who used oleophilic oil film to extract the oil continuous phase and left the aqueous phase to the MAIDI plate [77]; c). droplet-based liquid-liquid extraction inside a porous capillary [82]; d) the developed microfluidic probe (MFP) system [83]. 23

Figure 8. The diagram to define the contact angle θ_c [106], where Υ_{SL}, Υ_{SG} and Υ_{LG} are the interfacial tension between solid/liquid, solid/gas and liquid/ gas respectively. 31

Figure 9. TAS coating mechanism for the hydrophobic treatment following with hydrophilic treatment process[114]. 32

Figure 10. Laplace pressure generated at a) different cross-section geometry in hydrophobic surfaces; b) hydrophobic-more hydrophobic interface [117]. 33

Figure 11. Laplace pressure generated at geometrical microchannel expansions from a rectangle shape to a triangle shape [119, 120]. 34

Figure 12. Laplace pressure generated from expansion to the circular shape wall [121]. 35

Figure 13. Droplet generation strategies: a) co-flow in a capillary format; b) T-Junction in a planar chip format; 3) flow focusing [26]. 36

Figure 14. Diffusion Theories. a) The processes of molecule diffusion in a solution for steps 1-3; b) molecule radial diffusion through a semi-permeable cylindrical membrane (green part) connected with the tubing(blue parts), where the flow runs through the inner wall of the membrane, and where the flow rate is Q, the inner diameter is A, the concentration inside the inner tubing is C_1, the length of the membrane is L, thickness is ó, outer concentration is constant at C_2 and detected concentration C_{out}. 38

Figure 15. A direct injection methods Example: using a Hydrophilic capillary side wall into the main channel for the consistent merging of a $CaCl_2$ droplet to a buffer droplet [69]. 40

Figure 16. Droplets merging by changing the channel geometry methods. a) droplet passing merging in a flow focusing geometry [132]; b) pillar-induced droplet passive merging in microfluidic circuits [133]. 41

Figure 17. A passive merging method using the hydrophilic feature to slow down the former droplets to merge with the latter ones [41]. 41

Figure 18. Active droplet merging methods. a) EC-induced merging of two droplets with oppositely charged surfaces; b) DEP-induced merging process: i). when the voltage applied was 500 V, the two droplets were trapped at two electrodes edges; ii) when the voltage was increased to 780 V, the droplets stretched towards each other and merged, this action occurred at the left electrode, the initial location of the larger sized droplets [137]. ... 42

Figure 19. Processes for mixing during a). flow in as straight channel (blue dash part) and b). flow in the bent channel (red dash part) [143]. 44

Figure 20. Design of the first version of the silicon-based microfluidic probe. a) Applying one silicon fabricated needle-like device for insertion into and removing samples from animal-muscle tissue [15]; b) SolidWorks 3d module drawing of our first version design; suitable for readout from microscope (30mmX17 mm); 150 µm thick pyrex glass wafer will cover the top of the 375 µm silicon to form an enclosed channel; c) the needle includes two lumens; inspired by prior cantilever sensors microdevice for diagnostics [16]; d) side view of the microfabrication tip design. 48

Figure 21. Fabrication of the first version of silicon-based microfluidic probe. a). The laser cutting machine [3D micromac microSTRUCT C] used for making inlets holes and outlets holes on 3 inches silicon wafer, and 2 µm small holes on 125µm thick Pyrex glass; b). shape of the bottom view of a 2 µm hole cut on 125µm thick Pyrex glass; c) shape of the top view of a 2 µm hole cut on 125 µm thick Pyrex glass; d) laser cutting of 1 mm hole on the silicon wafer; e) the first version of the silicon-based microfluidic probe before dicing the 2 µm hole at the tip. 49

Figure 22. Mask showing the design of the second version of the needle. 50

Figure 23. Device layout and design of the membrane-at-needle-tip system. Note the G23 steel needle grinded to a flat 45-degree face with hydrophilic membrane attached by glue. 75

Figure 24. Device layout and design of the membrane-on-chip system. Note the oil and aqueous inputs, T-junction, and the membrane port. 76

Figure 25. Device Layout and design of membrane-in-pipette-tip system. Note the pipette's diameter, the membrane's location and membrane parameters. 77

Figure 26. Demonstration of the membrane-in-pipette-tip system for droplets a) delivery to and b) extraction from outside the needle. 80

Figure 27. Auto-controlled platform for a) sampling and b) delivery droplets using the membrane-in-pipette-tip system. 81

Figure 28. Demonstrate of air/ water sampling using the membrane-in-pipette tip system. 83

Figure 29. Chuck for holding the silicon device. For the top layer, there are 8 ports that connect to the external tube with the thread ¼-28 flat bottom fittings, which are labelled on the pictures. Holes with the numbers 1,2,3, and 4 are for the inlets, while holes with the numbers 5,6,7, and 8 are for the outlets. There is a copper bottom layer, which will be connected with the top layer by four M6 screws. 90

Figure 30. Dicing processes. a) Our device before dicing; b) Attaching wafer to the substrate process by the Norland Optical Adhesive 81 ("NOA81") to attach the wafer to the substrate process; c) UV curing the NOA 81 process; d) Another attaching wafer to substrate method by wax; e) the dicing machine alignment process; f) dicing in process; g) our wafers after dicing; f) after dewaxing Process. 91

Chapter 1: Introduction

This section first introduces the research background of sampling and delivery in biomedical practices and provides an overview of conventional hypodermic needles and microneedles. Then, we introduce the problem of Taylor dispersion in the conventional probes and explain this problem is overcome by using droplets in the microfluidic probes for sampling, delivering and transporting chemicals with high chemical, spatial and temporal resolution. In the end, we list the aims and organization of the current thesis.

1.1 Research background

Sampling and delivery of tiny amounts of body fluids for accurate analysis are of great interest for therapists and biologists. To maximize the effect of drugs on diseases, for instance, therapies must be specific and responsive to signals derived from the patient's body. Similarly, to fully understand the biological information of mechanisms, biologists have to accurately monitor the chemical signals. In this thesis, we developed an approach to monitor and react to chemical signals (i.e. inflammatory cytokine concentrations near the injury site or the neurotransmitters species in the mouse brain) with high chemical, spatial and temporal resolution.

The chemistry of any biological system change with time and place. For example, changes in neurotransmitters concentration in the extracellular space around synapses are known to occur in time scales ranging from milliseconds to seconds [1, 2]. It is also well known that several neurotransmitters coexist in a given synaptic region, and that they can be released at different times [3, 4]. There are also different neurons which are associated with transmitters which we are interested in [5]. Different designs of microfabricated Si probes have been

developed by several groups for monitoring several neurochemicals, including dopamine [6], glutamate [7], lactate and glucose with LODs of sub-mM. It has been shown by Bert [8] that glutamate changes occurring in 1 min can be completely dampened when samples are pooled, as opposed to discretised. Kinematic changes in enzyme monitoring can be achieved. Microdialysis sampling coupled with droplets and direct infusion mass spectrometry can be used for acetylcholine monitoring [9] at intervals lasting a few seconds.

How can these chemical signals be measured? Dyes that respond to electrical and chemical changes such as membrane potential, and calcium indicators (for example, Fluo-4) can illustrate the behaviour of a minimal set of molecules in optically accessible systems with rapid temporal responses. There are close relationships between calcium fluxes and neurotransmitters [10]. Gene-modified living creatures that produce fluorescent proteins can, directly or indirectly, reveal the concentration of some molecules. However, they rely on slow transcription processes as opposed to more rapid release and transport mechanisms. A real-time analytical chemistry laboratory, small enough to fit inside the brain of a mouse, does not exist.

A hypodermic needle is a sharp hollow probe which can be inserted below the skin or into the body. A hypodermic needle is generally used with a syringe to inject drugs into the body or extract fluids (e.g., blood) from the body. As this needle is extraordinarily smooth and sharp, it significantly reduces contamination as well as the trauma area after puncturing [11-14]. In the 1st century AD medical treatise, *De Medicina* by Aulus Cornelius Celsus, it refers to the use of early versions of syringes. These could be used to push liquids into existing orifices. In 1656, an intravenous injection for dogs was conducted by Sir Christopher Wren [15], while the first injection in humans was firstly performed by J.D. Major of Kiel and J.S. Elsholtz of

Berlin in the 1660s [16, 17]. Currently, hypodermic needle injections are as frequent as bandages and are a way of life for many people including people with diabetes and other minor patient groups such as drug addicts.

Microfabricated microneedle devices are high-aspect-ratio microdevices, and they are suitable for transdermal delivery and sampling of active substances. Instead of injection using a metal hypodermic needle, this microneedle can be applied for painless insertion and extraction of body fluids. Moreover, a skilled professional is not required to use the microneedle devices. And it may create even less trauma in the patient because of its small size [18]. Recently developed microneedles are designed in such a way to disrupt the stratum corneum, firstly, and then to improve the permeability of skin to drugs. A consequence of this is that drugs are delivered to the epidermis, then absorbed by blood vessels and lymphatics and from there sent to the circulation system [18].

The administration of multiple drugs by infusion is mostly done by making up a saline solution of the drug mixture in a single bag, or by making multiple bags and joining them in a single line. Generally, the hypodermic needle or the microneedle has one lumen (i.e. cavity). Therefore, delivery of sequences of drugs (multi-drug delivery) requires multiple injection lines/tubes, each carrying different drugs. In addition, the measurement of various chemical signals requires that we bring the monitoring instrument directly to the sampling point (expensive and impractical). A microfluidic probe containing just two fluid channels for multi-drug delivery and sampling can satisfy the need for multi-drug delivery and sampling.

The above-mentioned tools can undertake a continuous sampling of body fluid. However, these tools cannot sample and transport rapidly changing chemical signals from the insertion point to an analytical instrument without signal distortion because of the phenomenon

known as Taylor dispersion. Similarly, the same signal distortion problem also occurs when delivering sequences of different drugs to the injection point.

However, we can achieve these aims if we can sample and digitise the liquid contents from precise locations within a living creature at precise times. In a droplet-based microfluidic system, water-based liquids are carried by an immiscible oil (continuous phase) in a hydrophobic channel. If we discretise the liquid into droplets (delivery or sampling), each droplet is isolated and does not mix with neighbouring droplets. This overcomes the signal distortion caused by Taylor dispersion in a continuous flow.

The proposed droplet-based microfluidic probe will be able to extract nanolitres of the sample to off-chip chemical analysis instrumentation or deliver nanolitre droplets of chemicals to an injection site. The signals can be stored in the droplets to transport for a long time or a long distance without distortion. These reveal that the droplet strategy is able to sample, deliver and transport various time-changing chemicals with high chemical, spatial and temporal resolution, which is essential in research and clinical diagnostics development.

1.2 Aims and Objectives

In this thesis, the overall aim is to develop a droplet-based microfluidic probe system which can 1) extract minimum volumes of body fluid, 2) generate the extracted samples as droplets, 3) transport the sampled droplets without Taylor dispersion, 4) conduct on-line or off-line analysis, 5) ensure that no oil exits out of the probe to the tissue/body.

There are three specific objectives that need to be accomplished: firstly, we aim to design and fabricate a device which can insert into the tissue, sample or deliver droplets with good chemical, spatial and temporal resolution. Moreover, the system should have the Laplace

pressure as the flow barrier at the tip. Secondly, we aim to demonstrate the devices for delivery and sampling with droplets and create the flow barrier at the tip. The devices have to be able to perform droplet generation, droplet merging, mixing in a droplet for assay reactions and further on-line or off-line analysis.

Last but not the least, the third objective is that the developed droplet-based microfluidic probe system can perform the *in vitro* biological assay reactions to provide needle-in answer-out monitoring of chemical signals. It will be combined with *in vitro* assays using smaller volumes than ever before, which shows the system has the ability to be the next generation of the conventional needle.

1.3 Thesis Organization

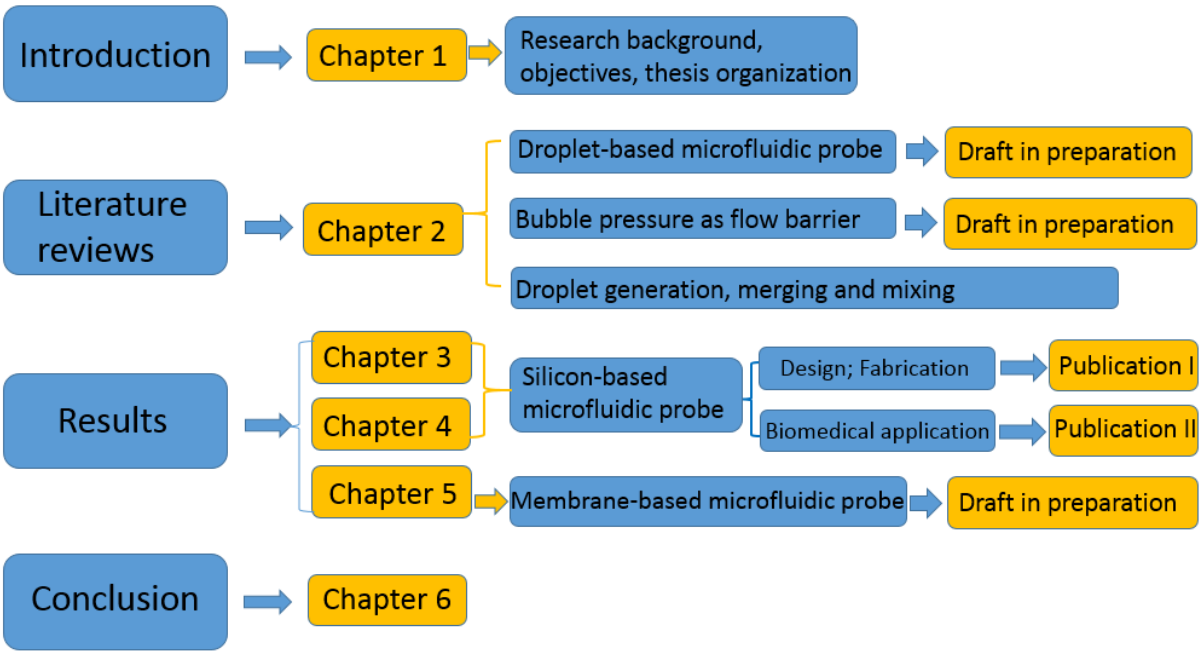

Figure 1. Thesis layout.

Figure 1 illustrates how this thesis is structured. Chapter 1 introduces the research background, objectives as well as the thesis outline. This section first introduces the research background of sampling and delivery in biomedical practices and provides an overview of

conventional hypodermic needles and microneedles. And then it points out the problem of Taylor dispersion in the conventional probes and its corresponding strategy that droplets can be applied in the probes to solve the signal distortion problem. Moreover, here it points out that the droplet-based microfluidic probe has the ability to sample and deliver chemicals with high chemical, spatial and temporal resolution. In the end, we list the objectives and organization of the current thesis.

Chapter 2 reviews droplet-based sampling probe systems and the use of Laplace pressure as a flow barrier, and also describes the theories involved in the thesis. Firstly, it described in detail how the droplets are applied with the microfluidic probe for the sampling and transportation of chemicals with chemical, spatial and temporal resolution to avoid the problem of Taylor dispersion. The strategy of 'droplets formed nearby the source with a flow barrier' is the focus of our microfluidic probe. Secondly, we illustrate in detail that Laplace pressure, serving as a flow barrier in our developed droplet-based microfluidic probe, could achieve safe chemical sampling and delivery. Only water-based droplets will pass through the tip while oil or gas will remain in the channel. Whenever delivering and sampling using the novel sampling probes presented in this thesis, the probes can prevent air/oil escaping into the body's circulation system or tissue, causing contamination, and therefore variations in pressure do not cause complications, e.g. blood pressure variation, body position, heart rate or other factors, which is another draft in preparation. Last but not the least, the basic theories of droplets merging, mixing in a droplet, and diffusion are also discussed, which build up important knowledge concerning the sampling probes' applications in the following chapters.

Chapters 3 and 4 focus on the results of our experiments with the silicon-based microfluidic probe systems that we developed. Firstly, Chapter 3 is based on Paper I, which discusses the design and microfabrication of the silicon-based probe systems, and the demonstration of the improved device for sampling and delivery with the droplet. The relationship between the recorded sample signals and the external dye concentration (10 to 40 µg/mL) indicates that this device is capable of quantitative, real-time measurements of rapidly varying chemical signals with a temporal resolution of around 3 seconds.

Chapter 4 is based on Paper II. Here the focus is on the application of the improved silicon-based microfluidic probe on H_2O_2 chemical sampling and further on-line detection using a commercial, single-step fluorescent H_2O_2 assay. The sampled H_2O_2 chemicals was immediately merged with the buffer droplet on board and carried away to mix and react, producing a sequence of droplets representing the H_2O_2 concentration as a function of time. After calibrating the device, we can calculate the concentration of H_2O_2 in the sampled liquid from the size and fluorescence intensity of each merged droplet, which reveals the device's potential for kinematic monitoring. It is expected that these systems, with the enclosed channels and minimal handling, could play an essential role in helping diagnostics technology to become reliable. Thousands of reactions can be recorded in a single run, which can expand the use of our developed probe for assay qualification.

Chapter 5 describes an alternative membrane-based probe system that we were trying to make using a hydrophilic membrane, namely membrane-in-pipette tip systems. We describe its design and microfabrication as well as a demonstration for sampling and delivery.

This is followed by Chapter 6, which provides an overall conclusion of the work done corresponding the objectives listed in section 1.2, along with the comparison between our

two developed systems and a view on the future of the sampling probes we have developed. I take the opportunity there to speculate on how our sampling probe might be used while speculating on opportunities for future development.

Chapter 2： Literature reviews

This chapter focuses on the reviews of the droplet-based microfluidic probe as well as Laplace pressure as a flow barrier. It also described the theories of droplet generation, droplets merging and mixing in a droplet, which build up important knowledge concerning the sampling probes' applications in the following chapters.

2.1 Droplet-based microfluidic probe systems

The temporal resolution of chemical signals that are sampled with the continuous flow is low because of Taylor dispersion. Droplets have been used to solve this problem by digitizing chemicals signals into discrete segments that can be transported for a long distance or a long time without loss of temporal or chemical precision. Different sampling probes have been used to sample fluid from a continuous medium, such as a cell culture or nerve tissue, and generate droplets for transport for external analysis. In this review, we describe key examples of this process and categorize them as follows: (1) aqueous phase sampling with downstream droplet formation, (2) pre-formed droplets which extract a sample from tissue, and (3) droplets formed nearby the tissue. Furthermore, we also list strategies for downstream analysis. Finally, we outlook the potential applications of droplets in sampling and delivering quick-changing signals.

2.1.1 Background

In 1953, Taylor dispersion was described as "the combined action of molecular diffusion and the variation of velocity over the cross section" [19]. Because of the dispersive phenomena, the distance that chemical signals (i.e. variation in concentration with time and

space) can be transported in the continuous phase is severely limited [19, 20], which cannot be avoided as this is the result of flow. The top part of Figure 2 shows pulses of imaginary chemical A and chemical B. Initially the pulses are separated from one another, but after a short distance the chemical pulses have merged and spread out [21]. In contrast, the bottom part of Figure 2 [21] shows that pulses of chemical A and B, when contained in droplets are not dispersed or merged after transport. This droplet-based approach prevents dispersion of signals during transport.

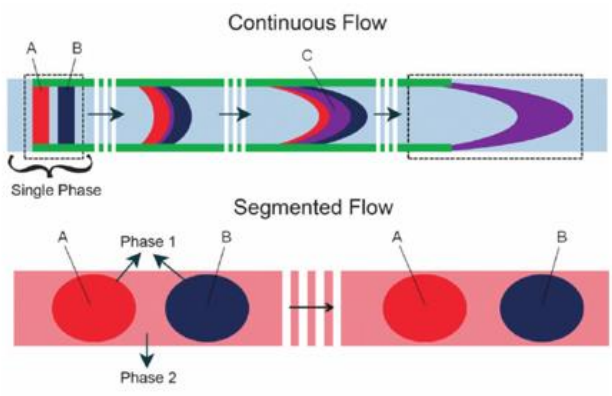

Figure 2. The picture to show how to use segmented flow to avoid the Taylor dispersion. Top part shows the continuous flow, where a and b are two different single phase, after transporting a distance, the signal dispersion happended at their connecting part, as part c. After a long distance, they all turned to be part c. Bottom is the picture to show how to use segmented flow to avoid the taylor dispersion. A different phase 2 was used to separate the component a and component b as phase 1. After transporting for a long distance, the signal still keep instant [21].

2.1.2 Theory of Taylor dispersion and measurement Theory

2.1.2.1 Theory of Taylor dispersion

Taylor dispersion acts to accelerate diffusion, which can reduce the resolution, precision and sensitivity of microfluidic devices for biosensors [22-24], DNA analysis [25-27], mass

spectrometry [28-30], surface patterning [31-34], and other applications. It results from the interaction of convection and diffusion within a pipe or channel.

Convection is the transport of fluid axially in the flow direction. The typical Poiseuille laminar flow in a low Reynolds number channel achieves its maximum flow velocity in the centre of the channel and decreases parabolically to zero at the walls. Volumes of fluid near the centre of the channel will move much faster than those near the walls. A group of molecules, initially near one-another is thus spread out. Diffusion, which makes the problem worse, is driven by a gradient in the chemical concentration of the diffusing species [35]. For example, when considering a group of molecules forming a pulse of a chemical, the sharper the gradient constituting that pulse, the more rapidly it disappears.

When liquid is transporting in a circular microchannels, Taylor–Aris dispersion controls the effective axial diffusivity, leading to an effective diffusivity written as [36]:

$$D_{eff} = D(1 + \frac{1}{48} {Pe_d}^2)$$

Where $Pe_d = d\bar{V}/D$ and d is the channel diameter, and $\bar{V}$ is the average value of the velocity in the Poiseuille flow. The Peclet number is ratio of convective fluxes to diffusive fluxes in the system. This equation clearly shows that diffusion along the axis of flow is greatly enhanced by high convection.

2.1.2.2 Measurement Theory

An *in vivo* measurement system should be concerned with three parameters: chemical sensitivity, spatial resolution, and temporal sensitivity. Chemical sensitivity refers to a variety of measurement parameters. These include the minimum and maximum concentrations that

can be detected, the smallest difference between two samples that can be resolved, and the specificity or selectivity of the measurement.

Spatial resolution is a well-understood concept in imaging, where the term voxel refers to a 3D volume, over which the information is averaged. The same principle applies to chemical sampling. The higher spatial resolution gives more localized information. We would also expect a high spatial resolution to enable the detection of more rapid chemical changes from smaller sources. Naturally, the cross-section of the probe where contact occurs with the tissue and flow rate is a primary determinant of spatial resolution. However, the volume of the extracted sample will also influence the spatial resolution. Drawing a large volume with a fine probe will average a larger chemical voxel, rather than drawing a small volume with the same size probe [37-40].

Temporal sensitivity refers to the time taken for the measured value to change in response to a step-change in the sample. This change may be fit to a single exponential, which allows for an easily defined time constant [41]. Temporal resolution may also be defined as $t_{res}=\Phi/f$, where f is the plug frequency (Hz), and Ø is the number of plugs required to observe a change (from 10 to 90% of a concentration step) [42]; in another example [43], Ø was defined as the number of plugs (or samples) needed to exchange 95% of molecules of interest. The response time of a complete system may also be limited by reaction kinetics at a sensor surface, but in this thesis, we are interested in the fundamental response time of the sampling process. This time is delay is created by movement of molecules from the signal source to the location of droplet break-up. For a probe that extracts volume from the source, this time is approximately equal to the volume of liquid between source and droplet, divided by the volume flow rate.

The temporal sensitivity can be reduced by extracting more fluid from the tissue, but this may damage or significantly interfere with the tissue.

For a probe that relies on diffusion across a membrane, the speed of molecular transport is proportional to the chemical gradient and permeability of the membrane [44].

A device could sample a small percentage of the chemical signal at a rapid rate, where the droplet has a small residence time with the membrane. However, capturing a high percentage of the source signal in a droplet requires the concentrations on either side of the membrane to approach equilibrium. Diffusion-based transport requires a longer residence time to approach equilibrium.

In a droplet system, we should consider the sampling rate and its relationship to the rate change of the thing being measured. Electrical engineers have addressed this problem through frequency analysis and arrived at a sampling theorem which states that the sampling rate (samples per second) should be twice as fast as the fastest changing component of the signal.

In this section, we survey examples where droplets have been applied to the delivery and sampling of chemical signals. We consider the spatial, temporal and chemical resolution of each. The work is divided into three categories: aqueous phase sampling with downstream droplet formation; preformed droplets which extract a sample from a source; and droplets formed nearby the source. We include a summary of detection methods, both on-chip and off-chip, and describe the expected development regarding these devices' and principles' potential applications.

2.1.3 Methods

We provide three case studies of using a droplet-based microfluidic sampling technique: (1) aqueous phase sampling with downstream droplet formation, (2) preformed droplets and extracting sample from tissue, and (3) droplets formed nearby the tissue.

2.1.3.1 Aqueous phase sampling with downstream droplet formation

This category is characterized by an aqueous phase sampling probe that draws liquid from within the tissue to a microfluidic device outside the tissue, which are diffusion through membrane (dialysis probe) and direct fluid extraction (push-pull cannula, push-pull microfabricated sampling probe, hydrophilic caplillary tube). The sampled fluid is then segmented at the external microfluidic devices.

2.1.3.1.1 Diffusion through membrane

Microdialysis is widely utilized as the sampling probe for in vivo monitoring [45], clinical studies [46-48] and pharmacokinetics [49]. However, the drawback of this probe is that it has a large sampling surface. The membrane is typically over 2 mm long and more than 200 µm in terms of its outer diameter. This limits the spatial resolution.

A modern trend is to apply microdialysis in various clinical situations, such as monitoring concentrations of glucose, lactate, glutamate, and urea [50]. The microdialysis probe makes it possible for sampling to be done frequently without any blood or tissue removals from the body. In the year 2000, microdialysis was used as a tool for *in vivo* pharmacokinetics monitoring [49].

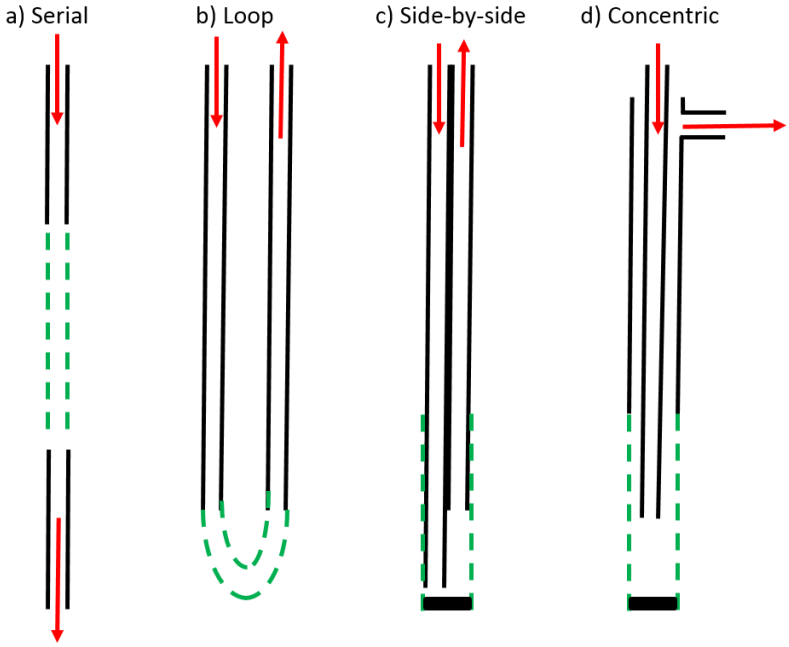

Figure 3. Microdialysis probe for serial, loop, side-by-side and concentric design.

Microdialysis probes can be designed as shown in Figure 3. Figure 3 a) illustrates a dialysis membrane (green dashed line) connected to an inlet and outlet. These are positioned in a serial arrangement, while the middle membrane part will work as the extraction region. Figure 3 b) – d) show a dialysis membrane connected with an inlet and outlet, which are positioned in a parallel arrangement. Here the bending tip part works as the sampling region. They can be categorised as a loop, side-by-side and concentric probe, respectively.

A concentration gradient causes the diffusion of substances, for instance molecules. Molecules existing at a higher concentration outside the dialysis membrane can diffuse into the dialysis membrane and vice versa. Continuously, the dialysis sampling probe can pull the dialysate, the part of a mixture which passes through the membrane in dialysis, from the sampling site. Further analysis of this is described in detail in the below section.

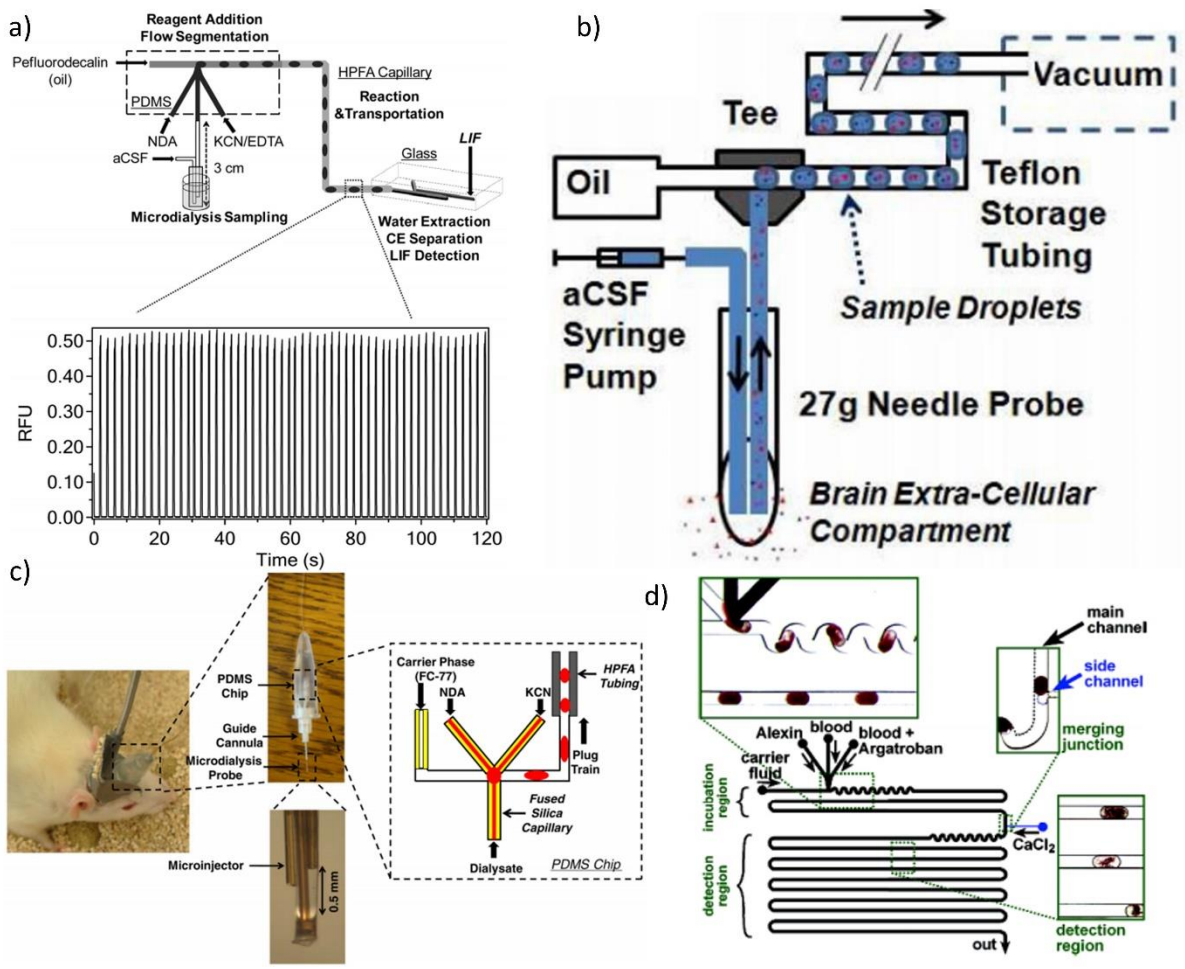

Figure 4. Aqueous phase sampling with downstream droplet formation methods. a) Robert Kennedy's group used the microdialysis probe for sampling, coupled with a droplet generation chip to transport chemicals to a CE system [51]; b) this group's research on low-flow push-pull probe system worked with a droplet system [42]; c) capillary was also used as the sampling probe, and attached is one with a 0.5mm probe and combined with droplet generator during the post-processing process [52]; d) a side hole closing channel provides droplet and merged with droplets for post-processing.

The microdialysis technique began in the early 1970s with Bito's group [53] and Delgado's group [54] in the USA. Since the mid-1970s, Urban Ungerstedt and his colleagues from the Karolinska Institute in Stockholm, Sweden [55, 56] have used a flexible microdialysis concentric catheter covered by a 10-30 mm dialysis membrane. The inlet tube is connected to a small portable pump while the outlet tube is connected to a microvial holder, which is

changed every 15-60 minutes. The collected sample can be brought to the laboratory for analysis of various analytes [56], including neurotransmitters [57].

Robert Kennedy's group used the microdialysis probe, shown in Figure 4 a), coupled to a droplet generation chip to transport chemical signals to a distant capillary electrophoresis system [51, 58]. The device has been used for the neurotransmitters sampling [59]. It has also been applied to a moving animal [60].

2.1.3.1.2 Direct fluid extraction

In 1961, Gaddum developed the push-pull cannula (PPC) perfusion [61] which was used for determining transmitter release in several tissues [62]. The structure of the PPC is shown as in Figure 2. Firstly, a solution is pushed in through the push cannula, which is located inside and protrudes to the pull cannula to some extent [63]. Secondly, the transmitters are released locally depending upon the perfusing fluid. Finally, the solution will be pulled out from the second outer needle, which has a bigger diameter and is located outside of the inner needle.

Microfabrication is a process that makes it feasible to achieve complicated structures as well as small enough features for the sampling probe. Kennedy's group has developed a series of deep reactive-ion etching (DRIE) procedures to fabricate pull−push sampling probes on silicon chips in batch [64] for *in vivo* monitoring of neurotransmitters.

Push-pull sampling probe has been assembled by hand from capillary tubes and been used for the brain since 1961 [62, 65]. In this method, the sample is continuously infused into the tissue through one inner tube. The sample will be withdrawn from a second tube that is placed parallel to the infusion tube.

A temporal resolution of 5 minutes can be achieved with low flow push-pull perfusion combined with off-line fraction collection and analysis by CE [40]. Lower temporal resolution of 16 s [66] and 45 s [67, 68] can be achieved by coupling low-flow push-pull perfusion on-line with CE for detection samples from the eye and brain respectively. Low-flow push-pull perfusion can be coupled with the segmented flow to achieve 7 s temporal resolution and spatial resolution of 0.016 mm^2 *in vivo* [42], the devices are shown in Figure 4 b). By further miniaturizing the probe inlet, they further show *in vitro* the potential for sampling at 200 ms resolution at 30 nL/mL *in vitro* with appropriate fluidics [42]. The droplet-based approach can be employed for moving animal detection. Figure 4 c) shows the 0.5mm diameter probe and is combined with the droplet generator in the post-processing process [52].

Song et al. used the hydrophilic capillary tube to sample the changing concentration solution of $CaCl_2$ (0.2–0.4 µL/ min) sample as droplets and merged them with assay droplets for post-processing. This is shown in Figure 4 d). The cross-section is 100 µm X 100 µm, but the length is unclear [69].

The M. Odijk group [70] presented a miniaturized hybrid push-pull perfusion probe for sampling with high spatial and temporal resolution. The development of this tool will ultimately enable the monitoring of neurotransmitters with unprecedented temporal (~1 s) and spatial (<100 µm) precision.

2.1.3.2 Preformed droplets and extracting sample from the tissue

This section summarizes the droplet-droplet extraction methods. The sampling probe length is almost 0. In this way, the Taylor dispersion problem was solved. However, it should be noted that a contamination problem will exist.

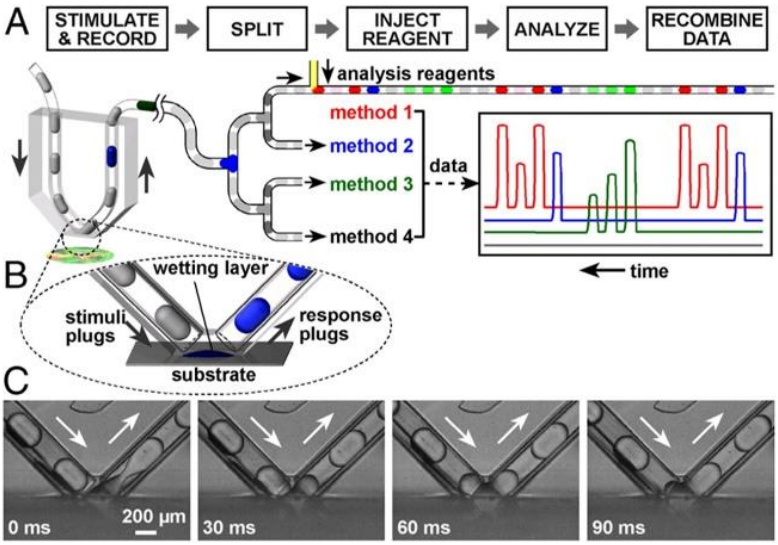

Figure 5. Pre-formed droplets and extracted sample from tissue methods. a) A conceptual schematic drawing of stimulation, recording, and analysis; b) schematic showing how the chemistrode works; c) time-lapse bright-field images (side view) of the droplet extracting contents at 0 ms, 30 ms, 60ms and 90 ms [43].

Chen et al. [43] provided an excellent example of the capability of the droplet to extract biochemical contents from a confluent cell layer and transport them downstream for various analyses. This is a method, shown in Figure 5, for sampling and/or introducing a matter to an environment that introduces firstly,an array of plugs through a first microchannel of a device into an exchange region of the device. It is here that mass transport between the environment and the plug fluid of at least one plug in the first array of plugs occurs, and the second array of plugs is subsequently formed. The exchange region is in fluid communication with the first microchannel. The method further comprises directing the second array of plugs into a

second microchannel downstream and in fluid communication with the exchange region. The contents we are focusing on for the sampling are the varying signals. These chemical signals were sampled with only minimal dispersion.

2.1.3.3 Droplets formed nearby the source

Droplets formed nearby the source is the segmentation method that was done using a microfluidic device which can be mounted near tissue. It has a minimal dead volume without a barrier We can also further categorize the examples by considering whether a membrane or other barrier exists between the microfluidic channel and the tissue to be sampled. Microfabricated probes are much smaller than other sampling probes and create smaller dead volume, which generates better spatial resolution [64].

2.1.3.3.1 Droplets formed at the source without a barrier

This method gives minimal dead volume nearly as 0 that helps to create a nanolitre volume fraction collector. Professor Qun Fang [71] developed one device that has three channels; the middle channel can have imparted significant pressure that sucks the liquid in, which is shown as Figure 6 a). It is a fully unsupervised compartment-on-demand for precise nanoliter assays of time-dependent steady-state enzyme kinetics and inhibition [72]. Figure 6 b) illustrates the sampling probe made of the pipette using the principle as the co-flow. A pipette tip can also be used in the experiments, where samples can be formed at the end. It is a simple demonstration of sampling at the tip for 3-bromopropan-1-ol detection [73].

MillDrop is a commercial product that direct sampling the chemicals and form as droplet format and does have a detection capacity. It can achieve up to 10 replicates, up to 94 different conditions, low sample volume required and reduced handling time.

2.1.3.3.2 Droplets formed at the source with a barrier

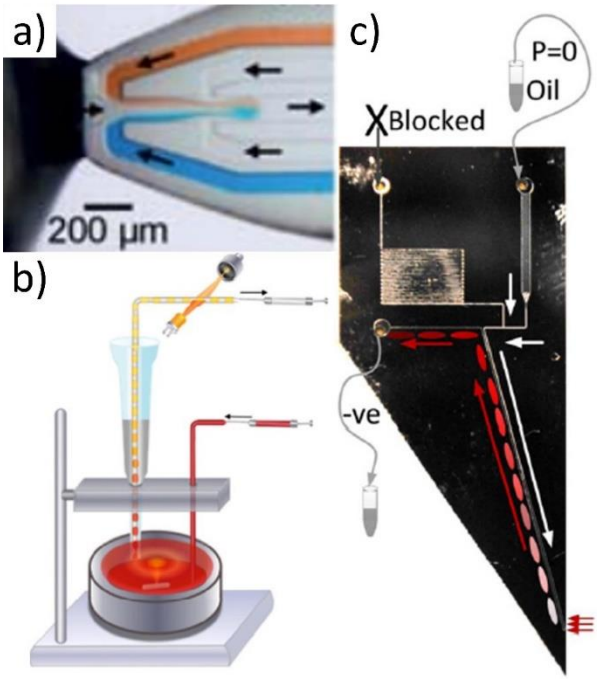

Figure 6. Droplets formed nearby the source methods. a). One device from professor Qun Fang's group [71] that has three channels; the middle channel can impart significant pressure that sucks the liquid in; b) droplets generated at the tip as flow. A simple demonstration of sampling at the tip for 3-bromopropan-1-ol detection [73]; c) sampling probe from our group with controlled barrier [41].

Our group has fabricated a silicon chip (Figure 6 c)) with only 2.8 pL microfluidic probe dead volume (only 7 of 100 µm X 2 µm X 2 µm), which was measured at around 3s temporal resolution. The hydrophilic structures at the tip generate the surface tension, where only the aqueous phase can be delivered or sampled through the tip [41], which will be described in Chapter 3 and Chapter 4. A hydrophilic membrane integrated with the commercial pipette tip system has also been achieved, it is low cost but works the same way. The sample can be sampled as droplets and transported as droplets with chemical resolution. It also has the Laplace pressure flow barrier that enables safe sampling, which will be described in Chapter 5.

2.1.3.4 Strategies for off-line droplet analysis

Conventional droplet-based detection methods were described in Qun Fang's review [74]. There are also other less common methods, for example using X-ray diffraction [75]. Moreover, the generated aqueous droplets can be enriched, delivered and further detected off-chip. Strategies are listed below that serve to remove the oil and enrich the droplets, and then the aqueous droplets can undertake the further detections, such as detection directly on MALDI mass spectrometer.

In Figure 7 a), the aqueous droplets can be placed one by one on the matrix-assisted laser desorption ionization (MALDI) plate together with part of the volatile perfluorinated oil. Evaporation of both phases happens before the plate is loaded into the MALDI mass spectrometer. The evaporation time can be completed within less than 60 s or less than 5 s when a flow of nitrogen gas is used to accelerate the process [76].

Figure 7 b) shows that the DeMello group [77] used oleophilic oil film to extract the oil continuous phase. Droplets generated in the interface device are transported to the MALDI target via the 200 µm inner diameter Teflon tubing. One oleophilic membrane was applied to remove the oil continuous phase, and the aqueous phase can be left suspended and placed one drop at a time on the hydrophilic part at the tip of the tubing on the MALDI plate. The droplet can be formed in liquid-gas microfluidic systems [78]. The main advantages here is that it creates the uniform water droplets purely in the air without oil or other second liquid carriers. Therefore, the final water droplets can be easily got without extra evaporating or oleophilic oil film steps to remove the carrier oil [79]. Here we focus on the final incubation stage where the oil can be extracted and aqueous droplets can be left as a single layer for further detection [80, 81]. Figure 7 c) depicts another possible method using the hydrophobic

and hydrophilic difference to extract the continuous oil continuous phase to obtain the aqueous phase by a porous capillary membrane. It is a simple and inexpensive device design. Similarly, as Figure 4 a) illustrates, a glass device containing an 'extraction bridge' was demonstrated to remove aqueous droplets from the oil channel for capillary electrophoresis [51].

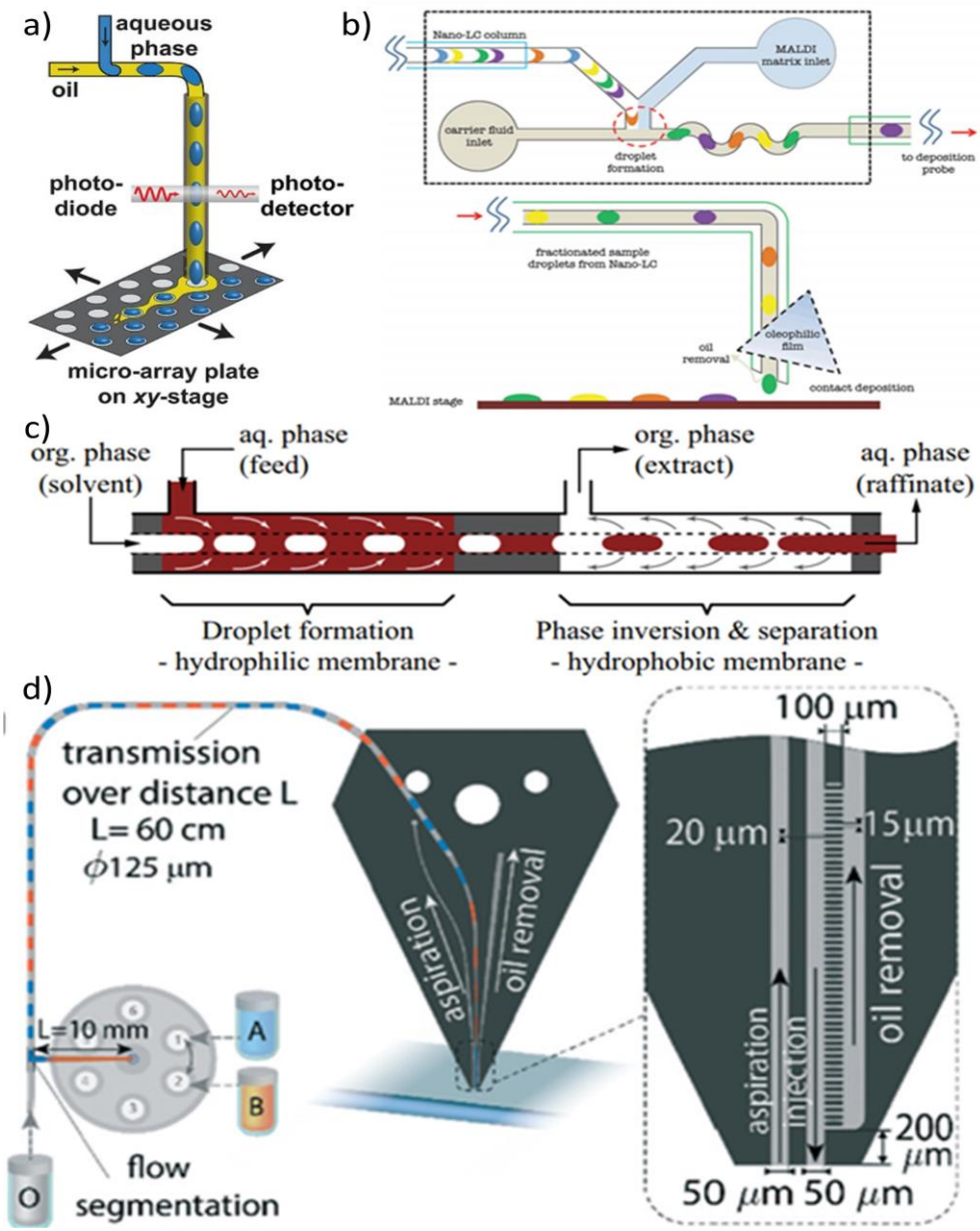

Figure 7. Off-chip water-based droplets enrichment methods. a) Schematic of droplet creation and spotting on a MALDI plate, where the hydrophobic carrier (oil) will evaporate quickly; b). schematic of the device from DeMello group who used oleophilic oil film to extract

the oil continuous phase and left the aqueous phase to the MAIDI plate [77]; c). droplet-based liquid-liquid extraction inside a porous capillary [82]; d) the developed microfluidic probe (MFP) system [83].

Figure 7 d) shows that Kaigala's group at IBM had developed a MFP system for writing chemical patterns [20, 84]. Negative pressure was provided at the probe's tip to remove the oil while the small hydrophilic features function to retain aqueous phase at the tip due to the surface tension. This device uses segmented flows to allow different chemicals to be delivered through the same orifice. Pressure balance has to be perfect otherwise oil leaks out.

2.1.4 Potential applications

Temporal resolution for conventional High-performance liquid chromatography (HPLC) will take minutes to achieve [85]. It will be difficult to distinguish between loss in temporal resolution due to dispersion and loss in accuracy due to sample degradation due to oxidation and/or enzyme activity. If the sensitivity of the analytical method and temporal resolution of the biosensor itself are sufficient, droplets with small sampling volumes (the size of each droplet) can be used to avoid the dispersion and detect in a controlled time and concentration to avoid the degradation problem [86-91].

The stored droplets can be trapped or accumulated in channels, capillaries or tubing. The droplets can be controlled by external electric or magnetic force or external pressure. Moreover, robotic stages and autosamplers can be coupled with the droplet generation step [52]. *In vivo* sampling methods can be achieved by sampling, transporting and storing signals for further detection. Note that it is crucial for real-time monitoring of neurotransmitters in the brain extracellular compartment so that the neuronal function and psychological disorders can be studied [1, 49, 92]. It is also vital to measure signalling chemicals in the

extracellular space for chemical communication [93, 94]. Developed smart assays have made it possible to monitor different neurotransmitters [98-103] simultaneously. Kinematic changes in enzyme monitoring can be achieved. Microdialysis sampling coupled with droplets and direct infusion mass spectrometry can be used for acetylcholine monitoring [9] at intervals lasting a few seconds.

Referring to the assay characteristics, the assay reactions could be slow reactions as well as immediate reactions. The droplet-based system can extract sub-nanoliter samples from the surrounding fluid and merge the sampled liquid with the detecting biosensor directly. These merged droplets can be stored and detected directly in the channel, enabling detection of fluorescent samples of nanoliter volumes taken at 1-second intervals. Using conventional methods such as a spectrophotometer, it is not practical to characterize samples at such a rapid rate, where we are talking about the temporal resolution. For the slow reaction assay, for example, the H_2O_2 detection assay which needs 15 minutes, we can detect fluorescence of the merged samples sharply at 15 minutes without any handling time. Also, it is possible to execute more rapid detection with this chip using a sensor which has a shorter reaction time. If the temporal resolution can reach lower than 1 second, we can, in fact, detect the reaction signal which is lower than 1 second.

2.1.5 Conclusion of droplet-based microfluidic probe systems

There have been many reviews of the droplet-based microfluidics devices, on-line detection methods. In this thesis, we highlight the significance of Taylor dispersion and show how droplet-based systems can help. We then survey examples where droplets had been applied to the delivery and/or sampling of chemical signals and pay particular attention to the

temporal, spatial and chemical resolution of each system. Continuously, we gave a former art on the methods that sampling and transporting by droplets with temporal, spatial and chemical resolution. They are: aqueous phase sampling with downstream droplet formation, preformed droplets and extracting a sample from tissue, and droplets formed nearby the tissue. Investigations of off-chip detection methods for contents in droplets were done. We also give an expected development trend on the potential applications of these devices.

2.2 Laplace pressure as a flow barrier

The oil or air phase has to be prevented from injecting into the tissue when the droplet-based microfluidic device is used as a needle. The non-aqueous phase does, however, have to be present at the injection site to partition the sampled liquid. This thesis focuses on developing new droplet-based microfluidic needles and probes with a flow barrier at the tip for safe chemicals delivery and sampling, which can be achieved by hydrophobic-hydrophilic interfacial Laplace pressure at the microfluidic probe tip. In this section, we introduce the Laplace pressure and its three governing parameters, i.e., surface tension, contact angle and hydraulic diameter.

2.2.1 Background

If the needle is inserted into a living creature, the pressure will vary with the heart rate, blood pressure, position of the body, and other factors, which are difficult to control. These variations in pressure require a high breakthrough pressure so that oil or air will not inadvertently escape. At that time, this high breakthrough pressure works as a flow barrier; this breakthrough pressure will be the Laplace pressure, which is defined as the pressure

difference between the inside and the outside of a spherical or curved fluid interface (such as bubbles or droplets). This Laplace pressure can be achieved at this hydrophobic-hydrophilic interface when it gets wet.

Flow control of droplets within microchannels is vital for microfluidic systems [95-99]. Interest has grown in Laplace pressure and its application to microfluidic devices as a driving force or flow barrier that enhances the flow control of microdevices. To control fluid behaviour within a microchannel for reliable microfluidic processing, a more effective and simpler flow-flow barrier designs are required [100]. Samples must be firstly delivered or sampled from the system and accurately located to a specific structure, for instance, a reaction chamber. Both processes can be achieved by using a Laplace pressure flow barrier.

Different channel features such as passive gating parts have applied Laplace pressure forces to stop aqueous droplets in microchannels without an external force [101-104]. The MFP was an example [83], and Kaigala's group applied it for writing chemical patterns [20, 84]. It is widely used to draw the chemical pattern on the surface, where they applied negative pressure to withdraw the oil phase and leave the aqueous phase at the tip by surface tension. Our group has successfully applied both the silicon 2 µm hydrophilic [41] features and hydrophilic membrane [105] in the chip to achieve safe Laplace pressure flow barrier. A flow barrier can serve to prevent the water going through while only the continuous gas or oil phase goes through, which can provide a safe delivery/ sampling environment.

The generated Laplace pressure can achieve controlled barrier for delivery/sampling, which all of our microfluidic probes are focusing on. Referring to droplet delivery, we can ensure no continuous oil-phase release from the device into the body (no contamination from oil/air, and it is safe); as for sampling, we shall guarantee that no blood will run back even

though the pressure outside the channel can be variable (for example, body movement or pressure difference). After reviewing the applications of the Laplace pressure, we will talk about the theory of Laplace pressure and its three relative parameters, i.e., surface tension, contact angle and hydraulic diameter.

2.2.2 Theory of Laplace pressure

Laplace pressure (ΔP) and the surface tension $\boldsymbol{\tau}$ relationship is described below in the following equation [106]:

Equation 1

$$\Delta \mathbf{p} = \boldsymbol{P_{inside}} - \boldsymbol{P_{outside}} = \boldsymbol{\tau}\left(\frac{\mathbf{1}}{\boldsymbol{R_1}} + \frac{\mathbf{1}}{\boldsymbol{R_2}}\right)$$

Where R_1 and R_2 are the principal radii of curvature and τ is the surface tension of the liquid/ air.

For the bubbles or droplets, R_1 and R_2 are actually the same. Therefore the Laplace pressure can be defined as [106]:

Equation 2

$$\Delta \mathbf{P} = \frac{\mathbf{2}\tau}{\mathbf{R}}$$

Where R is the principal radii of curvature formed by the fluid in contact. For an interface that is bounded by a solid surface, such as a microchannel or membrane pore, the Laplace pressure will relate to the contact angle as [106]:

Equation 3

$$\Delta \mathbf{P} = \frac{\mathbf{2}\tau}{\mathbf{R'cos\theta}}$$

Where $R'$is the hydraulic diameter of the structure containing the interface, and θ is the contact angle for the two fluids at the solid surface.

The principle of operation is based on the generated Laplace pressure flow barrier at the interface when either surface tension, contact angle, or hydraulic diameter of microchannels change gradually or abruptly in expansion regions or a neck based on Equation 3.

2.2.2.1 Surface tension （$\boldsymbol{\tau}$）

Surface tension is the first parameter that can affect the Laplace pressure. It is defined in a pragmatic way: if a line is drawn on the surface of an interface, then one can determine the equilibrium state by assuming that the molecules on one side of the line exert a force $\boldsymbol{\tau}$ per unit length of the line on the molecules on the other side. The $\boldsymbol{\tau}$ will be the surface tension, while the force is perpendicular to the line and tangent to the surface [106].

Surface energy E_A depends on the extension of the surface.

Equation 4

$$\mathbf{E}_{\boldsymbol{A}} = \boldsymbol{\sigma} \times \mathrm{d}\mathbf{A}$$

Where A is the total surface area, and σ is the energy per unit surface area. If a liquid droplet is free to change its shape, it will become sphere-shaped with less energy.

The surface tension can generate the work:

Equation 5

$$\boldsymbol{\tau} \times \mathbf{l} \times \mathbf{ds} = \boldsymbol{\tau} \times \mathbf{dA}$$

Where $\boldsymbol{\tau}$is the surface tension, A is the total surface area, with the distance s moving along the surface tension direction, with L the length being perpendicular to the surface tension direction.

From the principle of work ($\boldsymbol{\tau} \times dA$) and energy ($\sigma \times dA$), this work done must be equal to the increase in energy (surface energy), so that surface tension and surface energy are equivalent.

There are several issues that can affect the surface tension, and these are listed below.

The surface tension of water/mineral oil can be related to the temperature according to [107], as:

Equation 6

$$\boldsymbol{\tau}\left[\frac{\mathbf{mN}}{\mathbf{m}}\right] = \mathbf{51.83 - 0.103T}$$

Where *T* is the temperature in Celsius. If the room temperature *T* is 22 °C, surface tension is calculated at around 49.56 mN/m. The surface tension of one liquid may be altered locally through the addition of surfactants [108] or by applying the sunlight, even lasers [109] or magnetic fields [110].

2.2.2.2 Contact angle (*Θ*)

Contact angle is the second parameter that affects the Laplace pressure. In this section, we will define the contact angle and outlines how surface treatments can change the contact angle.

In 1805, Thomas Young defined the contact angle θ_c, as the angle formed by a liquid at the three-phase boundary where the liquid, gas, and solid intersect, as shown in Figure 8.

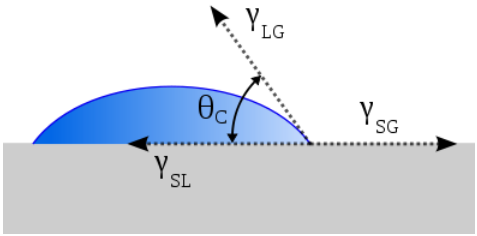

Figure 8. The diagram to define the contact angle θ_c [106], where γ_{SL}, γ_{SG} and γ_{LG} are the interfacial tension between solid/liquid, solid/gas and liquid/ gas respectively.

Summing the forces in the horizontal direction creates a relationship for the interfacial tension, which can be written as follows:

Equation 7

$$\gamma_{SG} = \gamma_{SL} + \gamma_{LG}\cos\theta$$

Where γ_{SL}, γ_{SG} and γ_{LG} are the interfacial tension between solid/liquid, solid/gas and liquid/ gas respectively.

Therefore, the contact angle represents a way to show liquid-solid adhesion. If the droplet is water, since γ_{SG} and γ_{LG} are constant, it is known from Figure 8 and Equation 7 that when γ_{SL} increases, the contact angle θ increases, standing for hydrophobic characteristics. Conversely, if the contact angle θ decreases, the surface is more hydrophilic. A surface with a contact angle of a droplet over 90° is hydrophobic, but less than 90° means it is hydrophilic.

Surface treatments directly affect the surface angle. Hydrophobic surface treatment can increase the contact angle while hydrophilic surface treatment can decrease the contact angle. Due to the wide usage of glass and silicon in industrial and academic research, surface treatment of these materials is of great importance.

The application of plasma is known to increase the surface energy, adhesion energy wettability or hydrophilic property. Plasma treatment as the most common method of surface modification enhances surface hydrophilicity (wettability) by increasing adhesion and surface

energies [111]. In fact, typical surface chemistry of silica will consist of Si-O-Si and Si-OH groups [112] in a ratio that is influenced by thermal treatment [113]. The effect of organic contamination from air, which adsorbs to the high-energy (when clean) silica surface. The role of oxygen plasma reaction plasma is to remove these layers to reveal the underlying hydrophilic surface, which has the dominant effect on the contact angle. Another similar method to remove these layers is to use piranha clean or KOH solution to clean the surfaces, which can convert the hydrophobic surface to hydrophilic or subsequently intensifies the adhesion capabilities.

Chemical treatments may also be used to make a surface hydrophobic. Tri Alkoxy Silane (TAS), OctadecylTrichlorosilane (OTS) and Sigmacote® (Sigma-Aldrich) are three such examples, which can react with the -OH group on the glass. Figure 9 presents the TAS hydrophobic coating process. This will make the Si-O long chain structure create a glass surface that is hydrophobic.

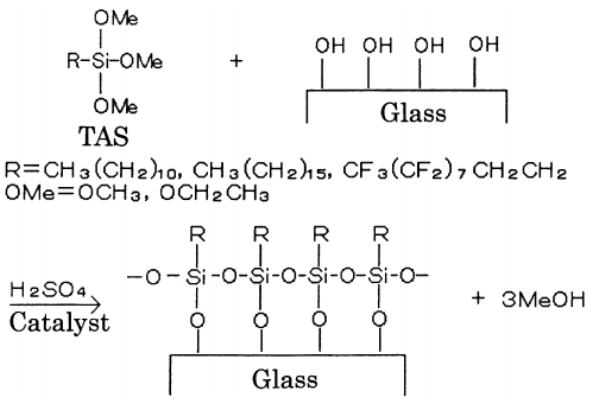

Figure 9. TAS coating mechanism for the hydrophobic treatment following with hydrophilic treatment process[114].

There are other methods that can make a surface hydrophobic. One promising approach to generate hydrophobic surfaces is to roughen glass surfaces at the submicron level, such as

using the help of TiO_2 nanoparticles which can grow on the inner surface by UV exposure using the so-gel process [115]. Other strategies such as laser or plasma etching, electrostatic spinning, phase separation, physical or chemical vapour deposition, and spraying have been explored for the preparation of hydrophobic surfaces [116]. The contact angle of the droplets and the solid surface can change the Laplace pressure based on Equation 3.

2.2.2.3 Hydraulic diameter (R')

This section examines the context of the hydraulic diameter change, which is the third factor that can be used to change the Laplace pressure. In each condition, the hydraulic diameter R' from above may be different based on the different shapes of the channel. The information here is concerned with shape categories, the sketches and the equations for Laplace pressure.

If the channel is a rectangle as shown in Figure 10 a), a Laplace pressure barrier can be formed by a sharp shrinkage of the cross-sectional width of this rectangle [117]. Figure 10 b) is one example, where Laplace pressure was generated at the interface between the hydrophobic phase and the more hydrophobic phase, where the contact angle changes.

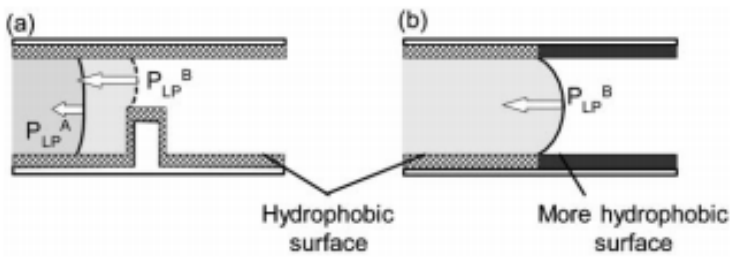

Figure 10. Laplace pressure generated at a) different cross-section geometry in hydrophobic surfaces; b) hydrophobic-more hydrophobic interface [117].

Equation 8

$$\Delta P = 2\tau cos\theta \left(\frac{1}{w} + \frac{1}{h}\right)$$

Where τ is the surface tension, w is the width and h is the channel depth, Θ is the contact angle.

The Laplace pressure is generated at geometrical microchannel expansions from a rectangle shape to a triangle shape (Figure 11) using the following expression developed by Chen et al. [118, 119].

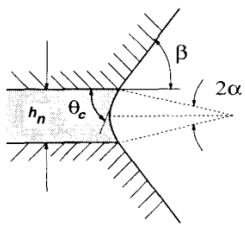

Figure 11. Laplace pressure generated at geometrical microchannel expansions from a rectangle shape to a triangle shape [119, 120].

Equation 9

$$\Delta P = \frac{2\tau_{LG}}{w\left[-\frac{w}{h}cos\theta_c + \frac{cos\theta_c - \frac{\alpha_w sin\beta}{sin\alpha_w}}{-cos\beta + \frac{sin\beta}{(sin\alpha_w)\left(\frac{\alpha_w}{sin\alpha_w} - cos\alpha_w\right)}}\right]}$$

Where τ is the surface tension, w is the width and h is the channel depth, Θ is the contact angle. β is the wedge angle in the width direction while the depth remains unchanged throughout the entire channel. The αw is circular arcs angle in width directions.

As shown in Figure 12, one microfluidic lab-on-a-disc platform used the expansion to a circular shape geometry [121].

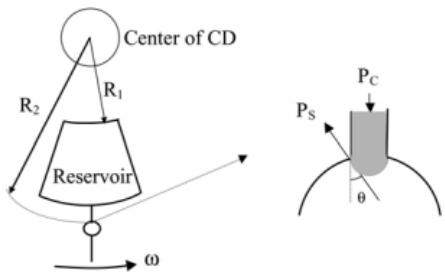

Figure 12. Laplace pressure generated from expansion to the circular shape wall [121].

Equation 10

$$\Delta P_c = \rho w^2 (R_2 - R_1)\left(\frac{R_1 + R_2}{2}\right)$$

2.2.3 Conclusion of Laplace pressure as a flow barrier

Here we address the importance of using Laplace pressure as the flow barrier. Moreover, we describe how the bubble-pressure flow barrier can be applied. The goal can be achieved by leveraging the Laplace pressure to restrict the flow of the oil phase in a droplet-based microfluidic system, where sampling or delivery is made possible by a transition from hydrophobic to hydrophilic surfaces. The Laplace pressure can be changed by liquid surface tension, contact angle, and channel hydraulic diameter. We describe the determining parameters and causes for all these three aspects.

2.3 Droplet generation, droplets merging, and mixing in a droplet

This section is concerned with the literature reviews of droplet generation, droplets merging and mixing in a droplet. These concepts build up important knowledge concerning the microfluidic probes' applications in the following chapters.

2.3.1 Droplet generation

Droplets have been used to sample and transport time-varying chemical signals [122], to avoid the problem of signal dispersion [19], as described in Section 2.1.1. This approach could transport chemicals from the sampling point to the measurement site without signal distortion. Moreover, all of the microfluidic probes we developed in this thesis follow with the strategy of 'droplets formed nearby the source with a barrier' (as described in section 2.1.3). Therefore, it is important to review and present the theory of droplet generation in this chapter.

Figure 13 shows the common three methods to generate the extracted samples as droplets in a microchannel, they are 1) co-flow in a capillary format; 2) T-Junction in a planar chip format; 3) flow focusing [26].

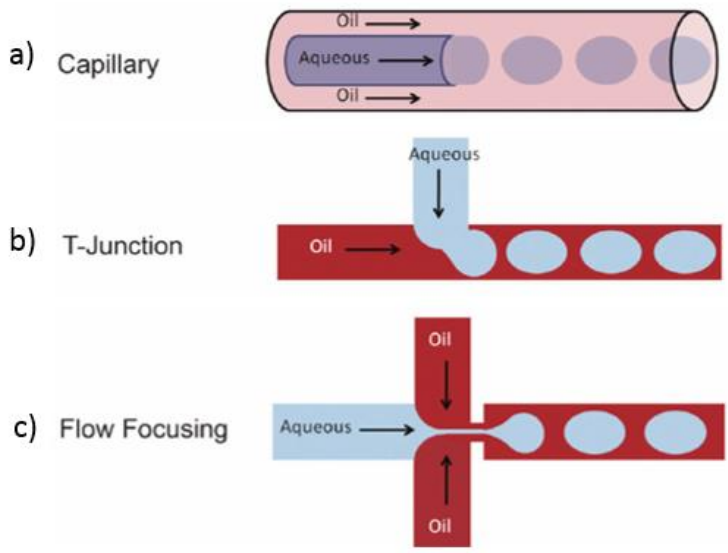

Figure 13. Droplet generation strategies: a) co-flow in a capillary format; b) T-Junction in a planar chip format; 3) flow focusing [26].

To achieve the aim that droplets formed nearby the source with a barrier, we should firstly ensure that the barrier existing at the tip of microchannel, which can be achieved by wetting

the hydrophobic-hydrophilic interface structures (as described in Section 2.2); we also should ensure that the barrier volume is as small as possible to reach the high temporal resolution (as described in Section 2.1). The wetted hydrophilic microfabricated features in a hydrophobic channel and the wetted hydrophilic membrane with the small pore sizes could be used as the barrier. Our silicon-based microfluidic probe is designed to use the T-junction in a planar chip format (as shown in Figure 13 b)), where the inlet aqueous inlet is only 2 µm diameter capillaries with the total dead volume of 2.8 pL, which will be described in Chapters 3 and 4. Our membrane-based system is designed to use the flow focusing in a planar chip format (as shown in Figure 13 c)), where the hydrophilic membrane with around 2.14 µm diameter pores was used for the aqueous phase inlet, which has been described in Chapter 5.

2.3.2 Diffusion

Taylor dispersion acts to enhance molecule diffusion, which can reduce the resolution. Moreover, diffusion through the membrane is important for the analysis of Chapter 5. Diffusion is caused by the gradient in chemical potential. It is the net movement of species (atoms or molecules) from a region of high chemical potential (or high concentration) to a region of low chemical potential (or low concentration) because of the random motion of the atoms or molecules. It can result in mixing or mass transport without requiring direct bulk motion and finally achieve equilibrium status. The process of molecule diffusion in a solution is shown in Figure 14 a).

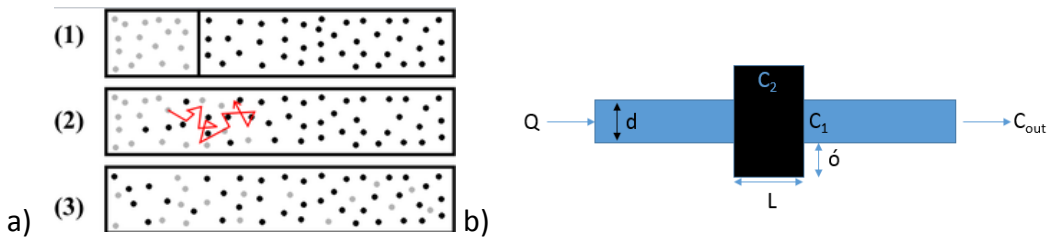

Figure 14. Diffusion Theories. a) The processes of molecule diffusion in a solution for steps 1-3; b) molecule radial diffusion through a semi-permeable cylindrical membrane (green part) connected with the tubing(blue parts), where the flow runs through the inner wall of the membrane, and where the flow rate is Q, the inner diameter is A, the concentration inside the inner tubing is C_1, the length of the membrane is L, thickness is ó, outer concentration is constant at C_2 and detected concentration C_{out}.

Considering the case of radial diffusion through a semi-permeable cylindrical membrane, the flux of molecules through the membrane (J_x, mol m^{-2} s^{-1}) is given by Fick's first law [123]:

EQUATION 11

$$J_x = -D\frac{\partial_c}{\partial_x} = \frac{1}{A}\frac{d_n}{d_t}$$

Where D is the diffusion coefficient (m^2/s)., A is the whole inner area of the membrane, c is the concentration (mol/m^3), n stands for the number of atoms (mol).

We also have:

EQUATION 12

$$\frac{d_c}{d_x} = \frac{C_1 - C_2}{ó}$$

Where ó is the thickness of the membrane, and C_2 is the molecule concentration outside of the membrane.

Therefore, by controlling the thickness of the membrane ó, the flow rate Q of fluid in the inner membrane and the targeted concentration C_2 (shown in Figure 14 b)), we can record the theoretical inner concentration C_1. When flow rate Q is so high, C_1 will be almost 0; but when the membrane thickness is extremely small, or the membrane inner contact surface A is extremely big, or the flow rate is almost 0, we can obtain C_1 being equal to C_2. So, to reach the nearly real time measurements ($C_1 = C_2$), we want: the membrane to be as thin as possible; the membrane area to be as big as possible; or the liquid flow rate at the inner wall being

almost 0. Considering the reality that a big membrane might be a problem. Droplets can form directly on the surface method and this is the environment for keeping the flow rate of droplets at 0, which makes $C_1 = C_2$.

2.3.3 Droplets merging

The first step for a droplet-based assay reaction is droplets merging, which is widely used in droplet-based microfluidics for chemical engineering and analytical chemistry. In this thesis, we demonstrate droplets merging, where the sampled droplets can be mixed with the assay droplets on board, which will be described in Chapter 4. Practical prerequisites for merging are that the droplets come into contact and overcome the stabilizing forces generated by surface tension and lubrication [124]. Merging can be categorized as passive merging and active merging [125]. Passive merging occurs spontaneously when the droplets meet, which can be organized for direct injection, or occur with a suitably shaped channel geometry [126] or partial hydrophilic surface treatment for droplet trapping. As for active merging, an electrical field (EC) [127], dielectrophoresis (DEP), thermocapillary effect or magnetic field [128] can be used.

2.3.3.1 Passive merging

In passive droplets merging, the channel geometry is the critical feature in achieving proper mixing. Three methods are described in this section: direct injection; changing channel cross-section dimensions (to adjust flow rate) and using hydrophilic features to trap the droplets.

Direct injection can be used to inject a different reagent into the passing droplets at the intersection of a microchannel and the main channel [218]. This strategy can create different

merged droplets populations having varied chemical information. Figure 15 illustrates the direct injection methods when merging can occur simply at a channel junction. Hydrophilic capillary side wall into the main channel for the consistent merging of $CaCl_2$ to the buffer droplet [69]. However, one inlet is always provided as one inlet. Another example for merging with the target reagent is a modular approach to droplet-based screening system using off-the-shelf components [129].

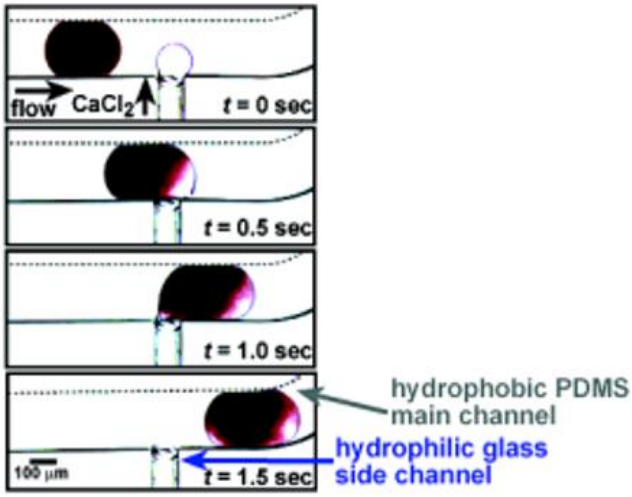

Figure 15. A direct injection methods Example: using a Hydrophilic capillary side wall into the main channel for the consistent merging of a $CaCl_2$ droplet to a buffer droplet [69].

It is difficult for a pair of droplets to merge in this case since they find it difficult to arrive at the same time and rate. Specially designed channel geometries can be helpful. One common flow focusing geometry for droplets merging consists of expanding the middle part of the channel (Figure 16 a)) [126, 130-132]. In this design, the droplet velocity decreases in the widening channel; where droplet merging happens. After this, the flow velocity increases again upon entry in the narrow channel, at which point the droplet merging occurs, as shown in Figure 16 a). Figure 16 b) presents an alternative approach for passively merging droplets

in a controlled manner, where the pillar slows down the former droplet and merges with the latter droplet.

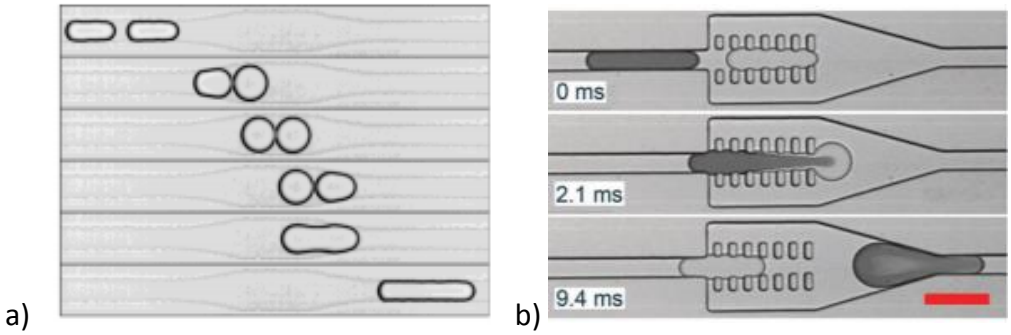

Figure 16. Droplets merging by changing the channel geometry methods. a) droplet passing merging in a flow focusing geometry [132]; b) pillar-induced droplet passive merging in microfluidic circuits [133].

Our silicon device [41] has its partially hydrophilic part at the junction where it traps the droplets. Figure 17 illustrates the layout of the silicon-based device, which has been used for merging the H_2O_2 samples and merged with H_2O_2 assay droplets on board. It is described in more details in Chapter 4.

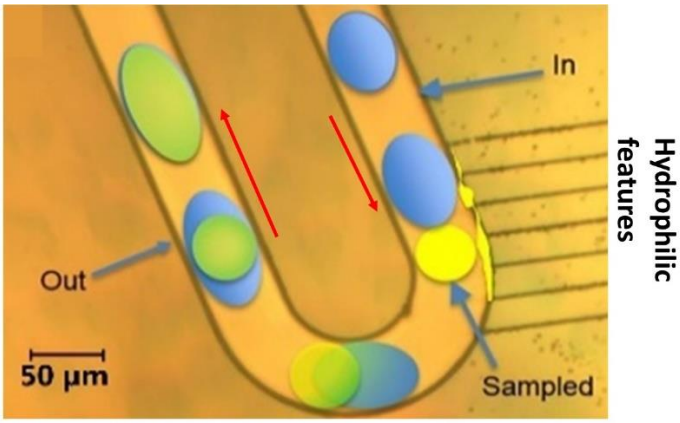

Figure 17. A passive merging method using the hydrophilic feature to slow down the former droplets to merge with the latter ones [41].

2.3.3.2 Active Merging

The widely used methods to achieve active merging serve to provide controlled EC, DEP, thermal capillary effect or magnetic fields at the location where two droplets meet. EC induces dynamic instability of the oil/water interface by the electric field, which continuously leads to the formation of a liquid bridge and continuous coalescence [134, 135]. Link *et al.* [136] showed that two droplets could be merged because of their oppositely charged surfaces, which will strongly attract each other when the droplets surfaces are nearby, as shown in Figure 18 a).

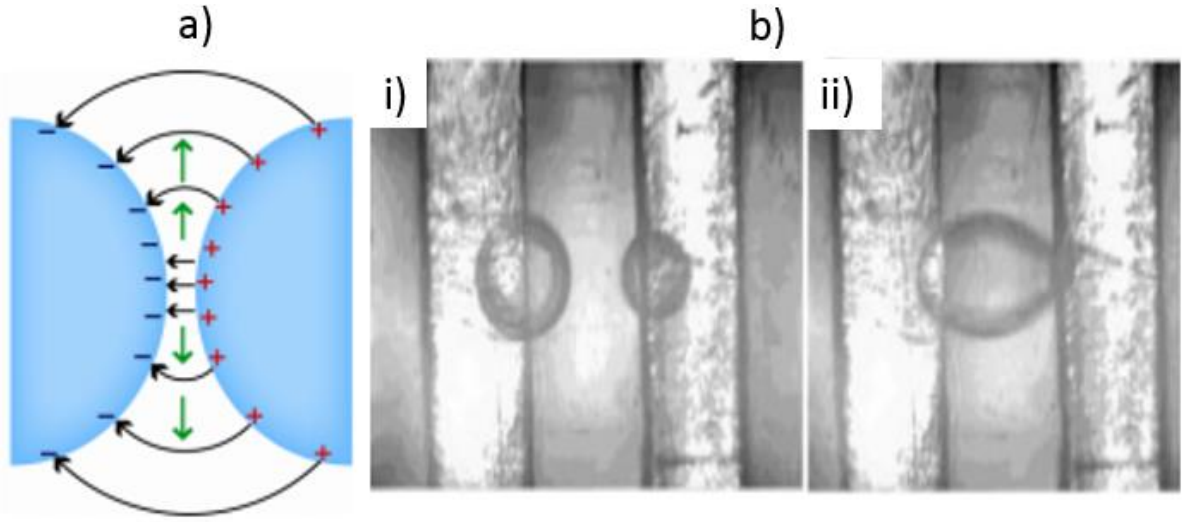

Figure 18. Active droplet merging methods. a) EC-induced merging of two droplets with oppositely charged surfaces; b) DEP-induced merging process: i). when the voltage applied was 500 V, the two droplets were trapped at two electrodes edges; ii) when the voltage was increased to 780 V, the droplets stretched towards each other and merged, this action occurred at the left electrode, the initial location of the larger sized droplets [137].

When the two droplets are subjected to a non-uniform electrical field, and the dielectric constants of the droplets and the ambient fluid are different. The electrical stress acting on the droplets' surface not only deforms the droplet, but also generates a net electrical force, which is referred to as the dielectrophoretic (DEP) force. This force causes the drop to move [137]. Figure 18 b) and c) show one example of the process. When the voltage applied was

500 V, the two droplets are trapped at the edges of two electrodes. When the electrical field strength was increased, the droplets swiftly stretched towards each other and coalesced. The merging of two adjacent droplets happens continuously are shown in Figure 18 b), until the droplets merged as depicted in Figure 18 c). However, this method has a drawback in that it requires high voltage, maybe up to several kV [119-121].

Droplets merging can also be achieved by uniform magnetic fields [138] for merging of two ferrofluid droplets. The thermo-capillary effect is another mechanism that produces active merging [128, 139-141]. The principle of heating two adjacent droplets with a focused laser beam was reported to change the surface tension as well as causing droplet disability. A consequence of this was effective droplets merging.

Merging can be categorized as passive merging and active merging [125]. Passive merging happens spontaneously when the droplets meet, which can be organized for direct injecting, or occur with a suitably shaped channel geometry [126] or partially hydrophilic surface treatment for droplet trapping. As for active merging, an electrical field (EC) [127], dielectrophoresis (DEP), thermocapillary effect or magnetic field [128] can be used. It is the first step for a droplet-based assay reaction, and then the second step will be mixing in a droplet, which will be described in the following section.

2.3.4 Mixing in a droplet

A droplet containing a sample must be mixed with a fluid containing the assay reagent for reaction after merging. When there is no flow, the two chemical reagents in one straight channel stay inside each hemisphere of a droplet, mixing only happens by diffusion [142]. Such mixing is too slow for fast kinetic reaction purposes. There are two main kinds of

situations for mixing two chemical reagents in a moving droplet. The first situation is flow in a straight channel. The flow pattern of each hemisphere of a droplet is shown as Figure 19 a), the shear force generated by walls will create flows that recirculate inside the droplet, which will accelerate the mixing of two chemical reagents.

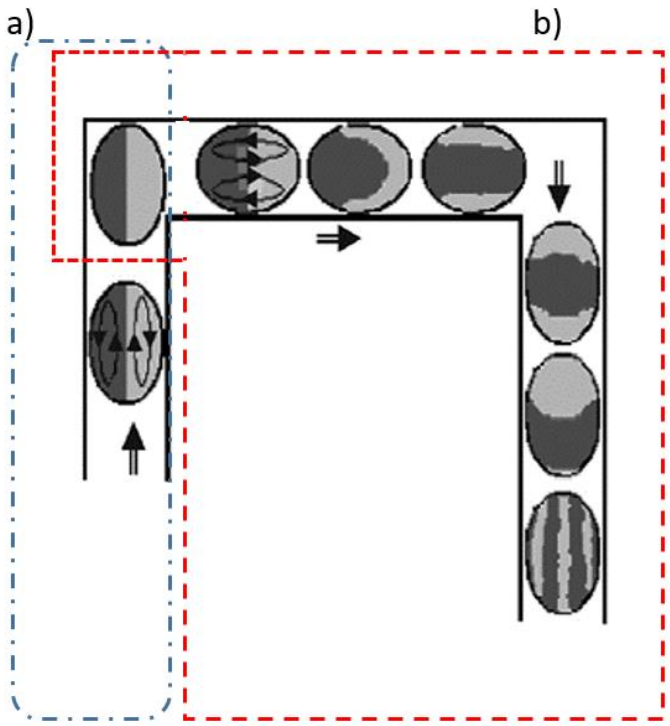

Figure 19. Processes for mixing during a). flow in as straight channel (blue dash part) and b). flow in the bent channel (red dash part) [143].

The second situation is the flow in a bent microchannel, which forces the flow patterns to change in the droplets as shown in Figure 19 b). At each bend, a reorientation of shear forces will happen which mixes the previous hemispheres. This can greatly reduce the mixing time.

2.4 Conclusion

In this chapter, we outline a review of the droplet-based microfluidic probe, a review of Laplace pressure as a flow barrier, the literature reviews about droplet generation, droplets merging, and mixing in a droplet. Firstly, using droplets in the microfluidic probe for sampling

and delivery of chemicals to avoid the Taylor dispersion with high chemical, spatial and temporal resolution has been pointed out. Moreover, sampling strategies had been categorized as follows: (1) aqueous phase sampling with downstream droplet formation, (2) pre-formed droplets and extracting samples from tissue, and (3) droplets formed nearby the tissue. Furthermore, we also list strategies for downstream analysis. Finally, we outlook the potential applications of droplets in sampling and delivering quick-changing signals. We will focus on the strategy of 'droplets formed nearby the tissue with a flow barrier at the tip on the development of our droplet-based microfluidic probe. Secondly, Laplace pressure to control the flow has been shown to have important applications, which is the innovative feature of the thesis. In terms of the applications, we focused on safe sampling and delivery control, which will be used in all of our developed devices. By changing either the surface tension, the contact angle or the hydraulic diameter, we can generate Laplace pressure by control, which can then be used as a flow barrier. We outline what will affect the surface tension and how to change the contact angle by surface treatment and how to categorize the microchannels.

Three methods to generate the extracted samples as droplets in microchannel has been listed, they are 1) co-flow in a capillary format; 2) T-Junction in a planar chip format; 3) flow focusing [26]. We have used the latter two points in our microfluidic probes. Our silicon-based microfluidic probe is designed to use the T-junction in a planar chip format, where the inlet aqueous inlet is only 2 µm diameter capillaries with the total dead volume of 2.8 pL, which was described in Chapters 3 and 4. Our membrane-based system is designed to use the flow focusing, where the hydrophilic membrane with small diameter pores was used for the aqueous phase inlet, which has been described in Chapter 5.

Droplets Merging and mixing are related to the chemical reaction on board, which will be used in Chapter 4. Merging can be categorized as passive merging (direct injection; more significant expansion channel to slow down the former droplet; small features to slow down the former droplet; partially hydrophilic pattern to slow down the former droplet to merge with the latter droplet) and active merging (using EC, DEP or the thermal-capillary effect to force two droplets to merge). As for mixing in a moving droplet, we categorize it as the flow in a straight microchannel and the flow in a bent microchannel.

Chapter 3: Design and microfabrication of a silicon-based microfluidic probe system

3.1 Background

Chapter 3 is based on Paper I. The design and microfabrication of our silicon-based microfabricated probe system, as well as the demonstration of this system for both sampling and delivery, are described in the paper published in Applied Physics Letters in 2017. Before that, I first describe the design and microfabrication of the first trial version as the background of this work.

Since hard material can be used to insert the tissue and microfabrication makes it easy to get the complicated structures, we tried to microfabricate our silicon-based device. In terms of size, a 375 µm thick silicon wafer 3 inches in diameter, as well as a 150 µm thick Pyrex glass, were chosen as substrate materials.

Figure 20 a) depicts the application of one silicon-based needle-like device, which can insert samples into animal-muscle tissue and remove samples from the tissue [15], while Figure 20 b) is our first microfabrication design, consisting of a T-junction forming a segmented flow (working principles are pictured in Figure 13 b)). This is followed by a descending channel that carries fluid to an aqueous-phase extraction hole at the tip of the needle and a return channel carrying oil, as shown in Figure 20 c). The first microfabrication design is shown below. The channel is around 50 µm thick at the needle tip, which has dimensions of 6.5 mm length and 425 µm thickness.

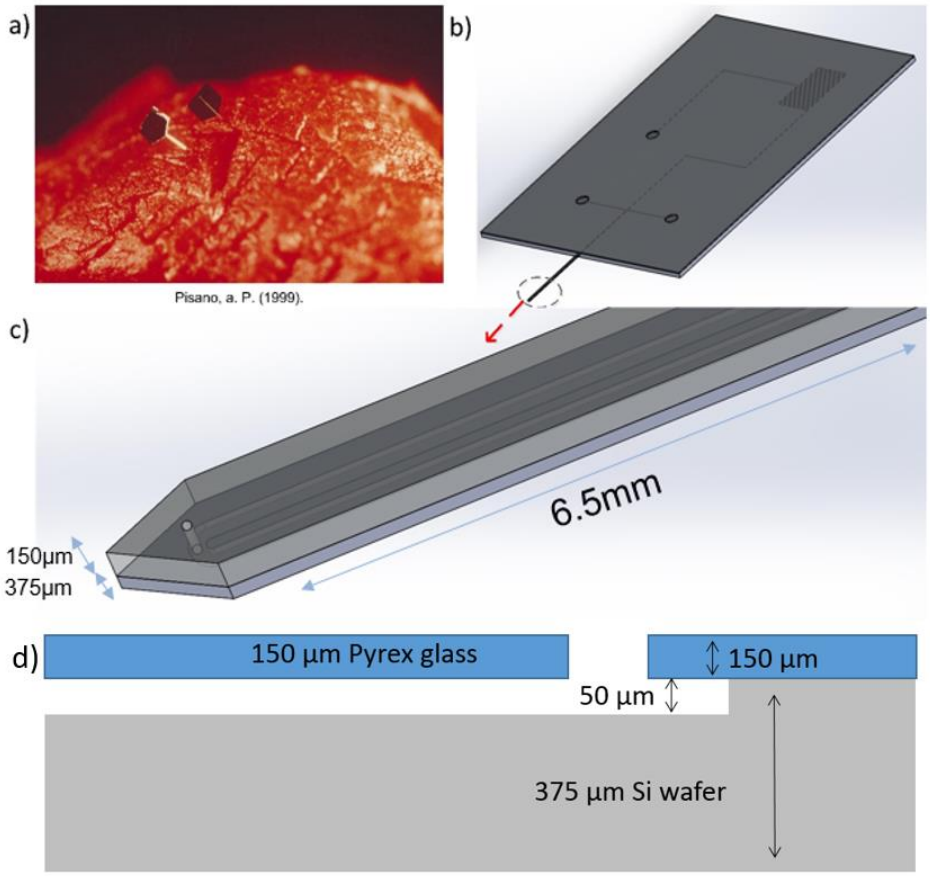

Figure 20. Design of the first version of the silicon-based microfluidic probe. a) Applying one silicon fabricated needle-like device for insertion into and removing samples from animal-muscle tissue [15]; b) SolidWorks 3d module drawing of our first version design; suitable for readout from microscope (30mmX17 mm); 150 µm thick pyrex glass wafer will cover the top of the 375 µm silicon to form an enclosed channel; c) the needle includes two lumens; inspired by prior cantilever sensors microdevice for diagnostics [16]; d) side view of the microfabrication tip design.

Assembling the chip as a circuit in the channel, we estimated the dimensions of the channels. We intended to laser-cut a series of holes in the Pyrex glass and conducted plasma treatment on them, after bonding the silicon wafer and the Pyrex glass to form an enclosed chip. The holes will, therefore, work as the extraction phase, as well as generating a high enough Laplace pressure.

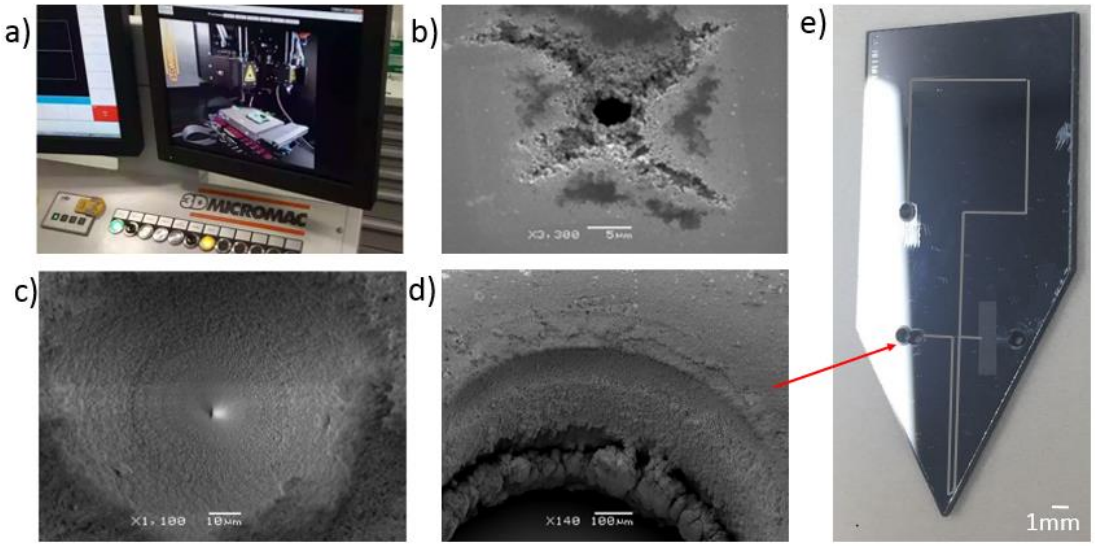

Figure 21. Fabrication of the first version of silicon-based microfluidic probe. a). The laser cutting machine [3D micromac microSTRUCT C] used for making inlets holes and outlets holes on 3 inches silicon wafer, and 2 µm small holes on 125µm thick Pyrex glass; b). shape of the bottom view of a 2 µm hole cut on 125µm thick Pyrex glass; c) shape of the top view of a 2 µm hole cut on 125 µm thick Pyrex glass; d) laser cutting of 1 mm hole on the silicon wafer; e) the first version of the silicon-based microfluidic probe before dicing the 2 µm hole at the tip.

Figure 21 above illustrates how to cut holes in a silicon wafer prior to bonding. We chose the 3D Micromac microSTRUCT 3D laser cutting machine (figure 21 a)) for making 2 µm holes in the Pyrex glass after the bonding process, as shown in Figure 21 b-c). 1 mm diameter inlet and outlet holes on in the 365 µm thick silicon can also be achieved, as shown in Figure 21 d).

However, the edge of the 1mm inlet and outlet holes created by the laser silicon-cutting process is not smooth enough for bonding, as shown in Figure 21 d). Finally, a sand-blasting machine (MicroCab+^{TM} (Danville materials)) was employed to put holes in the silicon for inlets and outlets with smooth surfaces for bonding, which is one innovative feature of our fabrication.

We fabricated and achieved the first version of the chip, as shown in Figure 21 e). We cut the holes in the glass after bonding, but we encountered certain problems. For example, the

holes in Pyrex glass are not consistent in hole dimensions, and a needle shape is difficult to achieve. We also prepared a chuck for holding the silicon device to run the microfluidics experiments, as shown in Appendix I.

We designed the second version of the chip. There are seven capillaries on the pattern. By a dicing process (as shown in Appendix II), the capillaries were exposed to the outside, forming the extraction region. This design is shown as the mask drawing with the dicing line (Figure 22).

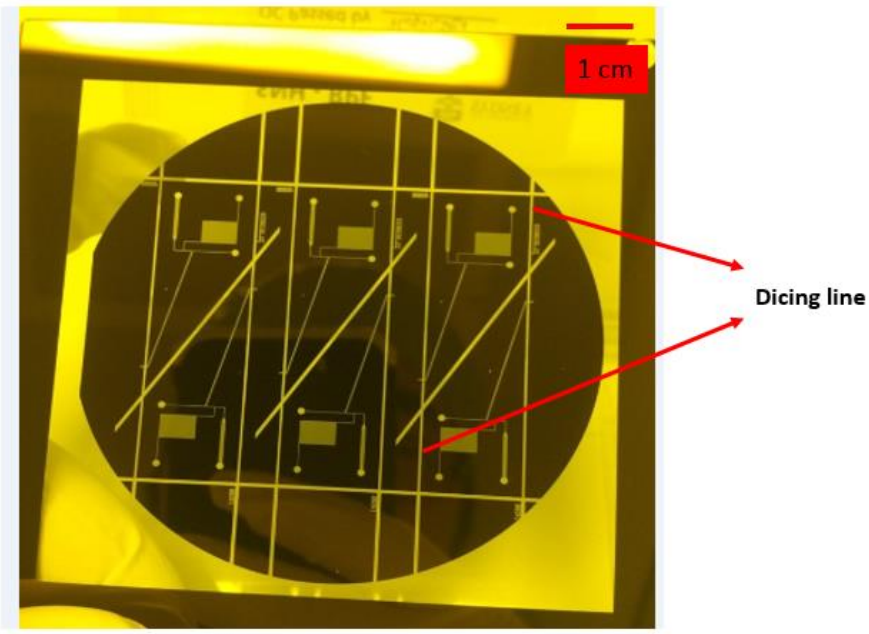

Figure 22. Mask showing the design of the second version of the needle.

3.2 Introduction to publication I

The design and microfabrication of the improved version of a silicon-based microfluidic probe are described. We made 7 capillaries that were 2 µm in diameter connecting the inner channel to the outside. The dice on these small features expose the sharp needle tip to the 2 µm features outside as a hydrophilic phase-extraction region with a bubble-pressure flow barrier. The demonstration of the device for delivery as well as sampling on board is also

described. The relationship between the recorded sample signals and the external dye concentration (10 to 40 µg/mL) indicates that this device is capable of quantitative, real-time measurements of rapidly varying chemical signals with a temporal resolution of around 3 seconds. Chemicals can be sampled as droplets and transported in droplets to preserve the chemical signals, which is crucial for real chemical and/or biological applications.

3.3 Author's contribution

I am the primary author of this paper, carried out all the data collection and wrote this work. Dr David Inglis coordinated the project and was also involved in publication preparation. The co-authors have also helped with the publication preparation process. G.Z. Liu and E. M. Goldys helped on the chemicals preparation. Y.G. Zhu comments and discusses on the microfluidic system.

The work was designed and mostly completed at Macquarie University. As for the first version of the device, I designed the device, drew the mask, and undertook the photolithography in MQ cleanroom and shipped it to ANFF-SA for the DRIE processing only. This was followed by my work on the bonding, dicing and post-processing aspects. Regarding the second version, I devised the new design, made the new mask, and did the photolithography. I had a one-month internship at ANFF-SA, where I completed the DRIE process by myself. Then I brought back the chip and did the bonding and dicing at Macquarie University. The experimental setup and the continuous experiments were all done at Macquarie University by myself.

3.4 Publication I

This work has been published in the Applied Physics letter journal:

S.L. Feng, G.Z. Liu, L.M. Jiang, Y.G. Zhu, E. M. Goldys, D.W. Inglis, "A Microfluidic Needle for Sampling and Delivery of Chemical Signals by Segmented Flows," Applied Physics Letters,111 (18), 183702, 2017.

Pages 53-57 of this thesis have been removed as they contain published material under copyright. Removed contents published as:

Feng, S., Liu, G., Jiang, L., Zhu, Y., Goldys, E. M., Inglis, D. W. (2017) A microfluidic needle for sampling and delivery of chemical signals by segmented flows, *Applied Physics Letters*, vol. 111, no. 18, 183702. https://doi.org/10.1063/1.4995657

Chapter 4: Biomedical application of a silicon-based microfluidic probe system

4.1 Background

Chapter 4 is based on Publication II. It presents the biomedical application of the silicon-based microfluidic probe. Droplets of the assay reagent are generated and sent to the needle tip using a mineral-oil carrier fluid. Droplets can be immediately generated while sampling, and the hydrophilic structure can slow down the droplets on board, which creates a good environment for droplets merging. Immediately merging sampled droplets with the on-line droplets, molecule mixing in a separated single droplet and on-board analysis can be achieved in the probe. The ability to characterize the commercial assay is also demonstrated here. The droplet approach facilitates thousands of detections in a single run and may help to quantify kinetic reactions in a low-cost and rapid way. The device has a dead volume of only 2.8 pL, which gives a high spatial, chemical and temporal resolution. We monitor the kinetics reactions using a commercial, single-step fluorescent H_2O_2 assay. The chip can provide an enclosed environment and be suitable for a slow reaction assay in a controlled period of time. Due to the high temporal resolution of the sampling probe, this system is also suitable for the study of rapid (~1 s) chemical changes in dynamic biological systems. The probes to be developed will function as a successful tool for the biologist or chemist wanting to monitor kinetics reactions with temporal, spatial and chemical resolution.

4.2 Introduction to publication II

This chapter shows the application of the silicon-based microfabricated microfluidic probe (as described in Chapter 3) for sampling, merging, reaction and quantitative detection of hydrogen peroxide (H_2O_2). This manuscript has been submitted to the journal Sensors and Actuators B: Chemical.

4.3 Author's contribution

I am the primary author of this paper, carried out all the data collection and wrote this chapter. David Inglis coordinated the work and was involved in publication preparation. The co-authors also assisted in the publication preparation process. S. Clement provided the H_2O_2 assay. Y. G. Zhu gave suggestions and comments on the device systems. Ewa M. Goldys gave suggestions and comments on the bioassay reaction.

4.4 Publication II

S.L. Feng, S. Clement, Y. G. Zhu, Ewa M. Goldys, D. W. Inglis, "Microfabricated probe for hydrogen peroxide detection," Sensors and Actuators B: Chemical, submitted on 3^{r} of September 2018.

Microfabricated probe for hydrogen peroxide detection

Shilun Feng[a, b*], Sandhya Clement[b, c], Yonggang Zhu[d], Ewa M. Goldys[b, c], and David W. Inglis[a, b*]

*Shilun.feng@students.mq.edu.au; +61 2 9850 9144.
*david.inglis@mq.edu.au; +61 2 9850 9144.

a. School of Engineering, Macquarie University, Sydney, NSW 2109, Australia

b. ARC Centre of Excellence for Nanoscale BioPhotonics (CNBP), Macquarie University, Sydney, NSW 2109, Australia

c. Graduate School of Biomedical Engineering, University of New South Wales, Sydney, NSW 2052, Australia

d. RMIT University, Melbourne, Australia, and Harbin Institute of Technology (Shenzhen)

A microfabricated needle-like probe has been designed and applied for hydrogen peroxide (H_2O_2) sampling and detection using a commercial, single-step fluorescent H_2O_2 assay. In this work, droplets of the assay reagent are generated and sent to the needle tip using a mineral-oil carrier fluid. At the needle tip, the sample is drawn into the device through 100 μm long hydrophilic capillaries by negative pressure. The sampled fluid is immediately merged with the assay droplet and carried away to mix and react, producing a sequence of droplets representing the H_2O_2 concentration as a function of time. We have characterized the assay fluorescence for small variations in the sample volume. With the calibration, we can calculate the concentration of H_2O_2 in the sampled liquid from the size and intensity of each merged droplet. This is a microfluidic data-logger system for on-site continuous sampling, controlled reaction, signals storage and on-line quantitative detection. It is a useful tool for monitoring dynamic chemical reactions in analytical chemistry and biological applications.

Keywords: microfluidics, sampling, merging, droplet, H_2O_2.

1. Introduction

Droplets can be used as independent micro-reactors for many chemical and biological applications[1], e.g. chemical synthesis[2], enzyme kinetics studies[3], bio-medical diagnostics[4] and biological agent detection[5]. The advantages of microfluidic droplet platforms for chemical reactions include smaller quantities of costly reagents, better biochemical reaction efficiency[6] and high throughput in terms of the number of reactions. Droplets can also be used to transport biochemical signals over long distance/ time with minimal dispersion[7]. This feature is useful for detecting rapid chemical changes in dynamic systems.

Slaney et al.[8] Used the two parallel 10 cm long, 20 μm ID capillaries to inject artificial cerebrospinal fluid into an injection site, while extracting fluid at the same rate. This fluid was then segmented into droplets immediately outside the brain for transport to a laser induced fluorescence measurement. This system achieved a temporal resolution of 7 s. They also showed that a smaller system using 10-mm long capillaries with an inner diameter of 10 μm could achieve a response time of 200 ms. However, this probe was used in-vitro and not inserted into tissue.

The same group also demonstrated a similar system that used a micro-dialysis membrane at the probe tip[7, 8]. The response time is longer, but the membrane contains the probe making a more practical system. In both cases, the sample is segmented after flowing through a channel for some millimeters[9], [10], allowing for Taylor dispersion of the chemical signal. In principle, a shorter response time can be achieved by segmenting immediately after sampling.

Chen et al.[11] did adjust this with a droplet-droplet extraction system for sampling biochemical signals from a cell culture. In their chemistrode, analytes produced in a cell culture were captured in passing droplets that were transported downstream for various analyses. Their work demonstrates an on-chip assay, where a reagent is merged/mixed with a passing sample droplet. However, their PDMS device had to be attached onto the cell culture dish to prevent the oil (continuous phase) from leaking out of the microfluidic system. Therefore, sampling within soft tissue is not possible.

To address the problem of the oil-phase leaking out of the probe at the sampling site, Feng et al. demonstrated the polymer[7] and silicon[12] devices that use Laplace pressure to allow aqueous fluids to enter and exit a microchannel, but not the oil phase. Laplace, or bubble pressure is also used as a gating mechanism to control the movement of liquid in centrifugal Lab-on-a-disc platforms[13]. Using our approach, sample is drawn into a hydrophobic microchannel through hydrophilic channels or a hydrophilic membrane. The sample is immediately segmented by the oil phase in the hydrophobic channel. In the work presented here, we apply the silicon device which has hydrophilic capillaries at its tip (100 μm long, 2 μm ID), to an on-chip fluorescence assay.

To conduct an on-chip assay, a droplet containing a sample must be mixed with a fluid containing the assay reagent. Merging of the droplets occurs when they touch each other and overcome the stabilizing forces caused by lubrication and surface tension[14]. Several designs have been used to bring droplets together including active merging and passive merging[15]. For droplets that are stabilized by surfactants, active merging is required. For example, the thermocapillary effect[16] or electrocoalescence[17] can be used. Without surfactants, the stability of the droplets is reduced, but it is possible to induce passive merging.

Following a merging event in a straight channel, the two substances form one droplet where each hemisphere is mixed. Mixing between the two halves occurs only by diffusion across this axis of symmetry[18], [19] . Mixing can be accelerated by generating advection in different directions inside the droplets. Flavie Sarrazin et al. used simple bends in the microchannel, which rotated the hemispheres[20]. At each bend, the internal loops are sheared and reoriented so that the internal fluids mix.

To demonstrate the on-chip assay, we have used a commercial H_2O_2 assay. H_2O_2 is a reactive oxygen species (ROS) molecules, which can damage DNA, inhibit bacterial oxidative phosphorylation[21]. In cell cultures, concentrations of between 20 to 50 μM have been shown to have limited cytotoxicity[22].The urinary H_2O_2 have been used as a biomarker for oxidative stress[23],[24] ,and the concentration ranges from the freshly voided urine from 55 healthy is ranging from 0.84 to 5.7 μM[25].

This is achieved by entraining droplets containing H_2O_2 assay reagent upstream of the sampling site. At the sampling site, the assay droplets merge with the sampled droplets with varying concentrations of H_2O_2, then flow downstream. Immediately following the merging event, a bend in the channel causes enhanced advection in the merged droplets. The droplets can be kept inside the enclosed channel, avoiding contact with the air or oxidation.

The merged signals can be stored and/or transported for analysis, enabling preserving digital chemicals information in the train of merged droplets.

2. Materials and methods

2.1 Instrumentation

The experimental setup for the microfluidic chip includes a Maesflow 4C (Fluigent) system for positive pressure control and a purpose-built system to apply and measure negative pressure. A Poly (methyl methacrylate) chuck was used to hold the chip and apply fluids and pressures. We recorded all images using an epi-fluorescence microscope with a monochrome camera (NIKON DS-Qi1Mc), a CoolLED pE300 light source, and appropriate filter cubes. Images and movies were analyzed and prepared using ImageJ. Figure 2 uses a custom grey-to-green look-up table. Fluorescence measurements of bulk solutions were carried out using a Cary Eclipse fluorescence spectrophotometer with a 5-nm spectral resolution for both excitation and emission.

The microfluidic device used is identical to those used in Feng et al. 2017[12], and is shown in Figure 1 a). The channels were photo-lithographically patterned and etched on the silicon chip. Sigma-Coat (Sigma Aldrich) was used to coat the channels in silane, creating a hydrophobic surface. The capillary channels at the needle tip were rendered hydrophilic by drawing 2-proponal containing 1% KOH into the device through the capillaries, while flowing pure 2-propanol through the main channel. A region around the capillary channels, but inside the main channel is also made hydrophilic. This feature is critical, as it anchors the sample droplet, enabling the merging of sample and assay.

2.2 Materials

The amount of H_2O_2 generated throughout our experiment is measured using an FBBBE probe (Product No. 14606, Cayman Chemicals, and USA). The FBBBE is a probe which is specifically designed for measuring intracellular H_2O_2 as it is capable of penetrating the cell wall[26]. The fluorescence of the FBBBE molecule (with Ex/ Em 480/512) increases with the amount of H_2O_2 (from 0 to 150 µM). For calibration, 30% hydrogen peroxide (H_2O_2) was used to make different concentrations of H_2O_2 samples; 50 mM HEPES buffer (pH=7.2) was used to dilute the H_2O_2 and the biosensor.

2.3 Droplet merging on chip

Figure 1 a) shows the layout and typical settings of the device. We set the oil (32 m bar) and biosensor (38 m bar) inputs using the Maesflow 4c (Fluigent) System. We applied negative pressure (-232 m bar) at the outlet; the needle tip is left in a small pool of solution to be sampled. Figure 1 b) depicts the process of sampling a yellow liquid and merging it with a dark-green droplet representing the biosensor. Figure 1 c) shows the measured droplet volumes for 20 continuous merging events. The volumes of the biosensor droplets are consistent with an average volume of 0.1600 ± 0.0025 nL. The volumes of the merged droplets are recorded to have an average of 0.213 ± 0.005 nL. We can calculate the sampled volume by subtracting the biosensor droplet volume (V_l) from the merged droplet volume V_m.

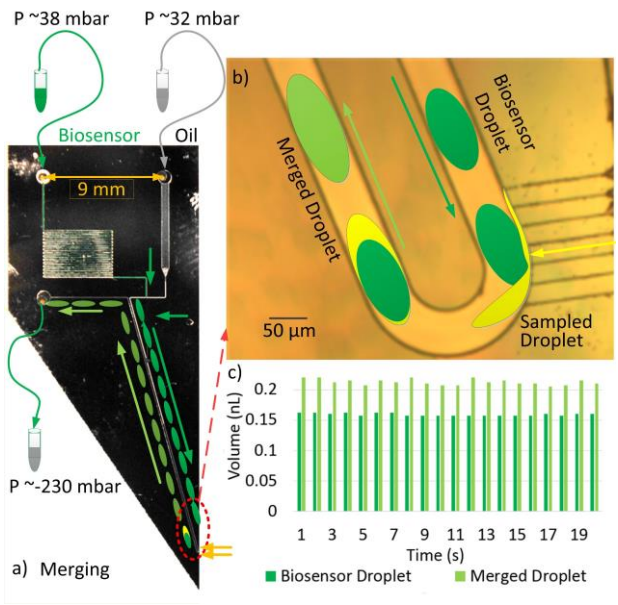

Figure 1 Working principle of our needle device for on-line droplets merging. a) There are two inlets (one for biosensor, one for oil, each under small positive pressure); there is one outlet with the negative pressure around -23 kPa. b) The detail of the merging process at the tip: 'sampled droplet' (yellow) from off-chip and 'biosensor droplet' (green) generated on board are mixed immediately after sampling. c) Chart showing the volumes of the biosensor and merged droplets for 20 sequential merging events with 0.160 ± 0.003 n L, 0.213 ± 0.005 n L respectively.

The sampled volume (0.0530 ± 0.0075 nL) may change due to pressure variations outside the device, while the volume of the biosensor droplet (V_I) is much more stable and does not need to be continuously monitored. The temporal resolution of the samples is around 1 s, as shown in Figure 1 c.

2.4 Estimated reaction time for two droplets merging

An important process in chemical and biological assays is the mixing of reagents. If two chemical droplets contact and merge into one droplet with no advection, only diffusion of molecules between the two droplets may take place. The time (t) for a chemical with diffusivity D in a volume of dimension x to reach equilibrium is approximately:

$$t = \frac{x^2}{D} \qquad \text{Eq.1}$$

For H_2O_2 in a 50-µm droplet, t is calculated as = 0.43 s. The assay for H_2O_2 has a practical reaction time of 15 minutes, so the mixing time due to diffusion is insignificant.

3. Results

3.1 Droplet merging

Our first result is to show that the HEPES buffer solution can be sampled by the chip and immediately mixed with biosensor droplets. Figure 2 shows a 90-µm long segment of 40-µM FBBBE biosensor mixing with a small amount of sampled 50 mM HEPES buffer (pH=7.2). 2 kPa was provided at the oil inlet, 4.8 kPa was provided at the biosensor inlet, both of which were provided by a Maesflow 4C (Fluigent) system. The negative pressure (-7 kPa) was provided at the outlet; 50 mM HEBES buffer was place at the needle tip for sampling. The microscope objective was a 10 X 0.3 APO, while the exposure time for the camera is 400 ms.

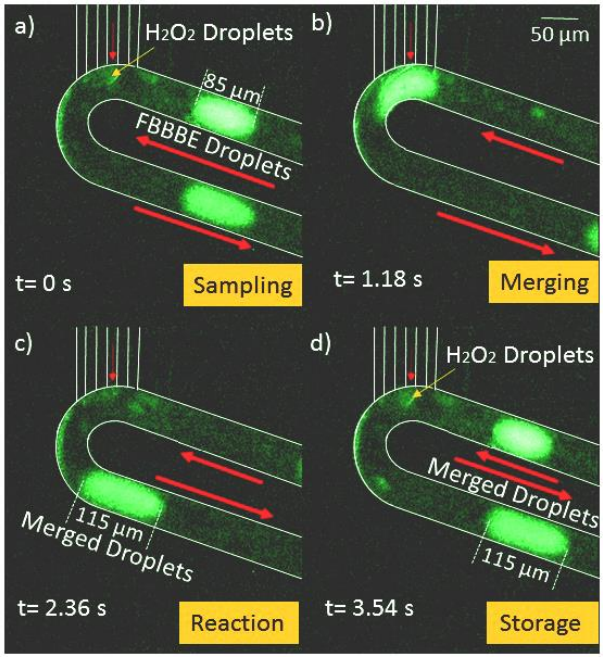

Figure 2 Demonstration of 40-µM FBBBE Biosensor droplet mixing with 50-mM HEPES buffer at the tip to form a 105-µm droplet. a) Biosensor droplet is traveling to tip; HEPES sample is flowing in through hydrophilic capillaries. b) Biosensor merges with HEPES sample. c) Merged droplet dispatched away from capillary. d) The cycle repeats with new biosensor droplet.

Figure 2 a) shows the sampling process of HEPES by the devices; Figure 2 b) shows the merging process of the 85 µm of 40 µM FBBBE biosensor solution with the sampled HEPES droplets; Figure 2 c) shows the merged droplet which has a length of 105 µm and a volume of 0.263 nL. Using this change in length we can calculate that approximately 0.038 nL of HEPES buffer was sampled; Figure 2 d) shows the merged, and rapidly mixed in the droplets is being transported away. Along with subsequent droplets, it is preserved on board while being transported downstream. The fluorescence of each merged droplet is used to measure the H_2O_2 concentration in the HEPES buffer after 15 minutes. In Figure 2, merged droplets are produced approximately once every 3.5 seconds. This digital sampling rate can be increased by increasing the pressure drop from the inlets to the outlet.

3.2 Evaluation of the FBBBE sensor with varying H_2O_2 and biosensor concentrations

The volume of sample that is added to the biosensor droplet is variable. If the pressure outside the device increases/decreases, more/less sample will be added. The concentration of the sensor and the analyte may therefore change from drop to drop. We investigated how these two parameters affect the fluorescence intensity of the assay over a reasonable range using a conventional spectrofluorometer. Figure 3 a) shows the reactions of the 10-50 µM FBBBE sensor probe with 30 µM H_2O_2. The fluorescence spectra (ex: 480 nm) were monitored after the merged solution had been left for 15 minutes. We observe a closely linear increase in the fluorescence signal with increasing FBBBE biosensor concentration.

Figure 3 b) shows the reactions of 10-80 µM H_2O_2 with 30 µM FBBBE sensor. The results also show a linear increase in the reading fluorescence signal intensity with the increase of H_2O_2 biosensor concentration. Therefore, we expect the fluorescence signal intensity to be approximately linear for changes to both H_2O_2 and FBBBE sensors concentrations in the examined ranges.

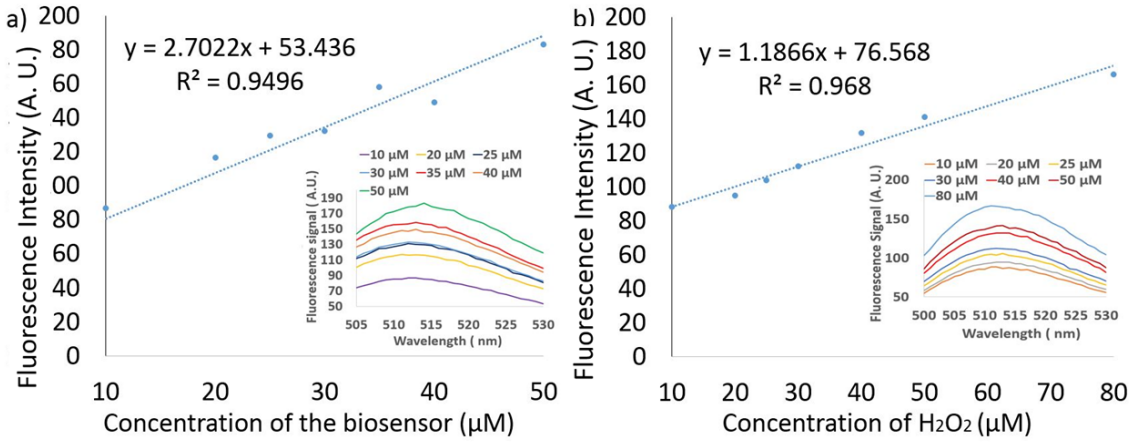

Figure 3 The performance of the FBBBE sensor with varying H_2O_2 and biosensor concentrations was evaluated by the Cary Eclipse Spectrophotometer. a) The Reading Fluorescence intensity is linear for FBBBE [10-50 µM] and H_2O_2 [30 µM]; b) The Reading Fluorescence intensity is linear for FBBBE [30 µM] and H_2O_2 [10-80 µM].

3.3 Validation of microfluidic device for H_2O_2 measurement

Different concentrations of H_2O_2 (0-150 µM) were mixed with 20 µM FBBBE biosensor off-chip. Then each merged solution was left in the dark at room temperature for 15 minutes before sampling by the microdevice. Here, both inlets are filled with oil and a negative pressure (-23 kPa) was provided at the outlet. The fluorescence intensity of the droplets was recorded by microscopy to validate the microfluidic system. Figure 4 shows the average intensity of 600 droplets for each concentration of H_2O_2. There is a linear increase in fluorescence with increasing concentration, demonstrating that this device can be used to measure different H_2O_2 concentrations.

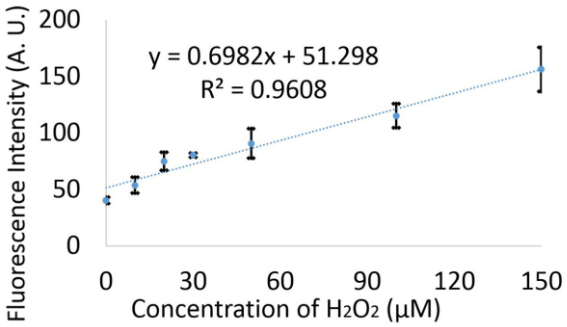

Figure 4 Validation of the biosensor in the droplet microfluidics system by using 20 µM FBBBE biosensor mixed with different concentrations of H_2O_2 in HEPES buffer. Each data point represents the fluorescent intensity of 600 droplets with each error bar giving one standard deviation.

3.4 Calibration of the microfluidic sampling system for biosensor reactions

We used the device to sample HEPES buffer containing various concentrations of H_2O_2. As shown in Figure 1, the FBBBE biosensor droplets are generated on board, and the peroxide-containing buffer is sampled through the capillaries. In this experiment, 1.7 kPa was provided at the oil inlet, 2.5 kPa was provided at the dye biosensor inlet; -330 m bar was provided at the outlet. Merged samples were obtained for 20 seconds then the flow was stopped. The samples were stored in the device for 15 minutes to allow the bioassay time to generate a satisfactory fluorescence signal. The fluorescence intensities and lengths of each stored droplet are then recorded.

For this particular experiment, we used biosensor droplets containing 40 µM FBBBE while 100 µM and 200 µM H_2O_2 in HEPES were sampled. The biosensor droplet volume is consistent and observed to be 0.191 ± 0.005 nL, while the merged droplet volume is variable at 0.249 ± 0.052 nL.

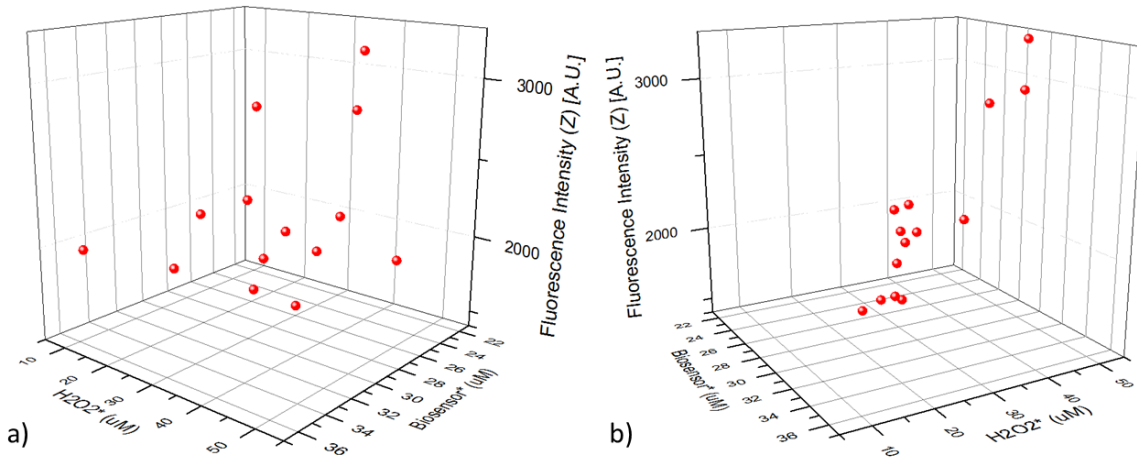

Figure 5 Calibration of biosensor system with varying H_2O_2 concentration a) View showing maximum data spread. b) Nearly orthogonal view showing a linear relationship. H_2O_2 is H_2O_2 concentration the in the merged droplet; Biosensor* is the Biosensor concentration in the merged droplet.*

Figure 5 shows the fluorescence intensity of the merged droplets after 15 minutes versus the peroxide concentration in the merged droplet ($C^*{}_{H_2O_2}$) and the biosensor concentration in the merged droplet ($C^*{}_{Sensor}$). These concentrations are calculated using the change in droplet volume. The data readily fit a 2-dimensional first-order linear function. (R^2=0.813).

The linear equation can be re-arranged to determine the hydrogen peroxide concentration in the droplet as a function of the fluorescence intensity (Z) and the biosensor concentration in the droplet:

$$C^*{}_{H_2O_2} = \frac{Z+2819-117.9\,C^*Sensor}{46.98} \qquad \text{Eq. 2}$$

Since the initial droplet size V_I and the biosensor concentration (C_{sensor}) prior to sampling are consistent, we can write an equation for the concentration of hydrogen peroxide outside the device ($C_{H_2O_2}$) in terms of known quantities and the directly measured variables:

$$C_{H_2O_2} = \left(\frac{Z+2819-117.9\,C_{sensor}\left(\frac{V_I}{V_m}\right)}{46.98}\right)\frac{V_m}{V_m-V_I} \qquad \text{Eq. 3}$$

Using the above equation, it is possible to calculate the concentration of H_2O_2 in the solution of interest.

4. Discussion

Our system can extract sub nL samples from surrounding fluid and merge the sampled liquid with the detecting biosensor directly. These merged droplets can be stored and detected directly in the channel, enabling fluorescence detection of samples with volume nL taken at 1 second intervals. Using conventional methods, such as a spectrophotometer, it is not practical to characterise samples at such a rapid rate. For the sensor we use in this article, 15 minutes is the optimal reaction time, so we can detect fluorescence of the merged samples sharply at 15 minutes without any handling time. Also, it is possible to perform more rapid detection with this chip using a sensor which has a shorter reaction time.

The size and rate of assay droplets are mainly controlled by the inlet pressures. The sampling rate (volume flow) is mainly controlled mainly by the difference between the external pressure and the negative pressure at the outlet. If this difference is too large, sample droplets may be released into the channel before an assay droplet arrives. Under normal operating conditions we did not observe this.

It is interesting to consider what fluid systems and surface treatments would result in stable droplets while giving a high breakthrough pressure. In such a system, the main micro-channel must be highly lipophilic, and hydrophobic, while the capillaries must be highly hydrophilic and lipophobic. We have not used any surfactants during the experiments as we expect this will render the capillaries lipophilic, destroying the Laplace pressure barrier that prevents the oil from escaping[27]. We have not experimented with other oil systems.

The length of the channel from the needle tip to the outlet is 28.4 mm. This channel length is sufficient to store 50 droplets at the flow rates used. In subsequent versions of the device, we will use a much longer channel or connect the outlet to a long tube to ensure continuous coupled measurements. Finally, with an improved chip-to-tube connection, sampled droplets could be stored and sent to a wide range of analytical tools.

The present system executes sampling, merging and reaction, which may also allow us to investigate the kinetics of assay reactions. As well as performing this long-reaction-time H_2O_2 assay (>15 minutes), our system is also the right tool for studying more rapid (~1 s) chemical changes in dynamic systems, and possibly high throughput charactersisation of assays. For example, small amounts of reagent can be merged with may different analytes of different concentrations in a single run of the chip, giving hundreds of individual reactions information. This can be used to reduce the cost and time effectively of developing new assays compared to the conventional methods.

5. Conclusions

We have demonstrated the use of an on-chip assay for varying hydrogen peroxide detections using droplet by the existing silicon data-logger system. Unlike prior work, the present approach segments the sample immediately upon entering the device to merge and react with the assay, and through the use of a hydrophilic barrier does not need a tight seal between device and tissue. The droplet approach facilitates thousands of detections in a single run and may be used to quantify the kinetic reactions in a low-cost and rapid way. This system is suitable for the studying of rapid (~1 s) chemical changes in dynamic biological systems.

Acknowledgements

The authors thank Dr Simon Doe, Dr Donghoon Chang, and Dr Jing-Hong Pai at the ANFF South Australia for input and guidance in fabricating the device. This fabrication work was performed (in part) at the South Australian node of the Australian National Fabrication Facility under the National Collaborative Research Infrastructure Strategy. This work was financially supported by Macquarie University Wireless Medical Devices Research Centre and the ARC Centre of Excellence for Nanoscale BioPhotonics CE140100003. We thank our colleague Dr Wei Deng from Macquarie University the useful discussions. The authors declare no conflicts of interest.

References

[1] T. Ishida, D. McLaughlin, Y. Tanaka, and T. Omata, "First-come-first-store microfluidic device of droplets using hydrophobic passive microvalves," *Sensors and Actuators B: Chemical,* vol. 254, pp. 1005-1010, 2018.

[2] P. Dubois *et al.*, "Ionic liquid droplet as e-microreactor," *Analytical Chemistry,* vol. 78, no. 14, pp. 4909-4917, 2006.

[3] F. Gielen *et al.*, "Interfacing Microwells with Nanoliter Compartments: A Sampler Generating High-Resolution Concentration Gradients for Quantitative Biochemical Analyses in Droplets," (in English), *Analytical Chemistry,* vol. 87, no. 1, pp. 624-632, Jan 6 2015.

[4] J. L. Garcia-Cordero and Z. H. Fan, "Sessile droplets for chemical and biological assays," *Lab on a Chip,* 10.1039/C7LC00366H vol. 17, no. 13, pp. 2150-2166, 2017.

[5] M. Nakano *et al.*, "Single-molecule reverse transcription polymerase chain reaction using water-in-oil emulsion," (in English), *Journal of Bioscience and Bioengineering,* vol. 99, no. 3, pp. 293-295, Mar 2005.

[6] S.-Y. Teh, R. Lin, L.-H. Hung, and A. P. Lee, "Droplet microfluidics," *Lab on a Chip,* vol. 8, no. 2, pp. 198-220, 2008.

[7] S. L. Feng, M. N. Nguyen, and D. W. Inglis, "Microfluidic Droplet Extraction by Hydrophilic Membrane," (in English), *Micromachines,* vol. 8, no. 11, Nov 2017.

[8] T. R. Slaney *et al.*, "Push–pull perfusion sampling with segmented flow for high temporal and spatial resolution in vivo chemical monitoring," *Analytical chemistry,* vol. 83, no. 13, pp. 5207-5213, 2011.

[9] M. Wang, G. T. Roman, K. Schultz, C. Jennings, and R. T. Kennedy, "Improved temporal resolution for in vivo microdialysis by using segmented flow," (in English), *Analytical Chemistry,* vol. 80, no. 14, pp. 5607-5615, Jul 15 2008.

[10] M. Wang, G. T. Roman, M. L. Perry, and R. T. Kennedy, "Microfluidic chip for high efficiency electrophoretic analysis of segmented flow from a microdialysis probe and in vivo chemical monitoring," *Analytical chemistry,* vol. 81, no. 21, pp. 9072-9078, 2009.

[11] D. Chen *et al.*, "The chemistrode: a droplet-based microfluidic device for stimulation and recording with high temporal, spatial, and chemical resolution," *Proceedings of the National Academy of Sciences,* vol. 105, no. 44, pp. 16843-16848, 2008.

[12] S. L. Feng, G. Z. Liu, L. M. Jiang, Y. G. Zhu, E. M. Goldys, and D. W. Inglis, "A microfluidic needle for sampling and delivery of chemical signals by segmented flows," (in English), *Applied Physics Letters,* vol. 111, no. 18, Oct 30 2017.

[13] A. Kazemzadeh, P. Ganesan, F. Ibrahim, M. M. Aeinehvand, L. Kulinsky, and M. J. Madou, "Gating valve on spinning microfluidic platforms: A flow switch/control concept," *Sensors and Actuators B: Chemical,* vol. 204, pp. 149-158, 2014.

[14] H. Gu, M. H. G. Duits, and F. Mugele, "Droplets Formation and Merging in Two-Phase Flow Microfluidics," (in English), *International Journal of Molecular Sciences,* vol. 12, no. 4, pp. 2572-2597, Apr 2011.

[15] H. Gu, M. H. Duits, and F. Mugele, "Droplets formation and merging in two-phase flow microfluidics," *International journal of molecular sciences,* vol. 12, no. 4, pp. 2572-2597, 2011.

[16] C. N. Baroud, J.-P. Delville, F. Gallaire, and R. Wunenburger, "Thermocapillary valve for droplet production and sorting," *Physical Review E,* vol. 75, no. 4, p. 046302, 2007.

[17] M. Zagnoni and J. M. Cooper, "On-chip electrocoalescence of microdroplets as a function of voltage, frequency and droplet size," *Lab on a Chip,* vol. 9, no. 18, pp. 2652-2658, 2009.

[18] C. N. Baroud, F. Gallaire, and R. Dangla, "Dynamics of microfluidic droplets," *Lab on a Chip,* vol. 10, no. 16, pp. 2032-2045, 2010.

[19] A. E. Kamholz and P. Yager, "Molecular diffusive scaling laws in pressure-driven microfluidic channels: deviation from one-dimensional Einstein approximations," *Sensors and Actuators B: Chemical,* vol. 82, no. 1, pp. 117-121, 2002.

[20] F. Sarrazin, L. Prat, N. Di Miceli, G. Cristobal, D. Link, and D. Weitz, "Mixing characterization inside microdroplets engineered on a microcoalescer," *Chemical Engineering Science,* vol. 62, no. 4, pp. 1042-1048, 2007.

[21] Y. Luo, H. Liu, Q. Rui, and Y. Tian, "Detection of extracellular H2O2 released from human liver cancer cells based on TiO2 nanoneedles with enhanced electron transfer of cytochrome c," *Analytical chemistry,* vol. 81, no. 8, pp. 3035-3041, 2009.

[22] B. Halliwell, M. V. Clement, and L. H. Long, "Hydrogen peroxide in the human body," *FEBS letters,* vol. 486, no. 1, pp. 10-13, 2000.

[23] B. Halliwell, L. H. Long, T. P. Yee, S. Lim, and R. Kelly, "Establishing biomarkers of oxidative stress: the measurement of hydrogen peroxide in human urine," *Current medicinal chemistry,* vol. 11, no. 9, pp. 1085-1092, 2004.

[24] D.-H. Wang *et al.*, "Urinary Hydrogen Peroxide as Biomarker," *General Methods in Biomarker Research and their Applications,* pp. 313-331, 2015.

[25] J. Yuen and I. Benzie, "Hydrogen peroxide in urine as a potential biomarker of whole body oxidative stress," *Free radical research,* vol. 37, no. 11, pp. 1209-1213, 2003.

[26] K. B. Daniel, A. Agrawal, M. Manchester, and S. M. Cohen, "Readily accessible fluorescent probes for sensitive biological imaging of hydrogen peroxide," *ChemBioChem,* vol. 14, no. 5, pp. 593-598, 2013.

[27] M. J. Rosen and J. T. Kunjappu, *Surfactants and interfacial phenomena*. John Wiley & Sons, 2012.

***Research Highlights**

Research highlights:

1. The probe solved the Taylor dispersion problem by droplets when transporting signals along the microchannel. Varying chemical signals can be sampled and transported with high temporal, spatial and chemical resolution. This system is suitable for the studying of rapid (~1 s) chemical changes in dynamic biological systems.
2. Laplace pressure can be generated at the needle tip by microfabrication of several hydrophilic features. This can provide a safe sampling and delivery environment, where only the aqueous liquid can go through the tip and the continuous oil phase will be kept inside the system. So it does not need a tight seal between device and tissue for delivery and sampling.
3. The sampled fluid is immediately merged with the assay droplet and carried away to mix and react, producing a sequence of droplets representing the H_2O_2 concentration as a function of time. With the calibration, we can calculate the concentration of H_2O_2 in the sampled liquid from the size and intensity of each merged droplet.
4. It is a useful tool for monitoring dynamic chemical reactions in analytical chemistry and biological applications. The approach facilitates thousands of detections in a single run and may be used to quantify the kinetic reactions in a low-cost and rapid way.

Author Biographies

Mr Shilun Feng had completed his Bachelor's degree since 2013 from Yanbian University, Jilin, China in Pharmaceutics. He completed his master's degree from Department of Micro and Nano Systems Technology (IMST), Buskerud and Vestfold University College (HBV), Tønsberg, Norway in Biomedical Microelectromechanical systems (Bio-MEMS). He is currently pursuing his PhD in Biomedical Engineering, focusing on microfabrication, biomedical microfluidics and 3D printing in the School of Engineering, Faculty of Science and Engineering, Macquarie University, Australia.

Dr Sandhya Clement received her PhD degree from the Department of Physics & Astronomy, Macquarie University, Australia in the year 2016 for the thesis titled "Towards photodynamic therapy with ionising radiation: nanoparticle-mediated singlet oxygen generation and quantification". Before coming to Australia, She was working as a Lecturer in the Department of Electronics and Communication Engineering, College of Engineering Munnar, Kerala, India from 2001-2012. She is now working as a Research Associate with Prof Ewa M. Goldys in the Graduate School of Biomedical Engineering, University of New South Wales, Australia. Her research focus is mainly on nanotheranostics with an emphasis on photodynamic therapy and Reactive Oxygen species quantification.

Professor Yonggang Zhu is currently a "Thousand Talents" Professor and director of Center for Microflows and Nanoflows at Harbin Institute of Technology (ShenZhen), China, and a joint Professor at School of Science, RMIT University, Australia. Prior to this, he held the positions of Senior Principal Research Scientist and Research Team Leader for the Microfluidics and Fluid Dynamics Team in CSIRO Australia, Senior Technology Fellow at Melbourne Centre for Nanofabrication. His current research interests include micro- and nanoscale thermal & fluid flows, lab on a chip devices, microtheraml systems, multiphase flows and micro-sensors. He has led many research and development projects in developing advanced technologies for chemical and biological sensing, new materials development, thermal management systems and industry applications. Prof. Zhu has published over 200 papers including book chapters, journal articles, conference papers and technical reports. He

is the winner of 2012 Australian Museum Eureka Science Prize for Outstanding Science in Support of Defence or National Security.

Professor Ewa M. Goldys is Deputy Director of the Australian Research Council Centre of Excellence in Nanoscale Biophotonics (cnbp.org.au). She is SHARP Professor at the Graduate School of Biomedical Engieering at the University of New South Wales, Sydney, Australia Previously she held a Personal Chair in the Department of Physics and Astronomy at Macquarie University, Sydney, Australia. She is Fellow of SPIE, Fellow of the Optical Society, Fellow of Australian Academy of Technology and Engineering, (ATSE) and winner of the 2016 Australian Museum Eureka Prize for 'Innovative Use of Technology'.

Her research spans the interface of ultrasensitive optical characterization, biotechnology, materials science and photonics. A portfolio of her works is centred on the development and understanding of luminescence emission in doped nanocrystals where she developed advanced methods of synthesis and characterisation of fluorescent nanoparticles for applications in fluorescence labelling. Her expertise in ultrasensitive optical characterisation and nanotechnology led to the development of novel approaches to biochemical and medical sensing and diagnostics. Current projects focus on label-free non-invasive high content cellular imaging and characterisation of cell subpopulations, on nanoparticle chemical sensors and theranostics.

Dr Inglis received a B.Sc in Engineering Physics from The University of Alberta in 2001 and a PhD in Electrical Engineering from Princeton University in 2007. He was an Australian Postdoctoral Fellow in the Physics Department of Macquarie University from 2008 to 2011. He is now a Senior Lecturer in the School of Engineering at Macquarie University.

Dr Inglis research interests lie in microfabrication for medicine and biology. He is well known for work on deterministic lateral displacement separations, and has published more than 30 research articles and patents that have been cited more than 2000 times.

Chapter 5: Design and fabrication of a membrane-in-pipette-tip system

5.1 Background

Our group achieved silicon-based microfluidic probes with a bubble-pressure flow barrier at the tip [41], described in Chapter 3 and Chapter 4. The microfabrication of silicon-based devices is time-consuming and expensive. For this reason, I also developed a membrane-based system, which is described in this chapter.

We describe our system as a membrane-in-pipette tip system. The porous hydrophilic membrane monoliths will be attached covalently to the walls of the channels in the plastic tip, which has small enough pores to cause a significant Laplace pressure when wet. It can generate a flow barrier for safe sampling and delivery using droplets.

During the design and fabrication of this membrane-in-pipette tip system, we also tried a membrane-at-needle-tip system as well as the membrane-on-chip system. Two systems mentioned were given up in this section because of microfabrication issues.

The fabrication of the tip part of the device was completed by our collaborator at Professor Emily Hilder's group in the University of South Australia, with the methods described in [144], but the device design and assembly were completed by us. Moreover, we set up the experiment to make the demonstration. I have demonstrated its capabilities for sampling and delivery of chemicals as droplets. The Laplace pressure flow barrier can be achieved at the pipette tip and is low cost, so we believe it has significant commercial potential.

5.2 Theory of membrane-based microfluidic probe systems

The membrane normally has the hydrophilic porous structures. When the water contacts with the membrane, the water will go and fill in the membrane automatically. If the negative pressure is applied inside the tip, the liquid inside the membrane will be extracted to the oil phase inside the tip. the oil around the tip can be used to break the extracted aqueous liquid into droplets. This droplet formation method is labelled flow focusing (as shown in Figure 13 c)).

Laplace pressure will be generated in the wet hydrophilic membrane [145] at the tip, which can generate a safe sampling/delivery barrier (see theory description in Section 2.2). In order to make the system operational, the membrane itself must have a preference for water over oil and contain pores that are small enough to generate significant Laplace pressure. This can generate a high-bubble-pressure barrier for safe sampling and delivery.

5.3 Design and fabrication

In this section, we describe three membrane-based microfluidic probe systems: a membrane-at-needle-tip system, a membrane-on-chip system and a membrane-in-pipette tip system. We glued a steel needle to one commercial membrane (Sartorius 16534-GUK Minisart Cellulose Acetate NML Syringe Filter, Sterile, Luer Lock Outlet, 0.2 µm, 28 mm), for the membrane-at-needle-tip system. We are not convinced about this system because the existing microfabrication issues limit its further application. We also developed the membrane-on-chip system [77] with the same membrane, but we encountered leakage problems before we could test the system in a biomedical application. Finally, we have successfully developed a membrane-in-pipette tip system with a home-made membrane and

the membrane (made by Professor Emily Hilder's group) is located in the pipette tip to avoid the microfabrication issues that above two systems met.

5.3.1 Membrane-at-needle-tip design and fabrication

We firstly used the hydrophilic membrane which is located and glued at the open end of a commercial G23 steel needle. This served to generate the Laplace pressure as the flow barrier at the tip. The initial design of the device was that a smaller tube would be inserted through the steel needle with one end on the membrane. When we provided negative pressure at the other end, the droplets could be generated using the co-flow principle.

We grinded the G23 steel needle to a flat 45-degree face. When the needle is pressed onto the membrane under a given force, the needle tip is glued with the membrane, as shown in Figure 23. We tried using a laser cutting technique to remove the glue, but we failed.

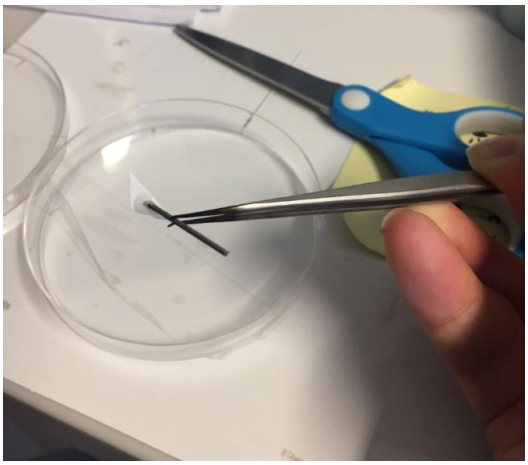

Figure 23. Device layout and design of the membrane-at-needle-tip system. Note the G23 steel needle grinded to a flat 45-degree face with hydrophilic membrane attached by glue.

5.3.2 Membrane-on-chip design and fabrication

Figure 24 depicts another developed membrane-on-chip system by our group and fabricated by one master student Michael Nguyen. We used the same hydrophilic commercial

membrane (Sartorius 16534--GUK Minisart Cellulose Acetate NML Syringe Filter, Sterile, Luer Lock Outlet, 0.2 µm, 28 mm) located at the sampling point in the chip and right above the channel to generate the Laplace pressure as the flow barrier. Below is a short description of the system while more details can be found in our publication [105].

There are three main parts: COC base, membrane, and lid. They were bonded together to form a single device. Using a method that is similar to embossing, the lid and the base were placed in a vacuum oven at 160 °C for 10 minutes. The assembly was annealed at the standard atmospheric pressure and 90 °C for 10 minutes; then the sample was left to cool to room temperature.

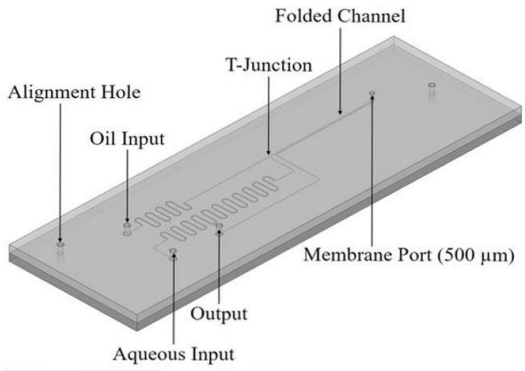

Figure 24. Device layout and design of the membrane-on-chip system. Note the oil and aqueous inputs, T-junction, and the membrane port.

For manufacturing simplicity, our entire channel, including the T-junction, was fabricated using a 100-µm bit on a micromachining mill to a depth of 100 µm. Upstream of the T-junction are two channels carrying oil and water respectively. Ports were arranged in a 9-mm by 9-mm square, the spacing of a 96-sample-well microtiter plate. In order to facilitate a smaller pressure difference at the T-junction, the water channel was made approximately 100 mm in length, while the oil channel, which carries more viscous fluid, was about 50 mm long.

The membrane, with its thickness, prevents the lid from contacting and bonding to the bottom substrate in a region of a few hundred microns around the membrane disk. When a droplet that is confined to the channel reaches this area, it begins to leak into the space around the membrane, so we did not continue this for further biological applications.

5.3.3 Membrane-in-pipette-tip system design and fabrication

This system avoids the microfabrication issues mentioned in the other mentioned systems. Figure 25 below shows one example of the finally designed membrane-in-pipette system device with the 200 µL gel-loading pipette tip (BIO-RAD). The whole device consists of a hydrophobic plastic tube (a pipette tip or IV cannula) that has a hydrophilic membrane at its tip and an inner smaller tubing all through to its open end near the membrane.

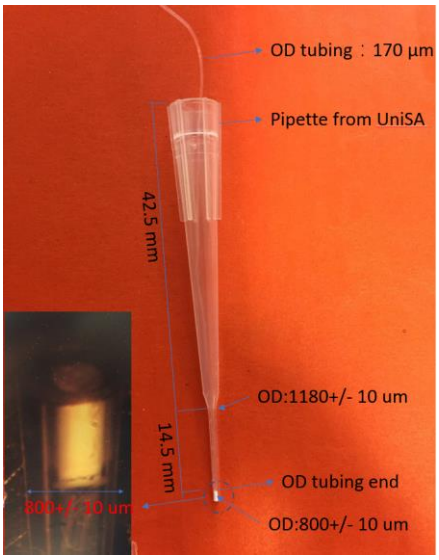

Figure 25. Device Layout and design of membrane-in-pipette-tip system. Note the pipette's diameter, the membrane's location and membrane parameters.

The hydrophilic porous polymer membrane covalently attached to the inner channel walls of the tip. The tip has an OD of 800 ± 10 µm. Meanwhile, the length can be adjusted by cutting the pipette with membrane using a regular scalpel, where the end is around 114.5mm from

the pipette's structure (a position with OD: 1180 ± 10 µm). We can then adjust the location of the end of the inner tube.

The hydrophilic membrane attached to the pipette tip was developed by collaborators from Professor Emily Hilder's group at the University of South Australia. The following procedure was provided by PhD candidate James Hsian-Meng. There are two main steps: surface modification of the pipette tips and a polymer monolith polymerization procedure.

For surface modification of pipette tips, the polypropylene pipette tip surface was modified using a methanolic-benzophenone solution and UV radiation, to allow adhesion of a polymer monolith onto the pipette tip wall during in-situ polymerisation. Methanolic-benzophenone solution was filled into the pipette tip and irradiated under an OAI Deep UV 260 nm curing system for about 10 minutes. The tips were then washed and dried in a 40 ^{o}C oven prior to use.

The next step is the polymer monolith polymerisation procedure. In a glass vial, 2-hydroxyethyl methacrylate acid (2HEMA, Sigma-Aldrich) and ethylene glycol dimethacrylate acid (EDMA, Sigma-Aldrich) were mixed together with 1% w/w of photo-initiator DMPA (2,2-dimethoxy-2-phenylacetophenone, Sigma-Aldrich). Subsequently, 60% of porogens mixture consisting of 1-dodecanol and cyclohexanol were added and degassed using nitrogen gas for 3 minutes. The solution was then aspirated into a pipette tip and irradiated using an OAI Deep UV 260 nm curing system for about 10 minutes. During polymerisation, it can be observed that the solution changed from transparent to opaque, and then to white when a solid structure of polymer monolith was formed at the end. The pipette tips were flushed with methanol to remove excess unreacted monomers and solvents. The tips were then dried in an oven at 40 ^{o}C overnight before use.

5.4 Results

Even though we tried the membrane-at-needle-tip system as well as the membrane-on-chip system, these two are failed in the design and microfabrication process for further biomedical applications, so we don't have results to show here. Below are some early results about the membrane-in-pipette-tip system.

5.4.1 Measurement of the wet membrane Laplace pressure

We did the experiments with a 200 µL standard pipette tip (Freloads, the same one as in Figure 26) and retained the 8 µL membrane. We firstly pushed in water to replace air until of the 8 µL membrane was wet, and then we pushed air in to replace the water. The breakthrough pressure for air going through the water was 100.8 ± 1 kPa.

The surface tension of air/water is around 70 mN/m and based on Equation 3 the radius of the pore will be around 1.4 cosθ µm. Since it is hydrophilic, if the contact angle is 40℃. the diameter of the hole will be approximately 2.14 µm.

Based on Equation 3, and with the same radius and contact angle with the measurement of air/ water, the surface tension of water/ mineral oil is 49.6 mN/m at room temperature (22 ℃) [146], so we can calculate that the theoretical Laplace pressure for water/oil with the hydrophilic membrane is 72 kPa. This value will decline if the contact angle increases (or the hydrophilic degree is less). We measured the oil breakthrough water pressure; the membrane was immersed in water, oil was pushed away the water and occupied the membrane, and the pressure was measured as being around 54 kPa.

5.4.2 Demonstration of sampling and delivery

Figure 26 depicts the 200 µL pipette with 8 µL membrane for droplet delivery to the needle and extraction from outside the needle. When the probe tip is placed in a water-based liquid, that liquid is wicked into the membrane.

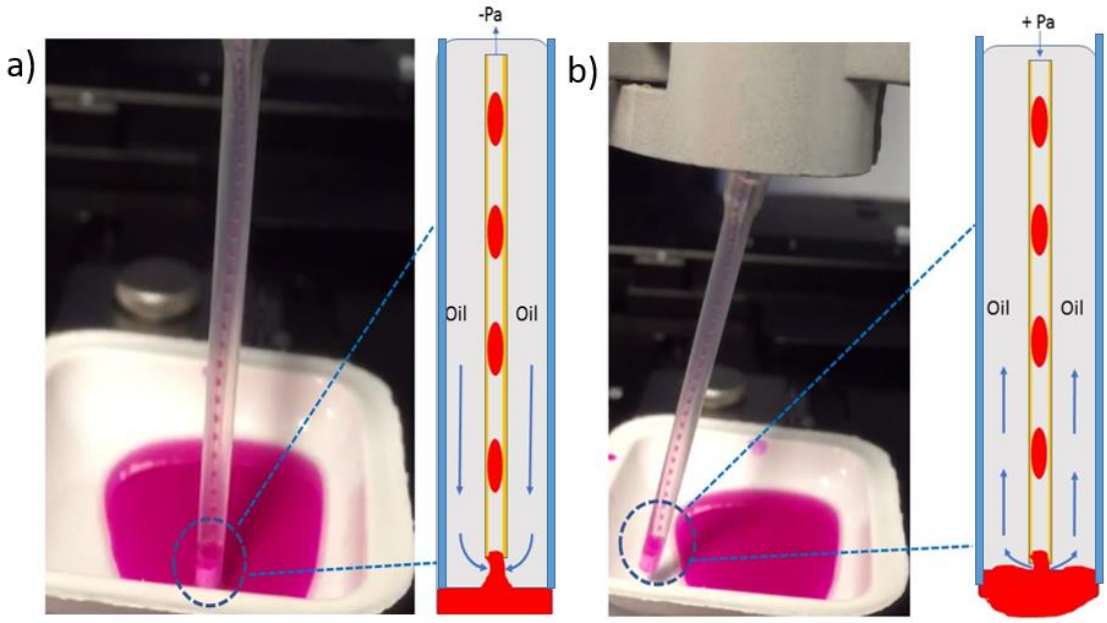

Figure 26. Demonstration of the membrane-in-pipette-tip system for droplets a) delivery to and b) extraction from outside the needle.

Meanwhile, the large probe and small tube are filled with mineral oil. If we apply negative pressure to the inner tube, the water-based sample is drawn into the probe, and nanoliter volumes of the sample form droplets or segmented flows and are transported up the small tube along with the immiscible oil to the detection site or stored in the long tube. The sampling rate is controlled by the pressures applied to the two tubes. These samples can be transported long distances without mixing or diluting, which helps to preserve the chemical signals for analysis.

If we apply positive pressure to the small tube and entrain water-in-oil droplets in it, those droplets exit the probe tip. However, the oil does not exit until the real pressure becomes larger than the Laplace pressure of oil/ water. In this way, we can entrain sequences of different droplets, that are able to deliver chemical signals. These signals are complex in terms of both content and timing.

5.4.3 Use of the automatic platform

A home-made controlled platform was used; the system is from an old 3D printing system as shown in Figure 27. It was manufactured by William Bales of TinkersProjects.com, programmed and adjusted to the x, y, z positions as shown.

Figure 27. Auto-controlled platform for a) sampling and b) delivery droplets using the membrane-in-pipette-tip system.

Multi-sampling and delivery by the controlled platform were done. To generate consistent droplets, we set the oil inlets as 10 kPa, outlet as -25 kPa, and submerged the tip in the water samples. Consistent droplets can be sampled at the needle tip, by changing three different

concentrations of dye (red, green and blue), as indicated in Figure 27 a), The delivered droplets can also be successfully loaded into the wells one by one on the MALDI plate, as indicated in Figure 27 b).

5.4.4 Chemical resolution analysis

Regarding the sampling tool shown in Figure 27 a), the inner diameter of the inner tube is around 1 mm. Negative pressure will be given at the inner tube outside the pipette, while the positive pressure will be given on the oil inlet to provide a continuous oil flow.

When the negative pressure is 50 kPa at the tip, we recorded the experiment on video which confirmed that the size of the generated droplets is consistent with the length of the water droplets is around 1.43 mm, while the length of the continuous oil-phase gap is around 7.41 mm. The volume of the water droplets is around 1.43 µL.

We sampled three different dyes, these being red, green and blue. We calculated the response flux, which we define as the volume needed to exchange one chemical for another in the droplet train. The volume needed from the green dye to the blue dye is around 5-6 droplets in an estimated time of 8 s. The volume of the membrane is calculated at around 7.15-8.58 µL based on the droplet number (5 droplets) and the single-droplet volume (1.43 µL). The volume of the membrane was around 8.00 µL, which is in the calculated range (7.15-8.58 µL).

5.5 Discussion and perspective

More experiments will be done in the future to examine the device, including the following: the relationships between different volumes of the porous hydrophilic membrane; different response fluxes; the relationships among the different flow rates; and how the volume results

to variations in the flow rate. Furthermore, gas/liquid sampling of the three colour dyes was achieved; the sampled droplets can be located on the glass slide one by one, which is shown in Figure 28, and can be used for off-line sample enrichment (described in Section 2.1), but this is still in the process of investigation.

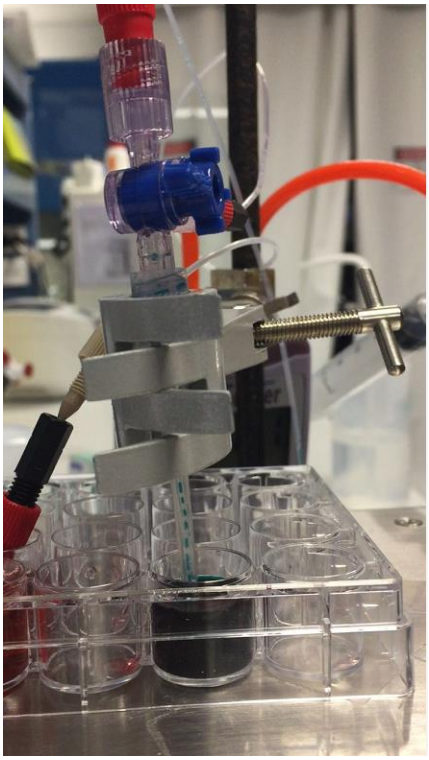

Figure 28. Demonstrate of air/ water sampling using the membrane-in-pipette tip system.

The volume of liquid held in the membrane located at the pipette tip is equal to the dead volume. This has a significant effect on the temporal resolution. It depends on the cross-section diameter of the pipette tip used as well as the length of the membrane inside the tip. So, as the next step, we choose the smallest pipette tip which can be used. The length can also be adjusted by cutting the pipette and the membrane using a regular scalpel.

In this work, a novel microfluidic membrane-in-pipette-tip system was used for *ex-vivo* detection. It has been demonstrated that this system can deliver a segmented flow and form segmented flows from aqueous surroundings for sampling. A novel, inexpensive microfluidic

membrane-in-pipette-tip sampling probe that can extract and transport nanolitre samples in droplet format has been developed. The device consists of a hydrophilic porous membrane covalently attached to the inner walls of a pipette tip. This membrane forms a phase-extraction region, and a Laplace pressure barrier can be generated at the porous membrane, which makes it a flow barrier for safe delivery and sampling of chemicals. One hydrophobic tube will be located in the middle of the plastic pipette, and it ends directly above the hydrophilic membrane. We demonstrated the sampling by the formation of segmented flows at the tip of our device and inside the inner tube. The negative pressure of the tubing generates forces to drag samples through the membrane and forms droplets in the tubing in the continuous mineral-oil phase using flow focusing principle. We also demonstrated the method of delivery by transporting the droplets to the membrane at the tip; the sample droplets can be released from the membrane to the outside of the tip. The automated controlled stage was used, which helped the tip to move to the desired positions. We achieved multisampling as well as sample delivery to the MALDI plate for further analysis.

5.6 Conclusion

In Chapter 5, we fabricated a membrane-in-pipette-tip system, where the hydrophilic membrane was located at the tip of a commercial pipette. We demonstrated its capability for sampling and delivery with droplets. It can be used with an automatic controlling platform and be moved to the desired x-y-z location. The only drawback is the large dead volume (around 8 µL), that will be improved in the next generation. On the positive side, the use of droplets to preserve chemical signals as well as employing a bubble-pressure flow barrier

have been succeeded and are inexpensive. For these reasons, we believe it has a significant commercial potential after further development.

Chapter 6 Conclusion and outlook

This thesis presents two types of novel droplet-based microfluidics probes (the silicon-based microfluidic probe and the membrane-based microfluidic probe) with enhanced performance over conventional needles (or similar probes) for sampling and delivery. Our droplet-based microfluidic-probe systems, proposed by us for the first time, are controlled by a bubble-pressure flow barrier at the probe tips for both sampling and delivery. The conclusions and future directions of this thesis are drawn as below.

6.1 Conclusions

We have met the aims listed in Chapter 1.2. Firstly, we have developed the droplet-based microfluidic probe system that can extract nanolitre volumes of chemical solutions as well as generate samples in a droplet format for transporting and analysis with good chemical, spatial and temporal resolution; the strategies are reviewed in Section 2.1. Moreover, the Laplace pressure was used as a flow barrier at the probe tip, which can ensure that no oil ever exits out of the probe to the tissue/body, which is reviewed in Section 2.2

Furthermore, we have successfully deigned and fabricated two systems: a silicon-based microfluidic device and a membrane-based microfluidic device. The silicon-based microfluidic probe is described in Chapter 3. We have demonstrated that the system can both sample and deliver chemical signals with droplets. The relationship between the recorded sample signals and the external dye concentration (10 to 40 μg/mL) indicates that this device is capable of quantitative, real-time measurements of rapidly varying chemical signals with a temporal resolution of around 3 seconds. We observed that a significant breakthrough pressure of 19 kPa was required to force oil out through the capillaries. We also made a membrane-based

microfluidic probe, namely a membrane-in-pipette-tip system which is described in Chapter 5. This kind of microfluidic probe harnesses the benefits of droplet-based fluid delivery and a high breakthrough pressure to prevent the continuous oil phase from leaving the needle tip. We located the hydrophilic membrane inside the membrane tip. It can generate a Laplace pressure of 54 kPa when the air is used to push the wetted membrane. It is low-cost and easy to fabricate.

Two kinds of microfluidic probes have been compared here. They have some things in common. Firstly, they all have the advantages of using droplets as well as having a flow barrier. Secondly, they all use the sampling method of 'Droplets formed at the source with a barrier' (in Section 2.1.3.3.2). Thirdly, they present a platform for on-line fluorescence detection. However, they also have differences. Firstly, seven hydrophilic capillaries (around 2 µm in diameter) with a dead volume of 2.8 pL are used in the silicon-based microfluidic probe to generate a high enough Laplace pressure (around 19 kPa) as a flow barrier. A hydrophilic membrane with a volume of around 8 µL was used in the membrane-based microfluidic probe to generate the bubble-pressure flow barrier, which has a worse temporal resolution. Reducing this volume is essential for the next step. The Laplace pressure generated at the wetted membrane tip was measured to be around 54 KPa, which is a bit higher than the one measured in the silicon-based probe. Secondly, the droplet-generation methods of the extracted samples are different. The silicon-based microfluidic probe uses the T-junction method to generate droplets, while the membrane-based microfluidic probe uses the flow focusing method to generate droplets. Thirdly, the silicon-based system can perform droplets merging, mixing in a droplet, and biological assay reactions, which gives needle-in answer-out monitoring of chemical signals. We have demonstrated the use of an on-chip assay for

hydrogen peroxide detections. The present approach segments the sample immediately upon entering the device to merge and react with the assay, and through the use of a hydrophilic barrier, a tight seal is not required. As well as performing this long-reaction-time H_2O_2 assay (>15 minutes), our system is also the right tool for studying more rapid (~1 s) chemical changes in dynamic systems. It is expected that these systems, with an enclosed channel and minimal handling, could play an essential role in improving the reliability of devices for diagnostics technology. Thousands of reactions can be recorded in a single run, which can expand the use of our developed probe for assay qualification. Last but not least, fabrication of the silicon-based microfluidic system is time-consuming and costly, while fabrication of the membrane-based microfluidic system is cheaper and easier to manufacture, and so has a large potential for commercialisation.

The needle has been in development for more than 450 years. It has led to our microfluidic needle-like probe, which may be commercialised or widely used as an inexpensive and safe tool for sampling, delivery, storing and monitoring of quickly changing chemical signals.

6.2 Future directions

In terms of the improvement of the membrane-based device, we can focus on increasing the temporal, spatial and chemical resolution for the detection. This can be achieved by making the membrane volume at the tip as small as possible. The dead volume depends on the inner diameter of the pipette tip as well as the length of the membrane. In future work, we will further miniaturise the pipette tip. The length can also be adjusted by cutting the pipette and the membrane using a regular scalpel.

For both the silicon-based microfluidic system and the membrane-based microfluidic system, only simple sampling and delivery have been performed. Two future aims are sampling and analysis of *in vivo* neurotransmitters from a mouse brain with chemical, spatial and temporal resolution, and delivery of multiple drugs into tissue while monitoring physiological response.

Appendix

Protocol 1: Chuck design and fabrication for lab use

To produce the microfluidics chip during the experiment, we designed and fabricated the chuck as Figure 29. The top layer structure has 8 ports, whereby 1-4 are for the inlets, and 5-8 are for the outlets. Each inlet ports and outlet port have a 9 mm gap; while ports 4 and 6 have a gap of 36 mm. There is a copper bottom layer, which will be connected with the top layer by four M6 screws. All the devices I created will follow this dimension arrangement, where the inlets and outlets will fit into the port.

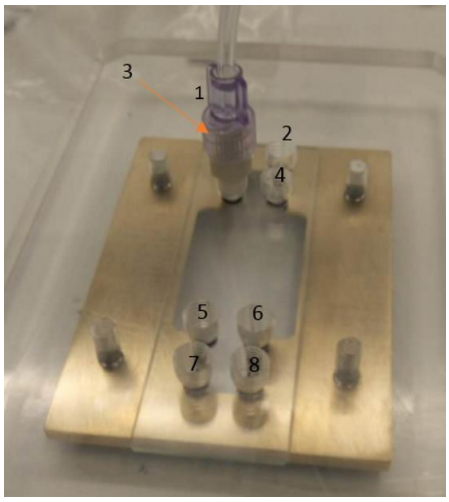

Figure 29. Chuck for holding the silicon device. For the top layer, there are 8 ports that connect to the external tube with the thread ¼-28 flat bottom fittings, which are labelled on the pictures. Holes with the numbers 1,2,3, and 4 are for the inlets, while holes with the numbers 5,6,7, and 8 are for the outlets. There is a copper bottom layer, which will be connected with the top layer by four M6 screws.

Protocol 2: Dicing of the silicon chip

We completed the dicing process at Macquarie University. Dicing was completed with the help of Dr Peter Dekker at the MQ Photonics Research Centre.

We prepared our wafer as shown in Figure 30 a), Norland Optical Adhesive 81 (NOA81) under UV treatment was used to bond the wafer to the platform for dicing as shown in Figure 30 b)-c). Using wax was another way to bond the wafer to the platform for dicing, as shown in Figure 30 d). Figure 30 e) is the alignment process before dicing, and Figure 30 f) shows that the dicing is in process. Figure 30 h) shows the dewaxing process either by a hot plate to remove the wax, or acetone to remove the NOA81 glue to obtain the parts we want.

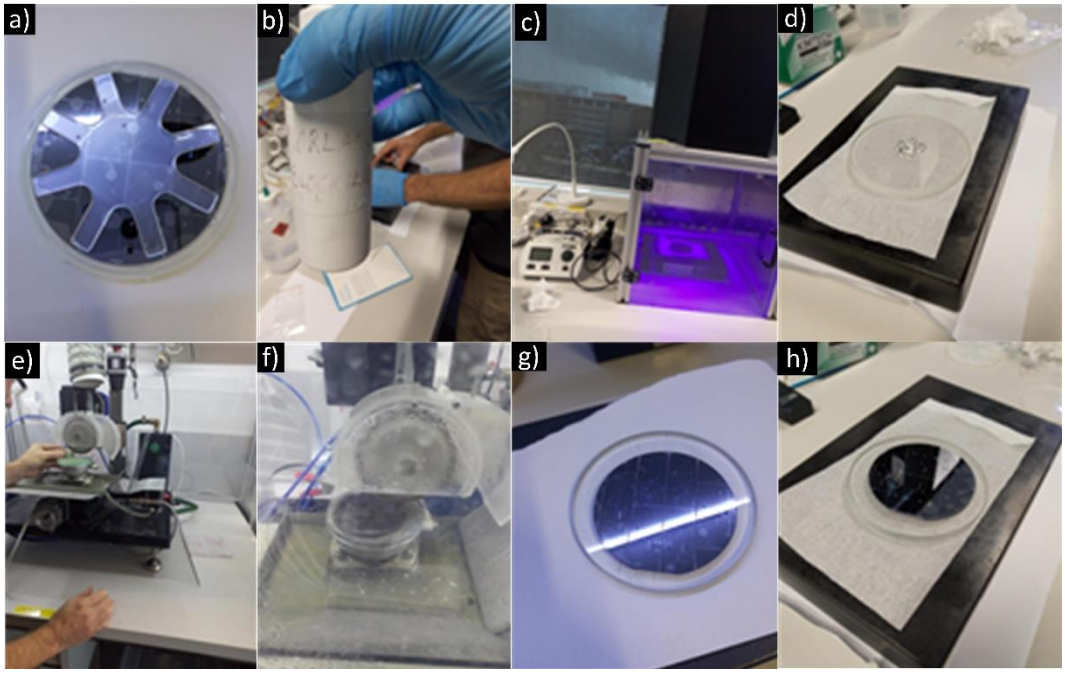

Figure 30. Dicing processes. a) Our device before dicing; b) Attaching wafer to the substrate process by the Norland Optical Adhesive 81 ("NOA81") to attach the wafer to the substrate process; c) UV curing the NOA 81 process; d) Another attaching wafer to substrate method by wax; e) the dicing machine alignment process; f) dicing in process; g) our wafers after dicing; f) after dewaxing Process.

Reference

[1] D. L. Robinson, A. Hermans, A. T. Seipel, and R. M. Wightman, "Monitoring rapid chemical communication in the brain," *Chemical reviews,* vol. 108, no. 7, pp. 2554-2584, 2008.

[2] M. Shou, C. R. Ferrario, K. N. Schultz, T. E. Robinson, and R. T. Kennedy, "Monitoring dopamine in vivo by microdialysis sampling and on-line CE-laser-induced fluorescence," *Analytical chemistry,* vol. 78, no. 19, pp. 6717-6725, 2006.

[3] F. Cesselin and M. Hamon, "Possible functional significance of the simultaneous release of several putative neurotransmitters by the same neuron," in *Annales d'endocrinologie*, vol. 45, no. 3, pp. 207-213, 1984.

[4] T. Hökfelt *et al.*, "Neuropeptides and classical transmitters. Localization and interaction," *Arzneimittel-Forschung,* vol. 42, no. 2A, pp. 196-201, 1992.

[5] I. Laing, A. Todd, C. Heizmann, and H. Schmidt, "Subpopulations of GABAergic neurons in laminae I–III of rat spinal dorsal horn defined by coexistence with classical transmitters, peptides, nitric oxide synthase or parvalbumin," *Neuroscience,* vol. 61, no. 1, pp. 123-132, 1994.

[6] M. K. Zachek, J. Park, P. Takmakov, R. M. Wightman, and G. S. McCarty, "Microfabricated FSCV-compatible microelectrode array for real-time monitoring of heterogeneous dopamine release," *Analyst,* vol. 135, no. 7, pp. 1556-1563, 2010.

[7] K. M. Wassum, V. M. Tolosa, J. Wang, E. Walker, H. G. Monbouquette, and N. T. Maidment, "Silicon wafer-based platinum microelectrode array biosensor for near real-time measurement of glutamate in vivo," *Sensors,* vol. 8, no. 8, pp. 5023-5036, 2008.

[8] L. Bert *et al.*, "In vivo temporal sequence of rat striatal glutamate, aspartate and dopamine efflux during apomorphine, nomifensine, NMDA and PDC in situ administration," *Neuropharmacology,* vol. 43, no. 5, pp. 825-835, 2002.

[9] P. Song, N. D. Hershey, O. S. Mabrouk, T. R. Slaney, and R. T. Kennedy, "Mass spectrometry “sensor” for in vivo acetylcholine monitoring," *Analytical chemistry,* vol. 84, no. 11, pp. 4659-4664, 2012.

[10] H. Bradford, J. Crowder, and E. White, "Inhibitory actions of opioid compounds on calcium fluxes and neurotransmitter release from mammalian cerebral cortical slices," *British journal of pharmacology,* vol. 88, no. 1, pp. 87-93, 1986.

[11] H. Elsheikh, B. Ali, A. Homeida, A. Lutfi, and H. Hapke, "The effects of fascioliasis on the activities of some drug-metabolizing enzymes in desert sheep liver," *British Veterinary Journal,* vol. 148, no. 3, pp. 249-257, 1992.

[12] S. G. Korenman, "Estrogen receptor assay in human breast cancer," *Journal of the National Cancer Institute,* vol. 55, no. 3, pp. 543-545, 1975.

[13] G. E. Scott and N. Zummo, "Sources of resistance in maize to kernel infection by Aspergillus flavus in the field," *Crop science,* vol. 28, no. 3, pp. 504-507, 1988.

[14] A. Leuchtmann and K. Clay, "Experimental infection of host grasses and sedges with Atkinsonella hypoxylon and Balansia cyperi (Balansiae, Clavicipitaceae)," *Mycologia,* pp. 291-297, 1988.

[15] A. Kotwal, "Innovation, diffusion and safety of a medical technology: a review of the literature on injection practices," (in English), *Social Science & Medicine,* vol. 60, no. 5, pp. 1133-1147, Mar 2005.

[16] S. Norn, P. R. Kruse, and E. Kruse, "[On the history of injection]," *Dan Medicinhist Arbog,* vol. 34, pp. 104-13, 2006.

[17] C. Ball, "The early development of intravenous apparatus," (in English), *Anaesthesia and Intensive Care,* vol. 34, pp. 22-26, Jun 2006.

[18] B. Xu, "High-aspect-ratio microdevices and methods for transdermal delivery and sampling of active substances," ed: Google Patents, 2009.

[19] G. Taylor, "Dispersion of Soluble Matter in Solvent Flowing Slowly through a Tube," *Proceedings of the Royal Society of London. Series A. Mathematical and Physical Sciences,* vol. 219, no. 1137, pp. 186-203, 1953.

[20] N. Ostromohov, M. Bercovici, and G. Kaigala, "Delivery of minimally dispersed liquid interfaces for sequential surface chemistry," *Lab on a Chip,* vol. 16, no. 16, pp. 3015-3023, 2016.

[21] X. C. i Solvas, "Droplet microfluidics: recent developments and future applications," *Chemical Communications,* vol. 47, no. 7, pp. 1936-1942, 2011.

[22] A. E. Kamholz, B. H. Weigl, B. A. Finlayson, and P. Yager, "Quantitative analysis of molecular interaction in a microfluidic channel: The T-sensor," (in English), *Analytical Chemistry,* vol. 71, no. 23, pp. 5340-5347, Dec 1 1999.

[23] K. Macounova, C. R. Cabrera, M. R. Holl, and P. Yager, "Generation of natural pH gradients in microfluidic channels for use in isoelectric focusing," (in English), *Analytical Chemistry,* vol. 72, no. 16, pp. 3745-3751, Aug 15 2000.

[24] J. Yang, Y. Huang, X. B. Wang, F. F. Becker, and P. R. C. Gascoyne, "Differential analysis of human leukocytes by dielectrophoretic field-flow-fractionation," (in English), *Biophysical Journal,* vol. 78, no. 5, pp. 2680-2689, May 2000.

[25] Y. H. Chen and S. H. Chen, "Analysis of DNA fragments by microchip electrophoresis fabricated on poly(methyl methacrylate) substrates using a wire-imprinting method," (in English), *Electrophoresis,* vol. 21, no. 1, pp. 165-170, Jan 2000.

[26] D. J. Ehrlich and P. Matsudaira, "Microfluidic devices for DNA analysis," (in English), *Trends in Biotechnology,* vol. 17, no. 8, pp. 315-319, Aug 1999.

[27] A. E. Kamholz and P. Yager, "Theoretical analysis of molecular diffusion in pressure-driven laminar flow in microfluidic channels," (in English), *Biophysical Journal,* vol. 80, no. 1, pp. 155-160, Jan 2001.

[28] J. H. Chan, A. T. Timperman, D. Qin, and R. Aebersold, "Microfabricated polymer devices for automated sample delivery of peptides for analysis by electrospray ionization tandem mass spectrometry," (in English), *Analytical Chemistry,* vol. 71, no. 20, pp. 4437-4444, Oct 15 1999.

[29] J. J. Li, J. F. Kelly, I. Chemushevich, D. J. Harrison, and P. Thibault, "Separation and identification of peptides from gel-isolated membrane proteins using a microfabricated device for combined capillary electrophoresis/nanoelectrospray mass spectrometry," (in English), *Analytical Chemistry,* vol. 72, no. 3, pp. 599-609, Feb 1 2000.

[30] D. M. Pinto, Y. B. Ning, and D. Figeys, "An enhanced microfluidic chip coupled to an electrospray Qstar mass spectrometer for protein identification," (in English), *Electrophoresis,* vol. 21, no. 1, pp. 181-190, Jan 2000.

[31] A. Bernard, E. Delamarche, H. Schmid, B. Michel, H. R. Bosshard, and H. Biebuyck, "Printing patterns of proteins," (in English), *Langmuir,* vol. 14, no. 9, pp. 2225-2229, Apr 28 1998.

[32] D. T. Chiu *et al.*, "Patterned deposition of cells and proteins onto surfaces by using three-dimensional microfluidic systems," (in English), *Proceedings of the National Academy of Sciences of the United States of America,* vol. 97, no. 6, pp. 2408-2413, Mar 14 2000.

[33] A. Folch and M. Toner, "Cellular micropatterns on biocompatible materials," (in English), *Biotechnology Progress,* vol. 14, no. 3, pp. 388-392, May-Jun 1998.

[34] P. J. A. Kenis, R. F. Ismagilov, and G. M. Whitesides, "Microfabrication inside capillaries using multiphase laminar flow patterning," (in English), *Science,* vol. 285, no. 5424, pp. 83-85, Jul 2 1999.

[35] S. Datta and S. Ghosal, "Characterizing dispersion in microfluidic channels," (in English), *Lab on a Chip,* vol. 9, no. 17, pp. 2537-2550, 2009.

[36] B. J. Kirby, *Micro-and nanoscale fluid mechanics: transport in microfluidic devices*. Cambridge university press, 2010.

[37] K. Thongkhao ‐ On, S. Kottegoda, J. S. Pulido, and S. A. Shippy, "Determination of amino acids in rat vitreous perfusates by capillary electrophoresis," *Electrophoresis,* vol. 25, no. 17, pp. 2978-2984, 2004.

[38] J. S. Pritchett, J. S. Pulido, and S. A. Shippy, "Measurement of Region-Specific Nitrate Levels of the Posterior Chamber of the Rat Eye Using Low-Flow Push− Pull Perfusion," *Analytical chemistry,* vol. 80, no. 14, pp. 5342-5349, 2008.

[39] K. Thongkhao-on, D. Wirtshafter, and S. A. Shippy, "Feeding specific glutamate surge in the rat lateral hypothalamus revealed by low-flow push–pull perfusion," *Pharmacology Biochemistry and Behavior,* vol. 89, no. 4, pp. 591-597, 2008.

[40] S. Kottegoda, I. Shaik, and S. A. Shippy, "Demonstration of low flow push–pull perfusion," *Journal of neuroscience methods,* vol. 121, no. 1, pp. 93-101, 2002.

[41] S. L. Feng, G. Z. Liu, L. M. Jiang, Y. G. Zhu, E. M. Goldys, and D. W. Inglis, "A microfluidic needle for sampling and delivery of chemical signals by segmented flows," (in English), *Applied Physics Letters,* vol. 111, no. 18, Oct 30 2017.

[42] T. R. Slaney *et al.*, "Push–pull perfusion sampling with segmented flow for high temporal and spatial resolution in vivo chemical monitoring," *Analytical chemistry,* vol. 83, no. 13, pp. 5207-5213, 2011.

[43] D. Chen *et al.*, "The chemistrode: a droplet-based microfluidic device for stimulation and recording with high temporal, spatial, and chemical resolution," *Proceedings of the National Academy of Sciences,* vol. 105, no. 44, pp. 16843-16848, 2008.

[44] H. C. Berg, *Random walks in biology*. Princeton University Press, 1993.

[45] R. T. Kennedy, "Emerging trends in in vivo neurochemical monitoring by microdialysis," *Current opinion in chemical biology,* vol. 17, no. 5, pp. 860-867, 2013.

[46] I. Timofeev *et al.*, "Cerebral extracellular chemistry and outcome following traumatic brain injury: a microdialysis study of 223 patients," *Brain,* vol. 134, no. 2, pp. 484-494, 2011.

[47] S. M. Bossers, R. D. de Boer, C. Boer, and S. M. Peerdeman, "The diagnostic accuracy of brain microdialysis during surgery: a qualitative systematic review," *Acta neurochirurgica,* vol. 155, no. 2, pp. 345-353, 2013.

[48] A. Helmy and P. Hutchinson, "Is cerebral microdialysis a clinical tool?," ed: Springer, 2013.

[49] D. J. Weiss, C. E. Lunte, and S. M. Lunte, "In vivo microdialysis as a tool for monitoring pharmacokinetics," *TrAC Trends in Analytical Chemistry,* vol. 19, no. 10, pp. 606-616, 2000.

[50] P. J. Hutchinson *et al.*, "Clinical cerebral microdialysis: a methodological study," *Journal of neurosurgery,* vol. 93, no. 1, pp. 37-43, 2000.

[51] M. Wang, G. T. Roman, M. L. Perry, and R. T. Kennedy, "Microfluidic chip for high efficiency electrophoretic analysis of segmented flow from a microdialysis probe and in vivo chemical monitoring," *Analytical chemistry,* vol. 81, no. 21, pp. 9072-9078, 2009.

[52] M. Wang, N. D. Hershey, O. S. Mabrouk, and R. T. Kennedy, "Collection, storage, and electrophoretic analysis of nanoliter microdialysis samples collected from awake animals in vivo," *Analytical and bioanalytical chemistry,* vol. 400, no. 7, pp. 2013-2023, 2011.

[53] L. Bito, H. Davson, E. Levin, M. Murray, and N. Snider, "The concentrations of free amino acids and other electrolytes in cerebrospinal fluid, in vivo dialysate of brain, and blood plasma of the dog," *Journal of neurochemistry,* vol. 13, no. 11, pp. 1057-1067, 1966.

[54] J. Delgado, "Dialytrode for long term intracerebral perfusion in awake monkeys," *Arch Int Pharmacodyn Ther,* vol. 198, pp. 9-21, 1972.

[55] U. Ungerstedt, "Microdialysis-a new bioanalytical sampling technique," *Current Separations,* vol. 7, no. 2, pp. 43-46, 1986.

[56] U. Ungerstedt, "Microdialysis–a new technique for monitoring local tissue events in the clinic," *Acta Anaesthesiologica Scandinavica,* vol. 41, no. S110, pp. 123-123, 1997.

[57] U. Ungerstedt, "Measurement of neurotransmitter release by intracranial dialysis," *Measurement of Neurotransmitter Release in vivo,* 1984.

[58] M. Wang, G. T. Roman, K. Schultz, C. Jennings, and R. T. Kennedy, "Improved temporal resolution for in vivo microdialysis by using segmented flow," *Analytical chemistry,* vol. 80, no. 14, pp. 5607-5615, 2008.

[59] C. A. Croushore and J. V. Sweedler, "Microfluidic systems for studying neurotransmitters and neurotransmission," *Lab on a Chip,* vol. 13, no. 9, pp. 1666-1676, 2013.

[60] Q. Fang, X.-T. Shi, Y.-Q. Sun, and Z.-L. Fang, "A flow injection microdialysis sampling chemiluminescence system for in vivo on-line monitoring of glucose in intravenous and subcutaneous tissue fluid microdialysates," *Analytical chemistry,* vol. 69, no. 17, pp. 3570-3577, 1997.

[61] A. Philippu, "Use of push-pull cannulae to determine the release of endogenous neurotransmitters in distinct brain areas of anaesthetized and freely moving animals," in *Measurement of neurotransmitter release in vivo*, vol. 6: Wiley New York, 1984, pp. 3-37.

[62] R. Myers, "An improved push-pull cannula system for perfusing an isolated region of the brain," *Physiology & behavior,* vol. 5, no. 2, pp. 243-246, 1970.

[63] J. C. Szerb, "Model experiments with Gaddum's push-pull cannulas," *Canadian journal of physiology and pharmacology,* vol. 45, no. 4, pp. 613-620, 1967.

[64] W. H. Lee, T. R. Slaney, R. W. Hower, and R. T. Kennedy, "Microfabricated sampling probes for in vivo monitoring of neurotransmitters," *Analytical chemistry,* vol. 85, no. 8, pp. 3828-3831, 2013.

[65] R. Myers, A. Adell, and M. Lankford, "Simultaneous comparison of cerebral dialysis and push–pull perfusion in the brain of rats: a critical review," *Neuroscience & Biobehavioral Reviews,* vol. 22, no. 3, pp. 371-387, 1998.

[66] E. E. Patterson II, J. S. Pritchett, and S. A. Shippy, "High temporal resolution coupling of low-flow push-pull perfusion to capillary electrophoresis for ascorbate analysis at the rat vitreoretinal interface," *Analyst,* vol. 134, no. 2, pp. 401-406, 2009.

[67] N. A. Cellar and R. T. Kennedy, "A capillary–PDMS hybrid chip for separations-based sensing of neurotransmitters in vivo," *Lab on a Chip,* vol. 6, no. 9, pp. 1205-1212, 2006.

[68] N. A. Cellar, S. T. Burns, J.-C. Meiners, H. Chen, and R. T. Kennedy, "Microfluidic chip for low-flow push-pull perfusion sampling in vivo with on-line analysis of amino acids," *Analytical chemistry,* vol. 77, no. 21, pp. 7067-7073, 2005.

[69] H. Song, H.-W. Li, M. S. Munson, T. G. Van Ha, and R. F. Ismagilov, "On-chip titration of an anticoagulant argatroban and determination of the clotting time within whole blood or plasma using a plug-based microfluidic system," *Analytical chemistry,* vol. 78, no. 14, pp. 4839-4849, 2006.

[70] F. T. G. van den Brink, A. Asthana, J. G. Bomer, E. Tolner, A. van den Maagdenberg, and M. Odijk, "Miniaturized hybrid push-pull perfusion probe for sampling with high spatial and temporal resolution," in *21st International Conference on Miniaturized Systems for Chemistry and Life Sciences*, 2017: Chemical and Biological Microstystems Society.

[71] M. Sun and Q. Fang, "High-throughput sample introduction for droplet-based screening with an on-chip integrated sampling probe and slotted-vial array," *Lab on a Chip,* vol. 10, no. 21, pp. 2864-2868, 2010.

[72] F. Gielen *et al.*, "A fully unsupervised compartment-on-demand platform for precise nanoliter assays of time-dependent steady-state enzyme kinetics and inhibition," *Analytical chemistry,* vol. 85, no. 9, pp. 4761-4769, 2013.

[73] F. Gielen *et al.*, "Interfacing microwells with nanoliter compartments: a sampler generating high-resolution concentration gradients for quantitative biochemical analyses in droplets," *Analytical chemistry,* vol. 87, no. 1, pp. 624-632, 2014.

[74] Y. Zhu and Q. Fang, "Analytical detection techniques for droplet microfluidics—A review," *Analytica chimica acta,* vol. 787, pp. 24-35, 2013.

[75] B. Zheng, J. D. Tice, L. S. Roach, and R. F. Ismagilov, "A droplet-based, composite PDMS/glass capillary microfluidic system for evaluating protein crystallization conditions by microbatch and vapor-diffusion methods with on-chip X-ray diffraction," (in English), *Angewandte Chemie-International Edition,* vol. 43, no. 19, pp. 2508-2511, 2004.

[76] S. K. K ster *et al.*, "Interfacing droplet microfluidics with matrix-assisted laser desorption/ionization mass spectrometry: label-free content analysis of single droplets," *Analytical chemistry,* vol. 85, no. 3, pp. 1285-1289, 2013.

[77] F. Pereira and X. Niu, "A nano LC-MALDI mass spectrometry droplet interface for the analysis of complex protein samples," *PLoS One,* vol. 8, no. 5, p. e63087, 2013.

[78] P. Tirandazi, "Droplet formation and entrainment in liquid-gas microfluidic systems," Boston, Massachusetts : Northeastern University, December 2017.

[79] L. Martín‐Banderas *et al.*, "Flow focusing: a versatile technology to produce size‐controlled and specific‐morphology microparticles," *Small,* vol. 1, no. 7, pp. 688-692, 2005.

[80] T. Kaminski and P. Garstecki, "Controlled droplet microfluidic systems for multistep chemical and biological assays," *Chemical Society Reviews,* vol. 46, no. 20, pp. 6210-6226, 2017.

[81] B. El Debs, R. Utharala, I. V. Balyasnikova, A. D. Griffiths, and C. A. Merten, "Functional single-cell hybridoma screening using droplet-based microfluidics," *Proceedings of the National Academy of Sciences,* vol. 109, no. 29, pp. 11570-11575, 2012.

[82] H. Breisig, M. Schmidt, H. Wolff, A. Jupke, and M. Wessling, "Droplet-based liquid–liquid extraction inside a porous capillary," *Chemical Engineering Journal,* vol. 307, pp. 143-149, 2017.

[83] G. V. Kaigala, R. D. Lovchik, U. Drechsler, and E. Delamarche, "A Vertical Microfluidic Probe," *Langmuir,* vol. 27, no. 9, pp. 5686-5693, May 3 2011.

[84] X. F. van Kooten, J. Autebert, and G. V. Kaigala, "Passive removal of immiscible spacers from segmented flows in a microfluidic probe," *Applied Physics Letters,* vol. 106, no. 7, p. 074102, 2015.

[85] P. Song, O. S. Mabrouk, N. D. Hershey, and R. T. Kennedy, "In vivo neurochemical monitoring using benzoyl chloride derivatization and liquid chromatography–mass spectrometry," *Analytical chemistry,* vol. 84, no. 1, pp. 412-419, 2011.

[86] B. H. Huynh, B. A. Fogarty, R. S. Martin, and S. M. Lunte, "On-line coupling of microdialysis sampling with microchip-based capillary electrophoresis," *Analytical chemistry,* vol. 76, no. 21, pp. 6440-6447, 2004.

[87] M. W. Lada, T. W. Vickroy, and R. T. Kennedy, "High temporal resolution monitoring of glutamate and aspartate in vivo using microdialysis on-line with capillary electrophoresis with laser-induced fluorescence detection," *Analytical chemistry,* vol. 69, no. 22, pp. 4560-4565, 1997.

[88] S. Parrot, V. Sauvinet, V. Riban, A. Depaulis, B. Renaud, and L. Denoroy, "High temporal resolution for in vivo monitoring of neurotransmitters in awake epileptic rats using brain microdialysis and capillary electrophoresis with laser-induced fluorescence detection," *Journal of neuroscience methods,* vol. 140, no. 1-2, pp. 29-38, 2004.

[89] S. Tucci, P. Rada, M. J. Sepúlveda, and L. Hernandez, "Glutamate measured by 6-s resolution brain microdialysis: capillary electrophoretic and laser-induced fluorescence detection application," *Journal of Chromatography B: Biomedical Sciences and Applications,* vol. 694, no. 2, pp. 343-349, 1997.

[90] L. Bert, F. Robert, L. Denoroy, L. Stoppini, and B. Renaud, "Enhanced temporal resolution for the microdialysis monitoring of catecholamines and excitatory amino acids using capillary electrophoresis with laser-induced fluorescence detection Analytical developments and in vitro validations," *Journal of Chromatography A,* vol. 755, no. 1, pp. 99-111, 1996.

[91] B. L. Hogan, S. M. Lunte, J. F. Stobaugh, and C. E. Lunte, "Online coupling of in vivo microdialysis sampling with capillary electrophoresis," *Analytical chemistry,* vol. 66, no. 5, pp. 596-602, 1994.

[92] C. J. Watson, B. J. Venton, and R. T. Kennedy, "In vivo measurements of neurotransmitters by microdialysis sampling," ed: ACS Publications, 2006.

[93] L. F. Agnati, D. Guidolin, M. Guescini, S. Genedani, and K. Fuxe, "Understanding wiring and volume transmission," *Brain research reviews,* vol. 64, no. 1, pp. 137-159, 2010.

[94] M. Zoli *et al.*, "The emergence of the volume transmission concept1," *Brain Research Reviews,* vol. 26, no. 2-3, pp. 136-147, 1998.

[95] G. H. W. Sanders and A. Manz, "Chip-based microsystems for genomic and proteomic analysis," (in English), *Trac-Trends in Analytical Chemistry,* vol. 19, no. 6, pp. 364-378, Jun 2000.

[96] E. Verpoorte, "Microfluidic chips for clinical and forensic analysis," *Electrophoresis,* vol. 23, no. 5, pp. 677-712, Mar 2002.

[97] J. Rossier, F. Reymond, and P. E. Michel, "Polymer microfluidic chips for electrochemical and biochemical analyses," (in English), *Electrophoresis,* vol. 23, no. 6, pp. 858-867, Mar 2002.

[98] D. Juncker *et al.*, "Autonomous microfluidic capillary system," (in English), *Analytical Chemistry,* vol. 74, no. 24, pp. 6139-6144, Dec 15 2002.

[99] M. A. Unger, H. P. Chou, T. Thorsen, A. Scherer, and S. R. Quake, "Monolithic microfabricated valves and pumps by multilayer soft lithography," (in English), *Science,* vol. 288, no. 5463, pp. 113-116, Apr 7 2000.

[100] N. Idota, A. Kikuchi, J. Kobayashi, K. Sakai, and T. Okano, "Microfluidic valves comprising nanolayered thermoresponsive polymer ‐ grafted capillaries," *Advanced Materials,* vol. 17, no. 22, pp. 2723-2727, 2005.

[101] H. Andersson, W. van der Wijngaart, P. Griss, F. Niklaus, and G. Stemme, "Hydrophobic valves of plasma deposited octafluorocyclobutane in DRIE channels," *Sensors and Actuators B: Chemical,* vol. 75, no. 1-2, pp. 136-141, 2001.

[102] K. Handique, D. Burke, C. Mastrangelo, and M. Burns, "Nanoliter liquid metering in microchannels using hydrophobic patterns," *Analytical chemistry,* vol. 72, no. 17, pp. 4100-4109, 2000.

[103] T.-S. Leu and P.-Y. Chang, "Pressure barrier of capillary stop valves in micro sample separators," *Sensors and Actuators A: Physical,* vol. 115, no. 2-3, pp. 508-515, 2004.

[104] P. Man, C. Mastrangelo, M. Burns, and D. Burke, "Microfabricated capillarity-driven stop valve and sample injector," in *Micro Electro Mechanical Systems, 1998. MEMS 98. Proceedings., The Eleventh Annual International Workshop on*, pp. 45-50: IEEE, 1998.

[105] S. L. Feng, M. N. Nguyen, and D. W. Inglis, "Microfluidic Droplet Extraction by Hydrophilic Membrane," (in English), *Micromachines,* vol. 8, no. 11, Nov 2017.

[106] J. P. Hurley and C. Garrod, "Principles of physics," *The Physics Teacher,* vol. 16, pp. 408-408, 1978.

[107] C. A. Stan, S. K. Tang, and G. M. Whitesides, "Independent control of drop size and velocity in microfluidic flow-focusing generators using variable temperature and flow rate," *Analytical chemistry,* vol. 81, no. 6, pp. 2399-2402, 2009.

[108] M. J. Rosen and J. T. Kunjappu, *Surfactants and interfacial phenomena*. John Wiley & Sons, 2012.

[109] K. Kumar *et al.*, "A chaotic self-oscillating sunlight-driven polymer actuator," *Nature Communications,* Article vol. 7, p. 11975, April 7 2016.

[110] M. Amiri and A. A. Dadkhah, "On reduction in the surface tension of water due to magnetic treatment," *Colloids and Surfaces A: Physicochemical and Engineering Aspects,* vol. 278, no. 1-3, pp. 252-255, 2006.

[111] T. Homola, J. Matoušek, M. Kormunda, L. Y. L. Wu, and M. Černák, "Plasma Treatment of Glass Surfaces Using Diffuse Coplanar Surface Barrier Discharge in Ambient Air," *Plasma Chemistry and Plasma Processing,* vol. 33, no. 5, pp. 881-894, 2013.

[112] E. Vansant, P. Van Der Voort, and K. Vrancken, "Chapter 3. The surface chemistry of silica," *Studies in surface science and catalysis,* vol. 93, pp. 59-77, 1995.

[113] A. Kanta, R. Sedev, and J. Ralston, "Thermally-and photoinduced changes in the water wettability of low-surface-area silica and titania," *Langmuir,* vol. 21, no. 6, pp. 2400-2407, 2005.

[114] T. Yamamoto, M. Okubo, N. Imai, and Y. Mori, "Improvement on hydrophilic and hydrophobic properties of glass surface treated by nonthermal plasma induced by silent corona discharge," *Plasma Chemistry and Plasma Processing,* vol. 24, no. 1, pp. 1-12, 2004.

[115] S. Pazokifard, S. Farrokhpay, M. Mirabedini, and M. Esfandeh, "Surface treatment of TiO2 nanoparticles via sol–gel method: Effect of silane type on hydrophobicity of the nanoparticles," *Progress in Organic Coatings,* vol. 87, pp. 36-44, 2015.

[116] E. Özmen, A. Durán, and Y. Castro, "Hydrophobic and oleophobic sol‐gel coatings on glass substrates for usage at high temperatures," *International Journal of Applied Glass Science,* vol. 9, no. 3, pp. 413-420, 2018.

[117] N. Ichikawa, K. Hosokawa, and R. Maeda, "Interface motion of capillary-driven flow in rectangular microchannel," *Journal of colloid and interface science,* vol. 280, no. 1, pp. 155-164, 2004.

[118] P. F. Man, C. H. Mastrangelo, M. A. Burns, and D. T. Burke, "Microfabricated capillarity-driven stop valve and sample injector," (in English), *Micro Electro Mechanical Systems - Ieee Eleventh Annual International Workshop Proceedings,* pp. 45-50, 1998.

[119] J. M. Chen, P.-C. Huang, and M.-G. Lin, "Analysis and experiment of capillary valves for microfluidics on a rotating disk," *Microfluidics and Nanofluidics,* vol. 4, no. 5, pp. 427-437, 2008.

[120] M. Mohammed, E. Abraham, and M. Desmulliez, "Rapid laser prototyping of valves for microfluidic autonomous systems," *Journal of micromechanics and microengineering,* vol. 23, no. 3, p. 035034, 2013.

[121] M. J. Madou, L. J. Lee, S. Daunert, S. Lai, and C.-H. Shih, "Design and fabrication of CD-like microfluidic platforms for diagnostics: microfluidic functions," *Biomedical Microdevices,* vol. 3, no. 3, pp. 245-254, 2001.

[122] N. Ostromohov, M. Bercovici, and G. V. Kaigala, "Delivery of minimally dispersed liquid interfaces for sequential surface chemistry," *Lab Chip,* vol. 16, no. 16, pp. 3015-23, Aug 02 2016.

[123] B. J. Zwolinski, H. Eyring, and C. E. Reese, "Diffusion and Membrane Permeability," *The Journal of physical chemistry,* vol. 53, no. 9, pp. 1426-1453, 1949.

[124] H. Gu, M. H. G. Duits, and F. Mugele, "Droplets Formation and Merging in Two-Phase Flow Microfluidics," (in English), *International Journal of Molecular Sciences,* vol. 12, no. 4, pp. 2572-2597, Apr 2011.

[125] H. Gu, M. H. Duits, and F. Mugele, "Droplets formation and merging in two-phase flow microfluidics," *International journal of molecular sciences,* vol. 12, no. 4, pp. 2572-2597, 2011.

[126] Y.-C. Tan, Y. L. Ho, and A. P. Lee, "Droplet coalescence by geometrically mediated flow in microfluidic channels," *Microfluidics and Nanofluidics,* vol. 3, no. 4, pp. 495-499, 2007.

[127] M. Zagnoni and J. M. Cooper, "On-chip electrocoalescence of microdroplets as a function of voltage, frequency and droplet size," *Lab on a Chip,* vol. 9, no. 18, pp. 2652-2658, 2009.

[128] C. N. Baroud, J.-P. Delville, F. Gallaire, and R. Wunenburger, "Thermocapillary valve for droplet production and sorting," *Physical Review E,* vol. 75, no. 4, p. 046302, 2007.

[129] V. Trivedi, A. Doshi, G. Kurup, E. Ereifej, P. Vandevord, and A. S. Basu, "A modular approach for the generation, storage, mixing, and detection of droplet libraries for high throughput screening," *Lab on a Chip,* vol. 10, no. 18, pp. 2433-2442, 2010.

[130] Y.-C. Tan, J. S. Fisher, A. I. Lee, V. Cristini, and A. P. Lee, "Design of microfluidic channel geometries for the control of droplet volume, chemical concentration, and sorting," *Lab on a Chip,* vol. 4, no. 4, pp. 292-298, 2004.

[131] K. Liu, H. Ding, Y. Chen, and X.-Z. Zhao, "Droplet-based synthetic method using microflow focusing and droplet fusion," *Microfluidics and Nanofluidics,* vol. 3, no. 2, pp. 239-243, 2007.

[132] N. Bremond, A. R. Thiam, and J. Bibette, "Decompressing emulsion droplets favors coalescence," *Physical review letters,* vol. 100, no. 2, p. 024501, 2008.

[133] X. Niu, S. Gulati, and J. B. Edel, "Pillar-induced droplet merging in microfluidic circuits," *Lab on a Chip,* vol. 8, no. 11, pp. 1837-1841, 2008.

[134] C. Priest, S. Herminghaus, and R. Seemann, "Controlled electrocoalescence in microfluidics: Targeting a single lamella," *Applied Physics Letters,* vol. 89, no. 13, p. 134101, 2006.

[135] A. R. Thiam, N. Bremond, and J. Bibette, "Breaking of an emulsion under an ac electric field," *Physical review letters,* vol. 102, no. 18, p. 188304, 2009.

[136] D. R. Link *et al.*, "Electric control of droplets in microfluidic devices," *Angewandte Chemie International Edition,* vol. 45, no. 16, pp. 2556-2560, 2006.

[137] P. Singh and N. Aubry, "Transport and deformation of droplets in a microdevice using dielectrophoresis," *Electrophoresis,* vol. 28, no. 4, pp. 644-657, 2007.

[138] V. Varma, A. Ray, Z. Wang, Z. Wang, and R. Ramanujan, "Droplet merging on a lab-on-a-chip platform by uniform magnetic fields," *Scientific reports,* vol. 6, p. 37671, 2016.

[139] E. Verneuil, M. a. Cordero, F. Gallaire, and C. N. Baroud, "Laser-induced force on a microfluidic drop: origin and magnitude," *Langmuir,* vol. 25, no. 9, pp. 5127-5134, 2009.

[140] R. M. Lorenz, J. S. Edgar, G. D. Jeffries, Y. Zhao, D. McGloin, and D. T. Chiu, "Vortex-trap-induced fusion of femtoliter-volume aqueous droplets," *Analytical chemistry,* vol. 79, no. 1, pp. 224-228, 2007.

[141] M. L. Cordero, D. R. Burnham, C. N. Baroud, and D. McGloin, "Thermocapillary manipulation of droplets using holographic beam shaping: Microfluidic pin ball," *Applied Physics Letters,* vol. 93, no. 3, p. 034107, 2008.

[142] C. N. Baroud, F. Gallaire, and R. Dangla, "Dynamics of microfluidic droplets," *Lab on a Chip,* vol. 10, no. 16, pp. 2032-2045, 2010.

[143] F. Sarrazin, L. Prat, N. Di Miceli, G. Cristobal, D. Link, and D. Weitz, "Mixing characterization inside microdroplets engineered on a microcoalescer," *Chemical Engineering Science,* vol. 62, no. 4, pp. 1042-1048, 2007.

[144] T. B. Stachowiak *et al.*, "Fabrication of porous polymer monoliths covalently attached to the walls of channels in plastic microdevices," *Electrophoresis,* vol. 24, no. 21, pp. 3689-3693, 2003.

[145] J. P. a. G. Hurley, Claude, "Principles of physics.," in *Principles of physics*Boston: Houghton Mifflin, 1978.

[146] T. Moritani, M. Yamada, and M. Seki, "Generation of uniform-size droplets by multistep hydrodynamic droplet division in microfluidic circuits," *Microfluidics and nanofluidics,* vol. 11, no. 5, pp. 601-610, 2011.